arXiv:2509.25116v2 [math.AP] 19 Mar 2026

Nonuniqueness of Leray–Hopf solutions to the unforced incompressible 3D Navier–Stokes Equation

Thomas Hou, Yixuan Wang, Changhe Yang

March 20, 2026

Abstract

The nonuniqueness of Leray–Hopf solutions to the unforced incompressible 3D Navier–Stokes equations is one of the central open problems in mathematical fluid dynamics. In this paper, we provide, to our knowledge, the first rigorous computer-assisted proof demonstrating such nonuniqueness. Inspired by earlier works [32, 1, 27], we construct a Leray–Hopf solution in the self-similar setting and then establish the existence of a second solution by analyzing the stability of the linearized operator around this profile, showing that it corresponds to an unstable perturbation. To achieve this, we develop an innovative numerical method that computes candidate solutions with high precision and propose a framework for rigorously establishing exact solutions in a neighborhood of these candidates, where the invertibility of the linearized operator is the key. Inspired by [13], we decompose the linearized operator into a coercive part plus a compact perturbation, which is further approximated by a finite-rank operator up to a small error. The invertibility of the linearized operator restricted to the image of this finite-rank approximation is then rigorously verified via construction of the inversion on its finite set of basis functions with residues incorporated properly. This certifies the existence of a profile and similarly an unstable eigenpair. Consequently, it yields a second solution–indeed, infinitely many Leray–Hopf solutions. The code is publicly available at: https://github.com/HouGroup2026/3d-navier-stokes-nonuniqueness

1 Introduction

In this paper, we study the three-dimensional incompressible Navier–Stokes equation on the whole space without forcing:

$$\begin{cases} \partial_t u + u \cdot \nabla u - \Delta u + \nabla p = 0, \\ \mathrm{div} u = 0, \\ u(t=0,x) = u_{\mathrm{in}}(x). \end{cases} \tag{1.1}$$

Leray [35], and later Hopf [28] for bounded domains, constructed weak solutions that exist for all time and satisfy energy inequalities. These solutions are termed Leray–Hopf solutions, and Leray's construction was moreover suitable, in the sense that it satisfies local energy inequality.

The main contribution of this paper is to develop a rigorous computer-assisted proof of the nonuniqueness of the Leray–Hopf solutions to (1.1).

Theorem 1 (Nonuniqueness of Leray–Hopf solutions) *There exist infinitely many distinct suitable Leray–Hopf solutions to the Navier–Stokes equation* (1.1) *on* $\mathbb{R}^3 \times [0,1]$ *with the same divergence-free initial condition* $u_{\mathrm{in}} = u_{\mathrm{loc}}$ *of compact support, with* $u_{\mathrm{loc}} \in C^\infty(\mathbb{R}^3 \setminus \{0\}) \cap L^q$ *for any* $q < 3$. *The solutions are* $L^s([0,1]; L^q(\mathbb{R}^3))$, *for any* $q \geqslant 2$, $\frac{3}{q} + \frac{2}{s} > 1$, *and smooth for positive times. They just miss the Prodi–Serrin condition that guarantees a unique solution, see* (1.3).

Our work is inspired by the works of Jia and Sverak [31, 32], which studied the forward self-similar Navier–Stokes equation and reduced nonuniqueness to spectral assumptions of the self-similar profiles. In [27], Guillod and Sverak provided numerical evidence that such spectral assumptions are

satisfied for the self-similar solution profiles that they constructed numerically. In [1], Albritton–Brue–Colombo built on this idea of unstable profiles in self-similar variables, but added a singular forcing term so that their background solution does not need to solve the Navier–Stokes equation exactly. In fact, their profile can be any divergence-free function. They instead leveraged the unstable vortex solutions constructed by Vishik [48, 49, 3] that are steady states of the 2D Euler equations, and lifted them to 3D axisymmetric vortex rings. The case of the unforced Navier–Stokes equations is much more challenging since it is almost impossible to find an explicit self-similar Leray–Hopf solution with an unstable eigenvalue.

In this paper, we adopt a different strategy by developing a novel computational method and an innovative computer-assisted strategy to rigorously verify the existence of a self-similar profile that solves the unforced Navier–Stokes equation exactly with an unstable eigenvalue. We then use the tools developed in [32] to establish the nonuniqueness of Leray–Hopf solutions, while reducing the spectral assumption simply to an unstable eigenvalue inspired by [1].

1.1 Leray–Hopf solution and strong-weak uniqueness

Two important types of solutions to (1.1) are the **Leray–Hopf solutions** and the **strong solutions**. We begin with the definition of Leray–Hopf solutions. We denote divergence-free function spaces using a subscript σ, and locally integrable function spaces using a subscript loc.

Definition 1 (Leray–Hopf solution) *[46] Let $T > 0$, $u_{\text{in}} \in L^2_\sigma$. A Leray–Hopf solution on $\mathbb{R}^3 \times [0,T)$ with initial data u_{in} is a divergence-free vector field*

$$u \in L^\infty_{\text{loc}}([0,T); L^2_\sigma(\mathbb{R}^3)) \cap L^2_{\text{loc}}([0,T); H^1_\sigma(\mathbb{R}^3)),$$

with the following properties:

1. It holds that for all test functions $v \in C^\infty_0([0,T); C^\infty_{0,\sigma}(\mathbb{R}^3))$:

$$-\int_0^T \langle u, \partial_t v\rangle + \int_0^T \langle \nabla u, \nabla v\rangle + \int_0^T \langle u\cdot\nabla u, v\rangle = \langle u_{\text{in}}, v(0,\cdot)\rangle.$$

2. u satisfies the energy inequality:

$$\frac{1}{2}\|u(t,\cdot)\|^2_{L^2} + \int_0^T \|\nabla u\|^2_{L^2} \leqslant \frac{1}{2}\|u_{\text{in}}\|^2_{L^2}.$$

Remark 1 (Suitability) Solutions built via Leray's original construction are, moreover, suitable, which means they satisfy the stronger local energy inequality:

$$(\partial_t - \Delta)\frac{1}{2}|u|^2 + |\nabla u|^2 + \operatorname{div}((\frac{1}{2}|u|^2 + p)u) \leqslant 0 \tag{1.2}$$

in a distributional sense. Local energy inequality plays an important role in partial regularity theory on the dimension of the potential singular sets, as in [9, 36].

A Leray–Hopf solution is weakly continuous in time [46] and exists globally. Its uniqueness is not guaranteed. A strong solution is a Leray–Hopf solution that satisfies the Prodi–Serrin [44, 45] condition in L^sL^q spaces:

$$u \in L^s_{\text{loc}}([0,T); L^q(\mathbb{R}^3)), \quad 3 < q < \infty, \quad 2 < s < \infty, \quad \frac{3}{q} + \frac{2}{s} \leqslant 1. \tag{1.3}$$

The critical case of $q = 3$ was established by Escauriaza–Seregin–Sverak [25]. Under this condition, the solution exhibits higher regularity [44, 45, 25],

$$u \in L^\infty_{\text{loc}}([0,T); H^1_\sigma(\mathbb{R}^3)) \cap L^2_{\text{loc}}([0,T); H^2_\sigma(\mathbb{R}^3)).$$

A global strong solution ensures the uniqueness of weak solutions. They are locally well-posed. However, the global-in-time existence of such solutions remains an open question. Therefore, we shift focus to studying the nonuniqueness of the Leray–Hopf solutions arising from blow-up times of strong solutions. In other words, we consider singular initial data u_{in}.

1.2 Self-similar setting

Self-similar solutions are thus a special class of solutions of interest that lie precisely at the boundary of the known well-posedness theory. A scale-invariant initial condition takes the form:

$$u_{\text{in}}(x) = \frac{1}{|x|} A(\frac{x}{|x|}), \tag{1.4}$$

with a singularity of $O(|x|^{-1})$ at the origin. The authors of [31, 32] seek solutions of the form:

$$u(t,x) = \frac{1}{\sqrt{t}} \widetilde{U}(\frac{x}{\sqrt{t}}), \tag{1.5}$$

which preserves the scaling structure. The readers should not confuse this self-similar setting, which starts from singular initial data, with the backward self-similar setting related to finite-time singularities from smooth initial data. Plugging (1.5) into the Navier–Stokes equation, we obtain:

$$\begin{cases} -\frac{1}{2}\widetilde{U} - \frac{1}{2}\xi \cdot \nabla \widetilde{U} + \Pi(\widetilde{U} \cdot \nabla \widetilde{U}) - \Delta \widetilde{U} = 0, \\ \text{div} \widetilde{U} = 0, \end{cases} \tag{1.6}$$

where $\xi = \frac{x}{\sqrt{t}}$ is the similarity variable and Π is the Leray projection. We stress that the pressure and the Leray projection formulations are interchangeable. The initial data, as per (1.4), translates into the following boundary condition for (1.6),

$$\widetilde{U}(\xi) = \frac{1}{|\xi|} A(\frac{\xi}{|\xi|}) + o(\frac{1}{|\xi|}), \quad |\xi| \to +\infty, \tag{1.7}$$

where the remainder term in fact decays at the sharper rate $O(\frac{1}{|\xi|^3})$, as shown in [31].

The divergence-free condition induces the following constraint on A:

$$\text{div}(\frac{1}{|x|} A(\frac{x}{|x|})) = 0. \tag{1.8}$$

In [31], the authors proved that for any admissible A, there exists a self-similar solution for (1.1). However, whether this solution is unique remains an open question.

1.3 Eigenvalue of the linearized operator and nonuniqueness

In [32], a sufficient condition for nonuniqueness was proposed. It involves analyzing the eigenvalues of the linearized operator $\mathcal{L}_{\widetilde{U}}$, defined by:

$$\mathcal{L}_{\widetilde{U}} v := \frac{1}{2} v + \frac{1}{2} \xi \cdot \nabla v - \Pi(\widetilde{U} \cdot \nabla v + v \cdot \nabla \widetilde{U}) + \Delta v. \tag{1.9}$$

To establish nonuniqueness, a second solution is sought in the form:

$$\widetilde{u}(t,x) = \frac{1}{\sqrt{t}} \widetilde{U}(\frac{x}{\sqrt{t}}) + \frac{1}{\sqrt{t}} \phi(t, \frac{x}{\sqrt{t}}).$$

Plugging this ansatz into (1.6) and introducing the rescaled time $\tau = \log t$, ϕ satisfies:

$$\begin{cases} \partial_\tau \phi - \mathcal{L}_{\widetilde{U}} \phi + \Pi(\phi \cdot \nabla \phi) = 0, \\ \text{div} \phi = 0. \end{cases} \tag{1.10}$$

We aim to find a nontrivial solution to (1.10) with initial data

$$\phi(\tau = -\infty, x) = 0.$$

In [32], the author considered a series of solutions parameterized by α. For a given parameterized initial data A_α, let $\widetilde{U}_\alpha$ denote the corresponding solution to (1.1) with the boundary condition $\widetilde{U}_\alpha(\xi) \sim \frac{A_\alpha(\xi)}{\xi}$ as $|\xi| \to +\infty$. Suppose that $L_{\widetilde{U}_\alpha}$ has a discrete eigenvalue λ_α satisfying $\Re(\lambda_\alpha) > -\frac{1}{4}$. They showed that if the trajectory of λ_α could cross the imaginary axis from negative to positive as α increases, then, under certain auxiliary assumptions, there exists a nontrivial solution to (1.10) and thus the solution to (1.1) is nonunique.

Remark 2 Note that due to the slow decay of $u_{\text{in}} = O(\frac{1}{|x|})$, the solution is not in L^2 and thus not a Leray–Hopf solution. However, in [32], the authors showed that such solutions can be localized to yield valid Leray–Hopf solutions.

In [1], the authors employed a similar approach to prove the nonuniqueness of Leray–Hopf solutions for the forced Navier–Stokes equation. The force corresponds to the right-hand side of the first equation of (1.1) of any divergence-free U, while we have to find a divergence-free profile U that solves the first equation of (1.6) exactly without any external forcing. They assumed that an unstable eigenvalue, with real part $a > 0$, exists for the linearized operator $\mathcal{L}_{\widetilde{U}}$ and found the unstable manifold associated with the most unstable eigenvalue. The perturbation of the solution follows the asymptotics $\phi = \widetilde{U}^{\text{lin}} + O(e^{2a\tau})$. Here, $\widetilde{U}^{\text{lin}}$ solves the linearized equation:

$$\partial_\tau \widetilde{U}^{\text{lin}} = \mathcal{L}_{\widetilde{U}} \widetilde{U}^{\text{lin}}, \tag{1.11}$$

and decays at the rate $O(e^{a\tau})$, converging to zero as $\tau \to -\infty$, indicating nonuniqueness.

Verification of eigenvalues. Having related the nonuniqueness of the Leray–Hopf solutions to the eigenvalue of the linearized operator in self-similar variables, we now focus on confirming the existence of an unstable eigenvalue. We aim to find a solution to the following system:

$$\begin{cases} -\frac{1}{2}\widetilde{U} - \frac{1}{2}\xi \cdot \nabla \widetilde{U} + \Pi(\widetilde{U} \cdot \nabla \widetilde{U}) - \Delta \widetilde{U} = 0, \\ -\frac{1}{2}\widetilde{v} - \frac{1}{2}\xi \cdot \nabla \widetilde{v} + \Pi(\widetilde{U} \cdot \nabla \widetilde{v} + \widetilde{v} \cdot \nabla \widetilde{U}) - \Delta \widetilde{v} = \widetilde{\lambda}\widetilde{v}, \quad \widetilde{\lambda} < 0, \\ \operatorname{div} \widetilde{U} = 0, \\ \operatorname{div} \widetilde{v} = 0. \end{cases} \tag{1.12}$$

Here, Π denotes the Leray projection. We remark that we flip a sign of the linearized operator in the second equation of (1.12) due to the convenience of elliptic estimates. If we can prove that $\mathcal{L}_{\widetilde{U}}$ has an eigenvalue with a positive real part for some $\widetilde{U}$ satisfying (1.6), then one can hope to show that the solution to (1.1) is nonunique. Through localization, this leads to the nonuniqueness of the Leray–Hopf solution. We will elaborate on this point in Section 2. Numerical evidence supporting the existence of such profiles was provided in [27].

Theorem 2 *There exists a weak solution* $(\widetilde{U}, \widetilde{v}, \widetilde{\lambda})$ *to the system* (1.12) *with* $\widetilde{U} \in H^1_{\text{loc}}, \widetilde{v} \in H^1$.

We adopt a computer-assisted framework to verify existence for (1.12). The strategy is to compute a high-accuracy numerical profile $\overline{U}$ and then construct a perturbation U so that $\overline{U} + U$ solves the equation exactly. This requires (i) a certified small residual for $\overline{U}$ and (ii) an invertibility estimate for the linearized operator around $\overline{U}$. To obtain (ii), we split the linearized operator into a coercive part and a compact remainder; the latter is rigorously approximated by a finite-rank operator with a quantitatively controlled tail. We then verify the spectral properties needed on this small matrix for the nonlinear estimates, combine them with coercivity in the linear estimates, and close a fixed-point argument; see Sections 3 and 4. A similar strategy also applied to $(\widetilde{v}, \widetilde{\lambda})$.

A subtle point is the regularity and decay of the exact profile $\widetilde{U} := \overline{U} + U$. From Proposition 1 we only know $U \in H^1$ with $\|U\|_{H^1} \lesssim \varepsilon^U$, which does not by itself identify $\widetilde{U}$ as a Leray–Hopf profile. To bridge this, we introduce a smooth radial cutoff and write $\widetilde{U} = U_{\text{near}} + U_{\text{far}}$, where U_{far} is divergence free, smooth, and constructed to match the exterior asymptotics of $\overline{U}$. In these variables, U_{near} solves the stationary self-similar Navier–Stokes system with variable coefficients determined by U_{far}; these coefficients are smooth, C^k–bounded, and decay polynomially, and the corresponding forcing is smooth and decays like $O(|\xi|^{-3})$ by our far-field analysis. We therefore combine local elliptic bootstrapping using the coercivity of the linearized operator to obtain $U_{\text{near}} \in H^m$ for all m, together with weighted energy bounds

$$|\xi|\, U_{\text{near}}, \quad |\xi|\, \nabla U_{\text{near}}, \quad |\xi|^2\, \nabla U_{\text{near}}, \quad |\xi|^2\, \nabla^2 U_{\text{near}} \ \in L^2.$$

A dyadic rescaling then yields the quantitative decay $|U_{\text{near}}(\xi)| = O(|\xi|^{-3/2})$ as $|\xi| \to \infty$; see Propositions 3 and 4. Consequently, $\widetilde{U}$ has the required regularity and far-field decay, and is a Leray–Hopf self-similar profile.

Outline of the nonuniqueness proof (Section 2.2). We combine the localization idea of Jia–Sverak [32] with the fixed-point framework of Jia–Sverak [32] and Albritton–Brue–Colombo [1]. The key innovation compared to [32] is that we perform localization and nonuniqueness arguments at the same time, bypassing the sophisticated spectral assumptions therein. Writing the solution as $u = \widetilde{u} + u^{\mathrm{cut}} + u^{\mathrm{cor}}$, we first *localize the scale-invariant initial data* by a Bogovskii decomposition $u_{\mathrm{in}} = u_{\mathrm{loc}} + w$, where u_{loc} is compactly supported and divergence free, and then set $u^{\mathrm{cut}} = -e^{t\Delta}w$ to cut off the far-field tail. Unlike [1], our self-similar profile $\widetilde{U}$ is not compactly supported; the new ingredient is to control the resulting *far-field interaction* via heat smoothing, which makes the associated linear term small when the localization radius R is large. Passing to similarity variables, we solve for the correction U^{cor} as a fixed point of a contraction Duhamel map generated by the semigroup $e^{\tau\mathcal{L}_{\widetilde{U}}}$. A key idea is to use a Riesz projection to split the dynamics into a stable part and an unstable part as in [32]; see also [12, 11]. The finitely many unstable modes will serve as free parameters at $\tau = 0$. Different choices of these unstable coordinates yield distinct solutions on $(-\infty, 0]$, producing infinitely many Leray–Hopf solutions with the same L^2 initial data u_{loc}.

In our construction of the Leray–Hopf solution $\overline{U}$ and the eigenfunction $\overline{v}$, we impose even symmetry in z for $\overline{U}$ and odd symmetry in z for $\overline{v}$. The odd parity of $\overline{v}$ breaks the base even symmetry of $\overline{U}$; thus the Leray–Hopf branch bifurcating in the $\overline{v}$-direction is symmetry-breaking, which was also observed by the previous work [27, 1].

1.4 Computer-assisted proofs

Our approach motivates the following assumption for approximate profiles:

Assumption 1 (Approximate profiles) *The tuple $(\overline{U}, \overline{P}, \overline{v}, \overline{q}, \overline{\lambda})$ is an approximate solution of* (1.12) *with small residuals:*

$$\begin{cases} -\frac{1}{2}\overline{U} - \frac{1}{2}\xi\cdot\nabla\overline{U} + \overline{U}\cdot\nabla\overline{U} - \Delta\overline{U} + \nabla\overline{P} = \mathrm{E}^U, \\ -\frac{1}{2}\overline{v} - \frac{1}{2}\xi\cdot\nabla\overline{v} + \overline{U}\cdot\nabla\overline{v} + \overline{v}\cdot\nabla\overline{U} + \nabla\overline{q} - \Delta\overline{v} = \overline{\lambda}\overline{v} + \mathrm{E}^v, \quad \overline{\lambda} < 0, \\ \mathrm{div}\overline{U} = 0, \\ \mathrm{div}\,\overline{v} = 0, \end{cases}$$

where $\overline{v}$ is normalized (i.e., $\|\overline{v}\|_{L^2} = 1$), and the orthogonality condition $\langle \mathrm{E}^v, \overline{v}\rangle = 0$ is satisfied upon a possible modification of $\overline{\lambda}$. The small residuals E^U and E^v are bounded by

$$\|\mathrm{E}^U\|_{L^2} \leqslant \varepsilon^U, \|\mathrm{E}^v\|_{L^2} \leqslant \varepsilon^v.$$

Here $\overline{U}, \overline{v} \in C^\infty_\sigma(\mathbb{R}^3\backslash\{0\}) \cap H^2_{\mathrm{loc}}$. In the far field, $\overline{U}$ satisfies the boundary condition

$$\overline{U}(\xi) = \frac{1}{|\xi|}A(\frac{\xi}{|\xi|}) + O(|\xi|^{-3}), \quad |\xi| \to +\infty, \tag{1.13}$$

which is consistent with the boundary condition in Section 1.2, for a suitable A with the divergence-free constraint (1.8)*. Moreover, for any index $j \geqslant 0$, we have*

$$\nabla^j\overline{U}(\xi) = \nabla^j(\frac{1}{|\xi|}A(\frac{\xi}{|\xi|})) + O(|\xi|^{-j-3}). \tag{1.14}$$

Our choice of the numerical basis guarantees the integrability and decay; see Sections 5.5 and 5.6.

Suppose we have constructed a sufficiently accurate approximate solution. The next step is to perform rigorous error analysis to confirm the existence of a nearby exact solution. This leads to our main theoretical results, summarized in the two propositions below:

Proposition 1 (Exact self-similar profile) *If Assumption 1 holds, then there exists a U satisfying the following equation in the distributional sense:*

$$\begin{cases} -\frac{1}{2}U - \frac{1}{2}\xi\cdot\nabla U - \Delta U + \Pi(\overline{U}\cdot\nabla U + U\cdot\nabla\overline{U} + U\cdot\nabla U) = -\Pi\mathrm{E}^U, \\ \mathrm{div}\,U = 0, \end{cases} \tag{1.15}$$

so that

$$\widetilde{U} = \overline{U} + U \tag{1.16}$$

solves the first and third equations of (1.12)*. Moreover, the perturbation* $U \in H^1$ *satisfies:*

$$\|U\|_{L^2} \lesssim \varepsilon^U.$$

Proposition 2 (Exact unstable eigenpair) *If Assumption 1 holds, then there exists* (λ, v) *satisfying the following equation in the distributional sense:*

$$\begin{cases} -\frac{1}{2}v - \frac{1}{2}\xi \cdot \nabla v - \Delta v + \Pi(\widetilde{U} \cdot \nabla v + U \cdot \nabla \overline{v} + v \cdot \nabla \widetilde{U} + \overline{v} \cdot \nabla U) = \overline{\lambda} v + \lambda \overline{v} + \lambda v - \Pi \mathrm{E}^v, \\ \operatorname{div} v = 0. \end{cases} \tag{1.17}$$

Here, $\widetilde{U} = \overline{U} + U$ *is the solution stated in Proposition 1. Hence,* $(\widetilde{\lambda}, \widetilde{v}) = (\overline{\lambda} + \lambda, \overline{v} + v)$ *is an eigenpair of the linearized operator and solves the second and fourth equations of* (1.12)*. Additionally,* $v \in H^1$ *satisfies the orthogonality condition* $\langle v, \overline{v} \rangle = 0$*, and the following estimate holds for* (v, λ)*:*

$$\|v\|_{L^2} + |\lambda| \lesssim \varepsilon^v.$$

Therefore, $\widetilde{v}$ *is nontrivial, and the eigenvalue* $\widetilde{\lambda}$ *is strictly negative.*

One can immediately see that Theorem 2 can be inferred by the two preceding propositions.

One of the main contributions of this paper is that we develop an innovative numerical framework to construct a smooth, axisymmetric, divergence-free candidate profile with high precision. A distinguished advantage of this framework is that we can start with any initial guess to search for a candidate unstable eigenmode. We refine our search iteratively by using gradient descent to locate a maximally unstable configuration. Specifically, we first solve the Navier–Stokes equations in a large finite domain using a finite element method, then extend it to the whole space by an analytic change of variables $r = \tan(\beta)$ and interpolate it on an exactly divergence-free spectral basis, which is essential for rigorous computer-assisted verification. We also use an iterative optimization method to further improve the accuracy of the approximate profile until a sufficiently small residual is reached. An important property of our numerical framework is that our constructed numerical solution $\overline{U}$ or $\overline{v}$ is smooth except at the origin. Moreover, $\overline{U}$ satisfies the far field boundary condition and the decay property to all orders. For more details, see Section 5.

We would like to point out that our Navier–Stokes nonuniqueness verification is far lighter than that for the 3D Euler singularity program [13, 15, 14], because viscosity yields genuine coercivity. In particular, the linearized operators enjoy relatively large coercivity coefficients in L^2: about 0.051 for the $\overline{U}$–equation and about 0.164 for the $\overline{v}$–equation (see Section 4.5). This allows us to work in standard L^2/H^1 norms without singular weights and to close the a posteriori bounds using only the L^2 residuals of $\overline{U}$ and $\overline{v}$ together with a few pointwise envelopes of L^∞ estimates. The discrete operators we assemble are modest (roughly 1200×1200), and the finite-rank verification reduces to eigenproblems of small sizes 25×25. Thanks to the strong damping reflected by the above coercivity and the effective approximation property of our generalized eigenfunctions, retaining 25 modes suffices to close the estimates via the Schauder fixed point theorem.

Moreover, we use a trigonometric tensor-product representation in (β, θ) for $\overline{U}$ and $\overline{v}$ after the change of variables $r = \tan\beta$ with a relatively small number of modes ($N = 600$ in the β-direction and $N = 300$ in the θ-direction). This representation enables us to perform analytic L^2 evaluation of the residuals E^U and E^v and also makes it easy for us to obtain relatively sharp upper bounds for $\|\overline{U}\|_{L^\infty}$ and $\|\overline{v}\|_{L^\infty}$ as well as their gradients. The only delicate numerical step is to evaluate the Q-inner products for the generalized eigenfunctions, which involve Bessel functions along the β-direction. We need to approximate the inner products using a 8th order quadrature and supply a rigorous $W^{8,\infty}$ error bound on the integrand, see Section 7 for more discussion. Altogether, viscous coercivity, low-dimensional spectral checks, and analytic trigonometric calculus make the present verification substantially simpler than that in the Euler setting.

We remark that a candidate solution was found in [27], but this approximate solution seems to be too large to apply our computer-assisted proof, in the sense that the approximation of the associated compact part of the linearized operator by a finite rank operator would require a large number of modes to reduce the residual error small enough for us to close the bootstrap argument, making the computer verification too expensive; see Section 4.2 for details.

1.5 Organization of the paper

In summary, our strategy consists of three main steps:

1. Construct an accurate approximate solution to the eigenvalue system (1.12).
2. Establish the existence of an exact solution (Theorem 2).
3. Prove the nonuniqueness of Leray–Hopf solutions (Theorem 1).

The rest of the paper is structured as follows. We first conclude nonuniqueness based on Theorem 2 in Section 2. Provided that Theorem 2 holds, we establish the smoothness of our profile by bootstrapping its regularity using elliptic estimates, even if the numerical profile is nonsmooth by itself only at the origin. We also show that the profile satisfies the boundary conditions necessary for the self-similar setting by establishing the fast decay of the perturbation. Then we adopt a fixed-point approach similar to [1] and [32] to establish nonuniqueness based on the unstable eigenpair, with a cutoff to obtain Leray–Hopf solutions.

In Section 3, we outline the framework for proving Theorem 2, which serves as a foundation for the numerical analysis of a broad class of problems. We believe that our framework is interesting in itself to establish eigenvalue properties rigorously for other problems. In Section 4, we apply this framework to our specific system and establish Theorem 2. We demonstrate the construction of a finite-rank operator to approximate the compact part of the linear operator, verify that this approximation has a sufficiently small error, and derive the necessary nonlinear estimates to complete the argument. For both the nonlinear terms and the approximation error, sharp estimates are essential to tighten the final bound.

Section 5 discusses the numerical implementation in detail. We introduce the setting of the finite element method used to obtain an approximate solution, and interpolate it on a spectral basis to ensure exact divergence-freeness. Section 6 details the numerical construction of the finite-rank approximation and verifies the invertibility of the linear operator on a finite-dimensional subspace. Finally, we describe the numerical methods that we will use to rigorously verify our numerical computations using interval arithmetic in Section 7 and collect some proofs in the Appendix.

1.6 Literature review

Now we review related literature on nonuniqueness besides the programs of Jia–Sverak and Guillod, and Albritton–Brue–Colombo. We also discuss relevant literature on computer-assisted proofs.

Nonuniqueness. One of the earliest examples of nonuniqueness to (1.1) dates back to Ladyzhenskaya [34], in a time-varying domain with force. Similar to the program of Jia, Sverak, and Guillod, Bressan, Murray, and Shen [6, 5] proposed some suggestive numerical evidence for nonuniqueness to the 2D Euler equations without forcing. In addition to the work using self-similar solutions, there is another important line of work leveraging convex integration, a powerful tool introduced to fluid dynamics that resulted in the proof of the Onsager conjecture by Isett [30] and Buckmaster–De-Lellis–Szekelyhidi–Vicol [7]. In particular, Buckmaster–Vicol [8] established that for any L^2 initial data, distributional solutions to (1.1) are nonunique, and Cheskidov–Luo [20, 21] established nonuniqueness in $L_t^{2-}L_x^\infty$ and $L_t^\infty L_x^{2-}$ for dimension $d \geqslant 2$. However, solutions obtained from convex integration schemes are very far from Leray regularity H_x^1. Very recently, Coiculescu–Palasek established nonuniqueness in a scaling critical space BMO^{-1} [22] where global well-posedness for

small initial data holds [33], using techniques from a dyadic model introduced by Palasek [43]. Later on, Cheskidov–Dai–Palasek [19] established nonuniqueness in the same space along with instantaneous blowup.

Computer-assisted proofs. The idea of combining rigorous analysis with numerical candidates has been successfully applied to problems in fluid dynamics, where the inherent complex nature of solutions prohibited analytical candidates: particularly in the search for backward self-similar singularities, culminating in the computer-assisted proof for the 3D incompressible Euler equation with cylindrical boundary by Chen–Hou [13, 15, 14] based on numerical investigation by Luo–Hou [41, 42]. We draw inspiration from the works of Chen–Hou [13], Elgindi–Pasqualotto [23] on the singularity formulation of the Boussinesq equation with only radial nonsmoothness, and Castro–Cordoba–Gomez-Serrano [10] on the construction of smooth rotating solutions of the inviscid surface quasi-geostrophic equation. We also remark the linear framework of Liu–Nakao–Oishi for eigenvalue verifications [40, 38, 39].

Stability analysis, especially linear stability, around the approximate solution is essential to conclude the computer-assisted proof, and we apply a coercive-compact decomposition of the linear operator. The compact part is approximated by a finite-rank operator, whose error, along with the residual of the approximate solution, will need to be verified rigorously by interval arithmetic. Our decomposition is obvious in a regular H^1 norm, unlike in [13], where building on results of 1D singularities in fluid models [16, 17], one needs to use singularly weighted estimates; see also [29, 18, 37] for the use of singular weights for singularity beyond self-similarity or full stability.

For numerical computation, we use traditional finite element methods for profile computation and spectral methods for rigorous verification. We remark that there has been encouraging recent progress in using Physics-Informed Neural Networks (PINNs) to construct self-similar blowup profiles, including the 2D Boussinesq system with boundary [51, 52, 50]. However, a rigorous computer-assisted proof is not yet available to rigorously justify these numerical profiles.

1.7 Notations

We denote by $\langle \cdot, \cdot \rangle_\Omega$ the L^2-inner product over a domain $\Omega \subset \mathbb{R}^3$. The Sobolev norm $\| \cdot \|_{W^{k,p}(\Omega)}$ for functions in the Sobolev space $W^{k,p}(\Omega)$ is defined by

$$\|f\|_{W^{k,p}(\Omega)} := \Big(\sum_{|\alpha| \leqslant k} \|\partial^\alpha f\|_{L^p(\Omega)}^p \Big)^{\frac{1}{p}},$$

where $\alpha = (\alpha_1, \alpha_2, \alpha_3)$ denotes a multi-index and $|\alpha| = \alpha_1 + \alpha_2 + \alpha_3$ is its order. In particular, we write $H^k(\Omega) := W^{k,2}(\Omega)$. These notations extend naturally to vector- and matrix-valued functions induced by the Frobenius norm. For example, for an $m \times n$ matrix function $A(x)$ with entries A_{ij}, we define its L^p norm as:

$$\|A\|_{L^p(\Omega)} := \Big\| \Big(\sum_{1 \leqslant i \leqslant m, 1 \leqslant j \leqslant n} |A_{ij}|^2 \Big)^{\frac{1}{2}} \Big\|_{L^p(\Omega)}.$$

When $\Omega = \mathbb{R}^3$, we can omit Ω.

We use C to denote a generic absolute constant, which may change from line to line. The notation $A \lesssim B$ indicates that $A \leqslant CB$ for some constant $C > 0$. Constants such as $K_0, K_1, \ldots$ are fixed throughout the paper. Constants $\eta_1, \eta_2, \ldots$ are tunable parameters that arise in both the analytical estimates and the computational components of the proof. We use $\varepsilon_1, \varepsilon_2, \ldots$ to denote error bounds that can be made arbitrarily small. Constants like $M_0, M_1, \ldots$ are abbreviations for long expressions. To indicate dependence, we use subscripts and superscripts such as K^U, though not necessarily functional dependence.

2 Nonuniqueness Based on Theorem 2

In this section, we detail the proof of Theorem 1 based on Theorem 2, addressing the nonuniqueness of Leray–Hopf solutions. First, we demonstrate the smoothness of the profile $\widetilde{U}$, along with its far-field decay. In particular, it satisfies the boundary conditions of a self-similar solution. Then, via an approach inspired by prior works [1, 32], we establish the nonuniqueness of Leray–Hopf weak solutions starting from homogeneous initial data after cutoff, as in [32]. An important idea is to perform a stable-unstable decomposition of the semigroup and demonstrate that each appropriate unstable mode at $t = 1$ corresponds to a distinct solution with the same initial data.

2.1 Regularity of the profile

We begin by proving the smoothness of the profile and that it satisfies the appropriate boundary condition. Notice that by Proposition 1 and Assumption 1, we know that $\widetilde{U} \in H^1_{\mathrm{loc}}$. We will perform a decomposition into far and near fields of the profile, and bootstrap the regularity based on the steady state equation (1.12).

To be precise, by Assumption 1, $\overline{U} \in C^\infty(\mathbb{R}^3\backslash\{0\}) \cap H^1_{\mathrm{loc}}$ is divergence free, and we construct $U_{\mathrm{far}} \in C^\infty$, also divergence free, such that $\overline{U} - U_{\mathrm{far}} \in H^1$. Let $\widetilde{\chi}$ be a smooth truncation function:

$$\widetilde{\chi}(\xi) = 0, \quad |\xi| \leqslant 1, \quad \widetilde{\chi}(\xi) = 1, \quad |\xi| \geqslant 2,$$

and define:

$$U_{\mathrm{far}} = \Pi(\widetilde{\chi}\overline{U}). \tag{2.1}$$

Then, U_{far} satisfies:

$$\begin{cases} U_{\mathrm{far}} = \widetilde{\chi}\overline{U} - \nabla P_c, \\ \operatorname{div} U_{\mathrm{far}} = 0, \end{cases} \tag{2.2}$$

where P_c solves:

$$\Delta P_c = \operatorname{div}(\widetilde{\chi}\overline{U}) = \overline{U} \cdot \nabla\widetilde{\chi}. \tag{2.3}$$

Here, the source term is of compact support and mean-zero, and we can invert the Laplacian in 3D to conclude that the function P_c is smooth, and $\nabla^j P_c$ decays sufficiently fast as $O(|\xi|^{-j-2})$, ensuring $\overline{U} - U_{\mathrm{far}} = (1 - \widetilde{\chi})\overline{U} + \nabla P_c \in H^1$. Then we decompose $\widetilde{U}$ into two components:

$$\widetilde{U} = U_{\mathrm{near}} + U_{\mathrm{far}}. \tag{2.4}$$

By Proposition 1 and (1.16), we know $U \in H^1$, and thus $U_{\mathrm{near}} = \widetilde{U} - U_{\mathrm{far}} = U + \overline{U} - U_{\mathrm{far}} \in H^1$. Moreover, U_{far} has the same far field asymptotics as $\overline{U}$:

$$\nabla^j U_{\mathrm{far}}(\xi) = \nabla^j\Big(\frac{1}{|\xi|}A\Big(\frac{\xi}{|\xi|}\Big)\Big) + O(|\xi|^{-j-3}). \tag{2.5}$$

With this decomposition, we are ready to establish the smoothness and decay properties of $\widetilde{U}$.

Proposition 3 (Smoothness) *The solution $\widetilde{U}$ in Proposition 1 is smooth.*

Sketch of proof for Proposition 3. U_{far} is smooth, so we only need to show the smoothness of U_{near}. We defer the full proof to Appendix F and outline the main steps of coercive estimates here.

Near–far split and the equation for U_{near}. Plug the decomposition (2.4) into equation (1.12), we obtain an equation for U_{near} below in the distributional sense,

$$-\tfrac{1}{2}U_{\mathrm{near}} - \tfrac{1}{2}\,\xi \cdot \nabla U_{\mathrm{near}} + \Pi(\widetilde{U} \cdot \nabla\widetilde{U}) - \Delta U_{\mathrm{near}} = F, \quad \nabla \cdot U_{\mathrm{near}} = 0,$$

where we have the decay of F by the asymptotics (2.5) and leading order cancellation

$$F := \tfrac{1}{2}U_{\mathrm{far}} + \tfrac{1}{2}\,\xi \cdot \nabla U_{\mathrm{far}} + \Delta U_{\mathrm{far}}, \quad \nabla^k F(\xi) = O(|\xi|^{-3-k}) \ \ (k \geqslant 0).$$

Mollification and the commutator. Let ρ_ϵ be a standard mollifier and set

$$u^\epsilon = \rho_\epsilon * U_{\text{near}}, \quad F^\epsilon = \rho_\epsilon * F.$$

Then $u^\epsilon \in H^\infty$, $\nabla \cdot u^\epsilon = 0$, and we obtain

$$-\tfrac{1}{2}u^\epsilon - \tfrac{1}{2}\,\xi \cdot \nabla u^\epsilon - \tfrac{1}{2}\,[\rho_\epsilon *,\, \xi \cdot \nabla] U_{\text{near}} + \rho_\epsilon * \Pi(\widetilde{U} \cdot \nabla \widetilde{U}) - \Delta u^\epsilon = F^\epsilon,$$

with the explicit commutator

$$[\rho_\epsilon *,\, \xi \cdot \nabla] U_{\text{near}} = \rho_\epsilon * (\xi \cdot \nabla U_{\text{near}}) - \xi \cdot \nabla (\rho_\epsilon * U_{\text{near}}) = -\int_{\mathbb{R}^3} \rho_\epsilon(y)\, y \cdot \nabla U_{\text{near}}(\xi - y)\, dy,$$

and the bound

$$\|[\nabla^{k-1}\rho_\epsilon *,\, \xi \cdot \nabla] U_{\text{near}}\|_{L^2} \leqslant C\,\epsilon\, \|U_{\text{near}}\|_{H^k} \quad \text{for all } k \geqslant 1.$$

Energy at level k and coercivity of drift and diffusion. Apply ∇^k, take inner products with $\nabla^k u^\epsilon$, and integrate by parts (localizing by a large cutoff χ_R and letting $R \to \infty$ at the end). One obtains

$$\langle -\Delta \nabla^k u^\epsilon, \nabla^k u^\epsilon \rangle = \|\nabla^{k+1} u^\epsilon\|_{L^2}^2,$$

and, using $\nabla \cdot \xi = 3$, we get

$$\langle -\tfrac{1}{2}\,\xi \cdot \nabla \nabla^k u^\epsilon, \nabla^k u^\epsilon \rangle = \tfrac{1}{4}\langle \nabla \cdot \xi, |\nabla^k u^\epsilon|^2 \rangle = \tfrac{3}{4}\,\|\nabla^k u^\epsilon\|_{L^2}^2.$$

Nonlinearity. Recall $\widetilde{U} = U_{\text{far}} + U_{\text{near}}$. For $k \geqslant 2$, $H^k(\mathbb{R}^3)$ embeds into L^∞, and we get

$$\|\rho_\epsilon * \nabla^{k-1}\Pi(\widetilde{U} \cdot \nabla \widetilde{U})\|_{L^2} \leqslant \|\nabla^{k-1}\Pi(\widetilde{U} \cdot \nabla \widetilde{U})\|_{L^2} \leqslant C_k(1 + \|U_{\text{near}}\|_{H^k}^2),$$

since U_{far} is smooth with the decay (2.5). For $k = 1$ we use a commutator representation,

$$\|\rho_\epsilon * \nabla^{k-1}\Pi(\widetilde{U} \cdot \nabla \widetilde{U})\|_{L^2} \leqslant C_k(1 + \|U_{\text{near}}\|_{H^k}^2 + \|u^\epsilon\|_{L^\infty}\|U_{\text{near}}\|_{H^k}) \leqslant C_k(1 + \|U_{\text{near}}\|_{H^k}^2 + \|u^\epsilon\|_{H^{k+1}}^{3/4}\|U_{\text{near}}\|_{H^k}^{5/4}).$$

The forcing term satisfies $\|\nabla^k F^\epsilon\|_{L^2} \leqslant C_k$.

Bootstrap. Collecting the previous bounds and treating $\|U_{\text{near}}\|_{H^k}$ as a constant render the bound

$$\|\nabla^{k+1} u^\epsilon\|_{L^2}^2 \leqslant C_k(1 + \|\nabla^{k+1} u^\epsilon\|_{L^2}^{7/4}),$$

with a constant independent of ϵ. We have a uniform bound on $\|u^\epsilon\|_{H^{k+1}}$ and letting $\epsilon \to 0$ yields $U_{\text{near}} \in H^{k+1}$. Starting from H^1 and iterating proves $U_{\text{near}} \in H^\infty$.

In particular, along with the decay of U_{far} (2.5), we get that

$$\widetilde{U} \in L^4 \cap L^\infty. \tag{2.6}$$

Proposition 4 (Far field asymptotics) *The solution $\widetilde{U}$ in Proposition 1 satisfies the boundary condition* (1.7) *with the same A as that associated with $\overline{U}$ in Assumption 1.*

Sketch of Proof for Proposition 4. Since U_{far} satisfies the desirable far field condition (2.5), we only need to establish U_{near} has decay $O(|\xi|^{-3/2})$ in the far field. We will establish that $|\xi|U_{\text{near}}, |\xi|^2\nabla^2 U_{\text{near}} \in L^2$, and use a dyadic Sobolev embedding to conclude the far field decay. We defer the full proof to Appendix F and outline the weighted estimates and dyadic rescaling.

Weighted L^2 at level 0. Let χ_R be a standard cutoff function with radius R, for example $1 - \widetilde{\chi}(\xi/R)$. Define the cutoff version of the radial weight $|\xi|^2$ as ϕ_L by:

$$\phi_L(\xi) := \phi\left(|\xi|/L\right), \qquad \phi(r) = r^2 \ (0 \leqslant r \leqslant 1), \quad \phi(r) = 4 \ (r \geqslant 2),$$

where ϕ is increasing and smooth. Test the near-field equation against $\chi_R\,\phi_L\,U_{\mathrm{near}}$, integrate by parts, and let $R\to\infty$. For the drift, we have

$$\langle -\frac{1}{2}\xi\cdot\nabla U_{\mathrm{near}},\phi_L U_{\mathrm{near}}\rangle=\frac{3}{4}\langle U_{\mathrm{near}},\phi_L U_{\mathrm{near}}\rangle+\frac{1}{4}\langle U_{\mathrm{near}},\xi\cdot\nabla\phi_L U_{\mathrm{near}}\rangle\geqslant\frac{3}{4}\langle U_{\mathrm{near}},\phi_L U_{\mathrm{near}}\rangle,$$

since ϕ_L is radially increasing. For the diffusion, we have

$$\langle -\Delta U_{\mathrm{near}},\phi_L U_{\mathrm{near}}\rangle=\langle\nabla U_{\mathrm{near}},\phi_L\nabla U_{\mathrm{near}}\rangle-\frac{1}{2}\langle U_{\mathrm{near}},\Delta\phi_L U_{\mathrm{near}}\rangle,$$

with $\Delta\phi_L$ uniformly bounded in L. For the nonlinear term, we split

$$|\langle\widetilde{U}\cdot\nabla\widetilde{U},\phi_L U_{\mathrm{near}}\rangle|=|\langle\widetilde{U}\cdot\nabla U_{\mathrm{far}},\phi_L U_{\mathrm{near}}\rangle-\frac{1}{2}\langle\widetilde{U}\cdot\nabla\phi_L,|U_{\mathrm{near}}|^2\rangle|\lesssim\sqrt{\langle U_{\mathrm{near}},\phi_L U_{\mathrm{near}}\rangle},$$

where we use the fact by (2.5) and (2.6) that $|\xi|\nabla U_{\mathrm{far}},\widetilde{U}\in L^4\cap L^\infty$, and the uniform bounds on derivatives of ϕ_L. For the pressure, we use the Riesz transform to represent $\Delta P=-\partial_i\partial_j(\widetilde{U}_i\widetilde{U}_j)$ and the Calderón–Zygmund theory gives $\|P\|_{L^2}\lesssim\|\widetilde{U}\|_{L^4}^2\lesssim 1$, hence we obtain

$$|\langle\nabla P,\,\phi_L U_{\mathrm{near}}\rangle|=|\langle P,\,\nabla\phi_L\cdot U_{\mathrm{near}}\rangle|\lesssim\sqrt{\langle U_{\mathrm{near}},\phi_L U_{\mathrm{near}}\rangle},$$

where we have used the fact that $|\nabla\phi_L|^2\lesssim\phi_L$. The forcing term has the same bound by the decay of F. Collecting the estimates yields a uniform bound on $\langle U_{\mathrm{near}},\phi_L U_{\mathrm{near}}\rangle+\langle\nabla U_{\mathrm{near}},\phi_L\nabla U_{\mathrm{near}}\rangle$, and we can take the limit $L\to\infty$ to conclude

$$|\xi|U_{\mathrm{near}}\in L^2,\qquad |\xi|\nabla U_{\mathrm{near}}\in L^2.$$

Weighted L^2 after one derivative. Differentiate the equation, test against $\chi_R\,\phi_L\,|\xi|^\alpha\,\nabla U_{\mathrm{near}}$ with $\alpha=0$ and $\alpha=2$, and repeat the previous bounds (now also using that $|\xi|^\alpha$ is an admissible weight for the pressure estimate). One obtains, after letting $R\to\infty$ and then $L\to\infty$,

$$|\xi|\,\nabla^2 U_{\mathrm{near}}\in L^2\quad\text{and}\quad |\xi|^2\nabla U_{\mathrm{near}},\ |\xi|^2\nabla^2 U_{\mathrm{near}}\in L^2.$$

Dyadic rescaling and decay. Fix $R>1$ and the annulus $A_R=\{\xi\in\mathbb{R}^3:\ R<|\xi|<2R\}$. Define $v(y):=U_{\mathrm{near}}(Ry)$ on $A_1=\{y:\ 1<|y|<2\}$. The local Sobolev embedding $H^2(A_1)\subset L^\infty(A_1)$ implies

$$\|U_{\mathrm{near}}\|_{L^\infty(A_R)}=\|v\|_{L^\infty(A_1)}\leqslant C\sum_{k=0}^{2}\|\nabla_y^k v\|_{L^2(A_1)}=C\sum_{k=0}^{2}R^{k-\frac{3}{2}}\|\nabla^k U_{\mathrm{near}}\|_{L^2(A_R)}.$$

Since $|\xi|\sim R$ on A_R and the global weighted bounds imply $\|\nabla^k U_{\mathrm{near}}\|_{L^2(A_R)}\leqslant CR^{-k}$ for $k=0,1,2$, we conclude

$$\|U_{\mathrm{near}}\|_{L^\infty(A_R)}\leqslant C\,R^{-3/2},$$

that is, $U_{\mathrm{near}}(\xi)=O(|\xi|^{-3/2})$ as $|\xi|\to\infty$, the desired decay.

Now we have established that $\widetilde{U}$ indeed induces a self-similar Leray–Hopf solution.

2.2 Nonuniqueness of Leray–Hopf solutions

Proof [Proof of Theorem 1]Let $\widetilde{u}$ be the self-similar solution corresponding to the profile $\widetilde{U}$ in Theorem 2. Recall that due to the slow decay of the scale-invariant initial data u_{in}, $\widetilde{u}$ is not a Leray-Hopf solution. Therefore, we introduce a suitable cutoff function u^{cut} and consider the following ansatz $u=\widetilde{u}+u^{\mathrm{cut}}+u^{\mathrm{cor}}$ to the Navier–Stokes equation (1.1), where u^{cor} is the correction to be constructed that renders non-unique solutions. We adopt the change of variables between physical coordinates (x,t) and self-similar coordinates (ξ,τ):

$$\widetilde{u}(x,t)=\frac{1}{\sqrt{t}}\widetilde{U}(\frac{x}{\sqrt{t}}),\quad u^{\mathrm{cut}}(x,t)=\frac{1}{\sqrt{t}}U^{\mathrm{cut}}(\frac{x}{\sqrt{t}},\log t),\quad u^{\mathrm{cor}}(x,t)=\frac{1}{\sqrt{t}}U^{\mathrm{cor}}(\frac{x}{\sqrt{t}},\log t).\qquad(2.7)$$

Please note that $u = \widetilde{u} + u^{\mathrm{cut}} + u^{\mathrm{cor}}$ is the Leray-Hopf solution that we construct in this subsection. It does not correspond to the correction U that we used in (1.16) to adjust $\overline{U}$; consequently, u does not satisfy the relation $u(t,x) = \frac{1}{\sqrt{t}} U(\frac{x}{\sqrt{t}}, \log t)$ with that U. We will first construct the cutoff function, as in [32]. Then we demonstrate that different choices of $u^{\mathrm{cor}}(\cdot, 1)$ correspond to different solutions in the rescaled time interval $\tau \in (-\infty, 0]$, as in [1] and [32]. Here, it is crucial to treat the stable and unstable parts separately via the Riesz projection, as in [32]; see also [12, 11].

Construction of cutoff. As in [32], via the Bogovskii operator, one can construct a decomposition of the initial condition $u_{\mathrm{in}} = u_{\mathrm{loc}} + w$ such that u_{loc} is compactly supported, divergence free, $w(x) = 0$ for $|x| < R$ and $\|w\|_{L^p} \lesssim R^{-(p-3)/p}$ based on the decay of u_{in}, for any $p > 3$. We will choose u_{loc} of compact support as the modified initial data for our Leray–Hopf solution u.

Now we define our cutoff function as

$$u^{\mathrm{cut}} = -e^{t\Delta} w,$$

where $e^{t\Delta}$ is the standard notation for the heat semigroup. Recall the standard smoothing estimate:

$$\|\nabla_x^k e^{t\Delta} f\|_{L^r} \lesssim t^{-\frac{k}{2}} t^{-\frac{3}{2}(\frac{1}{p} - \frac{1}{r})} \|f\|_{L^p}, \quad 1 \leqslant p \leqslant r \leqslant \infty. \tag{2.8}$$

By the similarity transform, we have the identities

$$\nabla_\xi^k U^{\mathrm{cut}}(\xi, \tau) = t^{\frac{k}{2} + \frac{1}{2}} (\nabla_x^k u^{\mathrm{cut}})(x,t)\Big|_{x = \sqrt{t}\xi}, \quad \|g(\sqrt{t}\,\cdot)\|_{L^r} = t^{-\frac{3}{2r}} \|g\|_{L^r}. \tag{2.9}$$

Combining (2.9), (2.8), and the bound on the p-norm of w, we conclude the estimate

$$\|U^{\mathrm{cut}}\|_{W^{k,r}} \lesssim t^{\frac{1}{2} - \frac{3}{2p}} \|w\|_{L^p} \lesssim (\frac{e^{\frac{\tau}{2}}}{R})^{(1 - \frac{3}{p})}. \tag{2.10}$$

We fix $p = 4$ from now on. The constants in the inequalities are independent of R and τ.

Duhamel setup. We will find solutions u^{cor} to the following perturbative equation to (1.1)

$$\partial_t u^{\mathrm{cor}} - \Delta u^{\mathrm{cor}} + \Pi(u \cdot \nabla u - \widetilde{u} \cdot \nabla \widetilde{u}) = 0, \quad \operatorname{div} u^{\mathrm{cor}} = 0,$$

with $u^{\mathrm{cor}} \to 0$ in L^2 as $t \to 0$ so that $u = \widetilde{u} + u^{\mathrm{cut}} + u^{\mathrm{cor}}$ will be a solution to the Navier–Stokes equation in L^2 with initial data $u_{\mathrm{in}} - w = u_{\mathrm{loc}}$. In similarity coordinates, the equation for U^{cor} reads

$$\partial_\tau U^{\mathrm{cor}} = \mathcal{L}_{\widetilde{U}} U^{\mathrm{cor}} + \mathcal{L}_{\mathrm{far}} U^{\mathrm{cor}} + F + N(U^{\mathrm{cor}}, U^{\mathrm{cor}}), \tag{2.11}$$

where we use the definition of $\mathcal{L}_{\widetilde{U}}$ in (1.9) and define the linear, quadratic, and residue terms as

$$\mathcal{L}_{\mathrm{far}} f := -\Pi(U^{\mathrm{cut}} \cdot \nabla f + f \cdot \nabla U^{\mathrm{cut}}), \quad N(f,g) := -\Pi(f \cdot \nabla g), \quad F := -\Pi(U^{\mathrm{cut}} \cdot \nabla U^{\mathrm{cut}} + \widetilde{U} \cdot \nabla U^{\mathrm{cut}} + U^{\mathrm{cut}} \cdot \nabla \widetilde{U}).$$

The Duhamel mapping, of which we want to show U^{cor} is a fixed point, reads

$$\mathcal{T}(U)(\cdot, \tau) := \int_{-\infty}^{\tau} e^{(\tau - s)\mathcal{L}_{\widetilde{U}}} (\mathcal{L}_{\mathrm{far}} U(\cdot, s) + F(\cdot, s) + N(U(\cdot, s), U(\cdot, s))) ds. \tag{2.12}$$

By (2.10), the fact that H^2 is an algebra, namely,

$$\|fg\|_{H^2} \lesssim \|f\|_{H^2} \|g\|_{H^2},$$

together with the fact that $U^{\mathrm{cut}}, \widetilde{U}$ are in $W^{\infty,4}$, we have

$$\|\mathcal{L}_{\mathrm{far}} f(\cdot, s)\|_{H^2} \lesssim (\frac{e^{\frac{s}{2}}}{R})^{(1 - \frac{3}{p})} \|f\|_{H^3}, \quad \|N(f,g)\|_{H^2} \lesssim \|f\|_{H^3} \|g\|_{H^3}, \quad \|F(\cdot, s)\|_{H^2} \lesssim (\frac{e^{\frac{s}{2}}}{R})^{(1 - \frac{3}{p})}. \tag{2.13}$$

Decomposition via Riesz projection. From Section 4.1 of [1], we know that for the operators defined on $L^2_\sigma \to L^2_\sigma$, $\mathcal{L}_{\widetilde{U}} - \mathcal{L}_0$ is a compact perturbation of $\mathcal{L}_0$, and thus $\mathcal{L}_{\widetilde{U}}$ has the same essential spectrum as $\mathcal{L}_0$, contained in the half-plane $\Re(\lambda) \leqslant -\frac{1}{4}$. Here we have used the same notation $\mathcal{L}_0 := \mathcal{L}_{\widetilde{U}}\big|_{\widetilde{U}\equiv 0}$ as in [1, 32]. The other spectral values are finite sets of eigenvalues with finite ranks.

We proceed as in the proof of Theorem 4.1 in [32] to decompose into stable and unstable subspaces $L^2_\sigma = X_s \oplus_j X_j$ via the Riesz projection $P_{\lambda_j} : L^2_\sigma \to X_j$. For every eigenvalue λ_j with a positive real part, we define $P_{\lambda_j} = \frac{1}{2\pi i}\int_{\Gamma_j}(\lambda - \mathcal{L}_{\widetilde{U}})^{-1}d\lambda$, where Γ_j is a suitable contour containing λ_j but no other spectral values. Here, each X_j is finite dimensional, and we define $P_s = I - \sum_j P_{\lambda_j}$. Finally, we denote $A_j = \mathcal{L}_{\widetilde{U}}|_{X_j}$ and $A_s = \mathcal{L}_{\widetilde{U}}|_{X_s}$. Using Jordan block computation, we have the following estimates for any $\delta > 0$ by [24]:

$$\begin{aligned} &e^{\Re(\lambda_j)\tau - \delta|\tau|}\|f\|_{L^2} \lesssim \|e^{\tau A_j} f\|_{L^2} \lesssim e^{\Re(\lambda_j)\tau + \delta|\tau|}\|f\|_{L^2}, \quad \forall f \in X_j, \forall \tau, \\ &\|e^{\tau A_s} f\|_{L^2} \lesssim e^{\delta\tau}\|f\|_{L^2}, \quad \forall f \in X_s, \tau > 0, \end{aligned} \tag{2.14}$$

since A_s has a growth bound equal to the maximum of its spectral bound and its essential spectrum (Lemma 4.2 of [1]), which is non-positive. We rewrite (2.12) as

$$\begin{aligned} \mathcal{T}(U)_s(\cdot,\tau) &:= \int_{-\infty}^{\tau} e^{(\tau-s)A_s} P_s(\mathcal{L}_{\text{far}}U + F + N(U,U))ds, \\ \mathcal{T}(U)_j(\cdot,\tau) &:= e^{\tau A_j}U_{j0} - \int_{\tau}^{0} e^{(\tau-s)A_j} P_j(\mathcal{L}_{\text{far}}U + F + N(U,U))ds, \end{aligned} \tag{2.15}$$

and we need to show the existence of fixed points $\mathcal{T}(U)_s = P_s U$, $\mathcal{T}(U)_j = P_j U$, for appropriately chosen $U_{j0} = P_j U(\cdot,0) \in X_j$. We remark that by Theorem 2, we have at least one unstable eigenmode with eigenvalue λ_j. The Riesz projections are moreover bounded since they are of finite rank.

Smoothing estimates of A_s. With the growth bound (2.14), we obtain the smoothing estimate as in Lemma 4.4 of [1]: for any $\delta > 0$, $\sigma_2 \geqslant \sigma_1 \geqslant 0$, there exists a constant depending on $\delta, \sigma_2, \sigma_1$ only, such that for any $f_s \in X_s \cap H^{\sigma_1}$ and $\tau > 0$, we have

$$\|e^{\tau A_s} f_s\|_{H^{\sigma_2}} \lesssim \tau^{-(\sigma_2-\sigma_1)/2} e^{\delta\tau}\|f_s\|_{H^{\sigma_1}}, \tag{2.16}$$

whose proof essentially combines the L^2 growth bound with a gain of regularity for the short time, as in Step 1 in the proof of Lemma 4.4 in [1]. Compact support of $\widetilde{U}$ is not essential for the proof therein, as only its boundedness in C^k norms is used in the standard estimates of energy dissipation along with a gain of regularity by the heat kernel, relating back to the equation in physical time.

Every finite-dimensional unstable eigenspace X_j is the kernel of $(A_j - \lambda_j)^{k_j}$ for some finite k_j. Thus it is spanned by basis functions $\{f_{j,k}\}$, where every $f_{j,k}$ satisfies

$$(A_j - \lambda_j)^{k_j} f_{j,k} = 0.$$

Similarly, we have a smoothing estimate for A_j, so the basis functions $f_{j,k}$ are smooth.

Contraction mapping. We recall $p = 4$ and fix $\delta = \frac{1}{2}\min\{\frac{p-3}{2p}, \min_j \Re(\lambda_j)\} > 0$. Consider the norm $\|U\|_X := \sup_{\tau<0} R^{\frac{p-3}{2p}} e^{-\delta\tau}\|U(\cdot,\tau)\|_{H^3}$. We will show that there exists a sufficiently large R such that the Duhamel mapping $\mathcal{T}$ in (2.15) induces a contraction on the unit ball of X.

Thanks to the integral computation for $\delta_1 > \delta$ that

$$\int_{-\infty}^{\tau}(\tau-s)^{-1/2}e^{\delta(\tau-s)}e^{\delta_1 s}ds \leqslant e^{\delta\tau}\Big(\int_{-\infty}^{\tau-1} e^{(\delta_1-\delta)s}ds + \int_{\tau-1}^{\tau}(\tau-s)^{-1/2}ds\Big) \lesssim e^{\delta\tau},$$

by (2.15), (2.16), and (2.13), we have for $\tau<0$,

$$\begin{aligned}\|\mathcal{T}(U)_s(\cdot,\tau)\|_{H^3} &\lesssim \int_{-\infty}^{\tau}(\tau-s)^{-1/2}e^{\delta(\tau-s)}((\frac{e^{\frac{s}{2}}}{R})^{(1-\frac{3}{p})}(1+\|U(\cdot,s)\|_{H^3})+\|U(\cdot,s)\|_{H^3}^2)ds\\ &\lesssim e^{\delta\tau}R^{-1+\frac{3}{p}}(1+\|U\|_X+\|U\|_X^2),\\ \|\mathcal{T}(U)_s(\cdot,\tau)-\mathcal{T}(V)_s(\cdot,\tau)\|_{H^3} &\lesssim \int_{-\infty}^{\tau}(\tau-s)^{-1/2}e^{\delta(\tau-s)}((\frac{e^{\frac{s}{2}}}{R})^{(1-\frac{3}{p})}+\|U\|_{H^3}+\|V\|_{H^3})\|U-V\|_{H^3}ds\\ &\lesssim e^{\delta\tau}R^{-1+\frac{3}{p}}(1+\|U\|_X+\|V\|_X)\|U-V\|_X.\end{aligned} \tag{2.17}$$

Multiplying $R^{\frac{p-3}{2p}}e^{-\delta\tau}$ to (2.17), and taking $\sup_{\tau<0}$ give

$$\|\mathcal{T}(U)_s\|_X\lesssim R^{-\frac{p-3}{2p}}\big(1+\|U\|_X+\|U\|_X^2\big),\quad \|\mathcal{T}(U)_s-\mathcal{T}(V)_s\|_X\lesssim R^{-\frac{p-3}{2p}}\big(1+\|U\|_X+\|V\|_X\big)\|U-V\|_X. \tag{2.18}$$

Thus, the stable part of $\mathcal{T}$ is a strict contraction on the unit ball of X for R sufficiently large.

Since $U_{j0}\in X_j$ are smooth, using (2.14), for $\tau<0$, we have similarly that

$$\begin{aligned}\|\mathcal{T}(U)_j(\cdot,\tau)\|_{H^3} &\lesssim e^{(\Re(\lambda_j)-\delta)\tau}\|U_{j0}\|_{H^3}+\int_{\tau}^{0}e^{(\Re(\lambda_j)-\delta)(\tau-s)}((\frac{e^{\frac{s}{2}}}{R})^{(1-\frac{3}{p})}(1+\|U\|_{H^3})+\|U\|_{H^3}^2)ds\\ &\lesssim e^{\delta\tau}\|U_{j0}\|_{H^3}+e^{\delta\tau}R^{-1+\frac{3}{p}}(1+\|U\|_X+\|U\|_X^2),\\ \|\mathcal{T}(U)_j(\cdot,\tau)-\mathcal{T}(V)_j(\cdot,\tau)\|_{H^3} &\lesssim \int_{\tau}^{0}e^{(\Re(\lambda_j)-\delta)(\tau-s)}((\frac{e^{\frac{s}{2}}}{R})^{(1-\frac{3}{p})}+\|U\|_{H^3}+\|V\|_{H^3})\|U-V\|_{H^3}ds\\ &\lesssim e^{\delta\tau}R^{-1+\frac{3}{p}}(1+\|U\|_X+\|V\|_X)\|U-V\|_X.\end{aligned}$$

Similarly, by multiplying $R^{\frac{p-3}{2p}}e^{-\delta\tau}$ to the above inequalities and taking $\sup_{\tau<0}$ give

$$\|\mathcal{T}(U)_j\|_X\lesssim R^{\frac{p-3}{2p}}\|U_{j0}\|_{H^3}+R^{-\frac{p-3}{2p}}(1+\|U\|_X+\|U\|_X^2), \tag{2.19}$$

$$\|\mathcal{T}(U)_j-\mathcal{T}(V)_j\|_X\lesssim R^{-\frac{p-3}{2p}}(1+\|U\|_X+\|V\|_X)\|U-V\|_X. \tag{2.20}$$

Denote $\alpha:=1-\frac{3}{p}=\frac{1}{4}$. For a small $\eta\in(0,1)$, consider the nonempty admissible set of the unit ball of X with fixed unstable projections at $\tau=0$:

$$\mathcal{D}_{R,\eta,U_{j0}}:=\Big\{\|U\|_X\leqslant 1:\ P_jU(\cdot,0)=U_{j0}\quad\forall j\Big\},$$

where $\sum_j R^{\alpha/2}\|U_{j0}\|_{H^3}\leqslant\eta$. Let C denote the maximal absolute constant in the inequalities (2.18), (2.19), and (2.20). Choose R so large that $C\sum_j R^{-\alpha/2}\leqslant\frac{1}{12}$, and then choose $\eta>0$ small enough so that $C\eta\leqslant\frac{1}{4}$. For any $U\in\mathcal{D}_{R,\eta,U_{j0}}$, we get by (2.18) and (2.19) that

$$\|\mathcal{T}(U)\|_X\ \leqslant\ CR^{\alpha/2}\sum_j\|U_{j0}\|_{H^3}+2C\sum_j R^{-\alpha/2}\big(1+\|U\|_X+\|U\|_X^2\big)\leqslant\tfrac{1}{4}+\tfrac{1}{2}<1,$$

and hence we have $\mathcal{T}(\mathcal{D}_{R,\eta,U_{j0}})\subset\mathcal{D}_{R,\eta,U_{j0}}$. Moreover, we obtain by (2.18) and (2.20) that

$$\|\mathcal{T}(U)-\mathcal{T}(V)\|_X\leqslant 2C\sum_j R^{-\alpha/2}\big(1+\|U\|_X+\|V\|_X\big)\|U-V\|_X\leqslant\tfrac{1}{2}\|U-V\|_X.$$

Thus $\mathcal{T}$ is a strict contraction on $\mathcal{D}_{R,\eta,U_{j0}}$. Hence, we conclude, via the Banach fixed point theorem, a solution to (2.12) and thus (2.11) for any small enough admissible U_{j0}, which contains infinitely many distinct solutions $U^{\rm cor}$, different by their projections at time $\tau=0$, i.e. $t=1$.

Conclusion of the proof. We compute by the scaling invariance of the heat semigroup

$$\widetilde{u}(x) + u^{\mathrm{cut}}(x) = \widetilde{u}(x) - e^{t\Delta}u^{\mathrm{in}}(x) + e^{t\Delta}u_{\mathrm{loc}}(x) = t^{-\frac{1}{2}}(\widetilde{U} - e^{\Delta}u^{\mathrm{in}})(\xi) + e^{t\Delta}u_{\mathrm{loc}}.$$

The decay estimate [31] implies $\widetilde{U} - e^{\Delta}u^{\mathrm{in}} \in L^q$ for any $q > 1$. u_{loc} is of compact support with $1/|x|$ at the origin, so it is in $L^{3-\epsilon}$ for any $\epsilon > 0$. Combined with the heat smoothing estimate (2.8) and the scaling (2.9), we get for $t \leqslant 1$, for constants independent of t, we have

$$\|\widetilde{u}(x) + u^{\mathrm{cut}}(x)\|_{L^q} \lesssim t^{\frac{3}{2q} - \frac{1}{2(1-\epsilon/3)}} + 1, \quad \limsup_{t\to 0} \|\widetilde{u}(x) + u^{\mathrm{cut}}(x) - u_{\mathrm{loc}}(x)\|_{L^2} \to 0. \tag{2.21}$$

Finally, $\|u^{\mathrm{cor}}\|_{L^2} = t^{1/4}\|U^{\mathrm{cor}}\|_{L^2} \to 0$ as $t \to 0$ so that $u \in L^\infty L^2$. Similarly, $\|\nabla u\|_{L^2} = t^{-1/4}\|\nabla U\|_{L^2}$ so that the H^1-norm of u is bounded by $t^{-1/4}$. Thus $u \in L^2H^1$, and we conclude the constructed $u = \widetilde{u} + u^{\mathrm{cut}} + u^{\mathrm{cor}}$ are infinitely many Leray–Hopf solutions with the same L^2 initial data u_{loc}. Similar to [1], we can establish their smoothness for positive times via the Duhamel representation. To be precise, we can bootstrap from $\sup_{\tau<0} e^{-\delta\tau}\|U^{\mathrm{per}}(\cdot,\tau)\|_{H^N} < \infty$ to $\sup_{\tau<0} e^{-\delta\tau}\|U^{\mathrm{per}}(\cdot,\tau)\|_{H^{N+1/2}} < \infty$ via the smoothing estimates (2.15), (2.16), and (2.13), similar to the estimate in (2.17). Their smoothness implies that they are moreover suitable and (1.2) holds with equality, as in [1].

By (2.21), the scaling (2.9), and $U^{\mathrm{cor}} \in H^3 \subset L^q$, we compute for $q \geqslant 2$,

$$\|u\|_{L^q} \leqslant \|u^{\mathrm{cut}} + \widetilde{u}\|_{L^q} + \|u^{\mathrm{cor}}\|_{L^q} \lesssim t^{\frac{3}{2q} - \frac{1}{2(1-\epsilon/3)}} + 1 + t^{\frac{3}{2q} - \frac{1}{2}} \lesssim t^{\frac{3}{2q} - \frac{1}{2(1-\epsilon/3)}} + 1.$$

Choosing $\epsilon > 0$ sufficiently small, we conclude the L^sL^q boundedness and the proof of Theorem 1. □

Remark 3 Our choice of localization is propagated in time via the heat smoothing. It would be interesting to explore an alternative approach based on a static spatial cutoff and direct estimates of the boundary terms generated by the cutoff. In particular, one may hope to combine such an approach with inner–outer gluing ideas used by Albritton–Brue–Colombo [2], to investigate whether an analogue of Theorem 1 could hold on smooth bounded domains (or the torus), e.g. under no-slip boundary conditions, at comparable levels of regularity. A natural starting point, similar to [2], would be to consider an ansatz of the form

$$u = \eta(\tilde{u} + u^{\mathrm{cor}}) + \psi,$$

where η is a cutoff, ψ corrects boundary/cutoff errors, and u^{cor} is intended to capture the nonuniqueness mechanism associated with unstable directions. Again, it is essential to run backward for the unstable directions, so that no assumption on the smallness of positive eigenvalues is needed for the cutoff terms. Another difficulty is that the correction fields u^{cor} and ψ are expected to satisfy a coupled system whose analysis appears more delicate in bounded geometries. We do not pursue these questions here and leave them for future work.

3 A Framework for Numerical Analysis

In this section, we introduce a framework for *a posteriori* numerical analysis. Consider a general nonlinear partial differential equation of the form:

$$J(\widetilde{w}) = 0. \tag{3.1}$$

Suppose we have an approximate solution $\overline{w}$, which satisfies

$$J(\overline{w}) = \mathrm{E},$$

where the residual E is small in a sense to be clarified later. Our goal is to find an exact solution $\widetilde{w} = \overline{w} + w$ that is close to $\overline{w}$ and satisfies

$$J(\overline{w} + w) = 0,$$

where w represents the error between the exact and approximate solutions.

We expand the equation in terms of the linearized operator L and the nonlinear part N as

$$Lw + N(w) + \mathrm{E} = 0. \tag{3.2}$$

If we can solve (3.2) for some w, then $\widetilde{w} = \overline{w} + w$ solves the original equation (3.1). Since w is small, the nonlinear term $N(w)$ should be negligible and (3.2) is almost linear. Therefore, the invertibility of the linear operator L essentially determines the well-posedness of the equation (3.2), and we can use a fixed-point argument to conclude the existence of a solution.

In this section, we will develop a framework of computer-assisted proof for the existence of solutions to equation (3.2), making the above heuristics rigorous. We will first introduce a simplified example of a nonlinear Poisson equation to illustrate and motivate our method in Section 3.1, followed by a general result in Section 3.2, when L is not exactly invertible but can be decomposed into a coercive part plus a compact part. We remark that instead of invoking the Banach fixed-point theorem via the proof of a contraction mapping, we will use the Schauder fixed-point theorem since our fixed-point map can be shown to have a gain of regularity. We spend more effort on compactness arguments for analysis, so that the computer-assisted proofs will be easier and to the minimal extent possible.

3.1 Toy model: nonlinear Poisson equation

We illustrate our framework with a simple toy model: the nonlinear Poisson equation on $D = [0,1]^3$:

$$\begin{cases} -\Delta\widetilde{w} + \widetilde{w}^2 = f, & \text{in } D, \\ \widetilde{w} = 0, & \text{on } \partial D. \end{cases}$$

In general, we do not know the existence of the solution. Suppose we have a bounded numerical solution $\overline{w}$ satisfying

$$\begin{cases} -\Delta\overline{w} + \overline{w}^2 = f + \mathrm{E}_w, & \text{in } D, \\ \overline{w} = 0, & \text{on } \partial D, \end{cases}$$

where E_w stands for the residual. If an exact solution exists, the error $w = \widetilde{w} - \overline{w}$ should satisfy

$$\begin{cases} -\Delta w + 2\overline{w}w + w^2 = -\mathrm{E}_w, & \text{in } D, \\ w = 0, & \text{on } \partial D. \end{cases} \tag{3.3}$$

In this formulation, we identify the linear and nonlinear components as:

$$Lw := -\Delta w + 2\overline{w}w, \quad N(w) := w^2.$$

We now analyze two cases. In the first case, we assume L is invertible and use a fixed-point argument to construct the solution. In the second case, where the invertibility of L is unknown, we will use a finite-rank perturbation to approximate the compact part and verify numerically the invertibility of L on the image of the finite-rank perturbation. In this subsection, since all of the norms and inner products are defined on D, we will omit the D dependence.

3.1.1 Simple case: $\overline{w} \geqslant 0$

First, we consider a simple case where $\overline{w} \geqslant 0$ and L is thus coercive. Specifically, we have

$$\langle Lw, w\rangle = \|\nabla w\|_{L^2}^2 + \langle 2\overline{w}, w^2\rangle \geqslant \|\nabla w\|_{L^2}^2.$$

Hence, by the Lax-Milgram theorem, L is invertible in $H_0^1(D)$. Now we define a fixed-point map $w^* = T(w)$ by solving in $H_0^1(D)$

$$Lw^* = -\mathrm{E}_w - N(w).$$

The solution w^* exists and satisfies

$$\|\nabla w^*\|_{L^2}^2 \leqslant \langle Lw^*, w^*\rangle \leqslant |\langle \mathrm{E}_w, w^*\rangle| + |\langle w^2, w^*\rangle|.$$

By Holder's inequality with multiple functions and Sobolev embedding, we have

$$\|\nabla w^*\|_{L^2}^2 \leqslant \|\mathrm{E}_w\|_{L^2}\|w^*\|_{L^2} + \|w\|_{L^3}^2\|w^*\|_{L^3} \lesssim (\|\mathrm{E}_w\|_{L^2} + \|\nabla w\|_{L^2}^2)\|\nabla w^*\|_{L^2},$$

where we have used the Poincaré inequality $\|w^*\|_{L^2} \lesssim \|\nabla w^*\|_{L^2}$ since w^* vanishes on ∂D.

Assume that the residual is small, i.e.,

$$\|\mathrm{E}_w\|_{L^2} \leqslant \varepsilon_w \ll 1.$$

Then the following estimate holds for w^*:

$$\|\nabla w^*\|_{L^2} \leqslant C(\varepsilon_w + \|\nabla w\|_{L^2}^2).$$

If ε_w is sufficiently small, we can choose a small radius r such that

$$C(\varepsilon_w + r^2) \leqslant r.$$

This implies the map T sends the ball

$$B_r := \{w \in H_0^1(D) : \|\nabla w\|_{L^2} \leqslant r\}$$

to itself. Next, we prove that T is continuous in a weaker topology. Let $w^* = T(w)$, $\widehat{w}^* = T(\widehat{w})$, for $w, \widehat{w} \in B_r$. Then we get

$$L(w^* - \widehat{w}^*) = w^2 - \widehat{w}^2 = (w - \widehat{w})(w + \widehat{w}),$$

and similarly, using coercivity and Sobolev embedding, we have

$$\|w^* - \widehat{w}^*\|_{L^3} \lesssim \|\nabla(w^* - \widehat{w}^*)\|_{L^2} \lesssim (\|\nabla w\|_{L^2} + \|\nabla \widehat{w}\|_{L^2})\|w - \widehat{w}\|_{L^3} \lesssim r\|w - \widehat{w}\|_{L^3}.$$

We know that T is continuous in L^3-norm on B_r. Since the bounded ball in H^1 is compact in L^3, by the Schauder fixed-point theorem, a solution to the equation (3.3) exists.

3.1.2 Difficult case: $\overline{w} \leqslant 0$

Next, we consider a more difficult case, where $\overline{w} \leqslant 0$. As before, we aim to establish the existence of a solution to equation (3.3). However, the operator L is no longer coercive, and directly proving its invertibility is challenging. To address this, we observe that the operator can be decomposed as $L = L_1 + L_2$, where $L_1 w := -\Delta w$ is coercive and $L_2 w := 2\overline{w}w$ is a compact perturbation.

Following the strategy in [13], we leverage computer-assisted methods to avoid directly verifying the invertibility of L. Specifically, we decompose w into $w = w_1 + w_2$ with:

$$\begin{aligned} -\Delta w_1 &= -\mathrm{E}_w - (w_1 + w_2)^2, \\ -\Delta w_2 + L_2 w_2 &= -L_2 w_1. \end{aligned}$$

Summing up the two equations implies (3.3). The key observation is that $w_2 = -L^{-1}L_2 w_1$. If L_2 were of of finite-rank instead, we would only need to verify the invertibility of L on a finite-dimensional space, which can be done numerically.

In our case, however, $L_2 = 2\overline{w}$ is compact but not of finite rank. To circumvent this, we approximate w_2 using a finite-rank operator. That is, we modify the system to:

$$-\Delta w_1 + L_{\text{res}} w_1 = -\mathrm{E}_w - (w_1 + w_2)^2, \tag{3.4}$$

$$-\Delta w_2 + L_2 w_2 = -L_{\text{ap}} w_1. \tag{3.5}$$

Here, L_{ap} is a finite rank approximation of L_2, and the residual $L_{\text{res}} := L_2 - L_{\text{ap}}$ is small and can be absorbed by the coercivity of L_1. Therefore, the modified linear part of equation (3.4), namely $-\Delta w_1 + L_{\text{res}} w_1$, remains coercive, enabling a fixed-point argument for the existence of w_1.

Now we show how to construct L_{ap}. To begin with, we choose an interpolation operator I_n with a finite rank n to approximate w. This operator, typically derived from finite element or spectral methods, ensures a small approximation error:

$$\|w - I_n w\|_{L^2} \leqslant \delta_0(n) \|\nabla w\|_{L^2},$$

where $\delta_0(n)$ tends to zero as n increases. We use $L_2 I_n$ to approximate L_2. Consider an associated basis $\Psi = (\psi_1, \ldots, \psi_n)$ of the image of I_n. We can represent $I_n w_1$ as:

$$I_n w_1 = \sum_{j=1}^{n} s_j(w_1) \psi_j,$$

where $s_j(w_1)$ are the projection coefficients. Next, we verify the invertibility of L by solving

$$-\Delta \phi_i + L_2 \phi_i = -L_2 \psi_i, i = 1, \ldots, n.$$

If this equation can be exactly solved, the solution of (3.5) is thus given by

$$w_2 = G w_1 := \sum_{j=1}^{n} s_j(w_1) \phi_j. \tag{3.6}$$

In practice, small numerical residuals are unavoidable. We will get approximate solutions ϕ_i with numerical residual r_i, that is:

$$L\phi_i = -L_2 \psi_i + r_i, i = 1, \ldots, n.$$

These residuals are expected to be small, ensuring that the overall approximation remains accurate enough. We can absorb this residual into ψ_i by slightly modifying L_{ap} as:

$$L_{\text{ap}} w_1 := L_2 I_n w_1 + R w_1, \quad R w_1 := -\sum_{j=1}^{n} s_j(w_1) r_j.$$

Then w_2 defined by (3.6) solves the equation (3.5) precisely. Here, we need to numerically verify that G is bounded and R is small in $L^2(D)$, i.e.,

$$\|R w_1\|_{L^2} \leqslant \varepsilon_R \|w_1\|_{L^2}, \quad \|G w_1\|_{L^2} \lesssim \|w_1\|_{L^2}.$$

The boundedness of G ensures the invertibility of L within the finite-dimensional space. Moreover, since the residual R is small, $L_{\text{res}} = L_2(I - I_n) - R$ also remains small as we want.

Finally, by substituting (3.6) into (3.4), we address the first equation in our modified system:

$$-\Delta w_1 + L_{\text{res}} w_1 + (w_1 + G w_1)^2 = -\mathrm{E}_w.$$

Using the Poincare's inequality, which gives $\|w_1\|_{L^2} \lesssim \|\nabla w_1\|_{L^2}$, we obtain

$$\begin{aligned}
&\langle -\Delta w_1 + L_{\text{res}} w_1, w_1 \rangle = \langle -\Delta w_1, w_1 \rangle + \langle 2\overline{w}(w_1 - I_n w_1), w_1 \rangle - \langle R w_1, w_1 \rangle \\
&\geqslant \|\nabla w_1\|_{L^2}^2 - 2\|\overline{w}\|_{L^\infty} \|w_1 - I_n w_1\|_{L^2} \|w_1\|_{L^2} - \|R w_1\|_{L^2} \|w_1\|_{L^2} \geqslant (1 - C\delta_0(n) - C\varepsilon_R) \|\nabla w_1\|_{L^2}^2.
\end{aligned}$$

Thus, coercivity is preserved with large n and small ε_R. Consequently, a fixed-point argument similar to the simpler scenario ensures the existence of a solution to equation (3.3).

3.2 Generalization

In this section, we formalize the methods and ideas introduced earlier into a general theorem. For our toy model, the essential structure of the linear operator is characterized by its decomposition into a coercive part and a compact perturbation. Accordingly, we impose the following assumption for the linear operator in the equation (3.2):

Assumption 2 (A priori bounds) *Let $\mathcal{H}^0$ be a Hilbert space equipped with inner product $\langle\cdot,\cdot\rangle_{\mathcal{H}^0}$ and corresponding norm $\|\cdot\|_{\mathcal{H}^0}$. Suppose $\mathcal{H}^1 \subset \mathcal{B} \subset \mathcal{H}^0$ are dense subsets of $\mathcal{H}^0$, respectively endowed with stronger norms $\mathcal{H}^1$, $\mathcal{B}$, and that the identity embedding $\mathcal{H}^1 \to \mathcal{B}$ is compact. In particular, there exists a constant $K_0 > 0$ such that*

$$\|f\|_{\mathcal{H}^0} \leqslant K_0\|f\|_{\mathcal{H}^1}, \quad \|f\|_{\mathcal{H}^0} \lesssim \|f\|_{\mathcal{B}}, \quad \forall f \in \mathcal{H}_1. \tag{3.7}$$

The operator L admits the decomposition:

$$L = L_1 + L_2,$$

where L_1 is coercive and bounded, and L_2 is a compact perturbation. Specifically, we impose:

1. Coercivity of L_1 for a constant $K_1 > 0$:

$$\langle L_1 f, f\rangle_{\mathcal{H}^0} \geqslant K_1\|f\|^2_{\mathcal{H}^1}, \quad \forall f \in \mathcal{H}^1. \tag{3.8}$$

2. Boundedness of L_1 as a bilinear form, where the exact constant is not important:

$$|\langle L_1 f, g\rangle_{\mathcal{H}^0}| \lesssim \|f\|_{\mathcal{H}^1}\|g\|_{\mathcal{H}^1}, \quad \forall f \in \mathcal{H}^1. \tag{3.9}$$

3. Compactness of L_2 via boundedness in $\mathcal{H}^0$ for a constant $K_2 > 0$:

$$\|L_2 f\|_{\mathcal{H}^0} \leqslant K_2\|f\|_{\mathcal{H}^0}, \quad \forall f \in \mathcal{H}^0. \tag{3.10}$$

3.2.1 Finite rank approximation

Following our earlier approach, we now construct a finite-rank approximation of the operator L_2. First, we select an interpolation operator I_n satisfying:

$$\|f - I_n f\|_{\mathcal{H}^0} \leqslant \delta_1(n)\|f\|_{\mathcal{H}^1},$$

where $\delta_1(n)$ tends to zero as n increases. Consider an associated basis $\Psi = (\psi_1, \ldots, \psi_n)$ of the image of I_n. We express $I_n f$ in terms of its basis functions:

$$I_n f = S(f) \cdot \Psi := \sum_{j=1}^{n} s_j(f)\psi_j.$$

Next, we construct a set of functions $\Phi = (\phi_1, \ldots, \phi_n)$ satisfying:

$$L\phi_i = -L_2\psi_i + r_i, i = 1, \ldots, n, \tag{3.11}$$

where $R = (r_1, \ldots, r_n)^T$ represents the small residual terms. The finite-rank approximation operator L_{ap} is defined as:

$$L_{\text{ap}} w_1 = \sum_{j=1}^{n} s_j(w_1)(L_2\psi_j - r_j).$$

The residual of this approximation is given by:

$$L_{\text{res}} w_1 := (L_2 - L_{\text{ap}})w_1 = L_2(I - I_n)w_1 + \sum_{j=1}^{n} s_j(w_1)r_j. \tag{3.12}$$

We then decompose the equation (3.2) into the following system:

$$L_1 w_1 + L_{\text{res}} w_1 = -\mathrm{E} - N(w_1 + w_2), \quad L w_2 = -L_{\text{ap}} w_1. \tag{3.13}$$

With the definitions of ϕ_j and s_j established, the solution w_2 is explicitly represented as:

$$w_2 = G w_1 := \sum_{j=1}^{n} s_j(w_1)\phi_j.$$

The boundedness of the operator G guarantees the invertibility of L within this finite-dimensional space. In summary, to validate the numerical approach, we will verify the following assumption:

Assumption 3 (Finite-rank approximation) *For any n, consider the finite-rank operator I_n. We assume that the interpolation error satisfies:*

$$\|I_n f - f\|_{\mathcal{H}^0} \leqslant \delta_1(n)\|f\|_{\mathcal{H}^1}, \quad \forall f \in \mathcal{H}^1. \tag{3.14}$$

Suppose Φ solves equation (3.11) with a small residual R, specifically:

$$\|R\|_{\mathcal{H}^0} \leqslant \varepsilon_1,$$

where ε_1, though dependent on n, can be made sufficiently small in practice. The coefficients $S(f)$ and the solution Φ satisfy the bounds:

$$|S(f)| \lesssim \|f\|_{\mathcal{H}^0}, \quad |S(f)| \leqslant \gamma_1(n)\|f\|_{\mathcal{H}^1}, \quad \|\Phi\|_{\mathcal{H}^1} \leqslant \gamma_2(n). \tag{3.15}$$

Here, in the first estimate of (3.15), we therefore have a gain of regularity that

$$\|G w_1\|_{\mathcal{H}^1} \lesssim \|w_1\|_{\mathcal{H}^0},$$

which is crucial for the continuity estimate in a weaker topology $\mathcal{B}$ to follow, while the precise constant is not important.

3.2.2 Residual and nonlinear terms

In this subsection, we analyze the first equation of (3.13). Having established the coercivity of L_1 and the smallness of L_{res}, we now shift our focus to the residual and nonlinear terms. Regarding the residual term, we pose the following assumption:

Assumption 4 (Residual estimate) *The residual* E *is sufficiently small:*

$$\|\mathrm{E}\|_{\mathcal{H}^0} \leqslant \varepsilon_2,$$

where ε_2 quantifies the permissible magnitude of the residual.

For the nonlinear term, we pose the following assumption:

Assumption 5 (Nonlinear estimate) *The nonlinear term $N(w)$ satisfies the bounded estimate:*

$$|\langle N(u), w\rangle_{\mathcal{H}^0}| \leqslant K_3\|u\|_{\mathcal{H}^1}^2\|w\|_{\mathcal{H}^1},$$

and the continuous estimate

$$|\langle N(u_1) - N(u_2), w_1 - w_2\rangle_{\mathcal{H}^0}| \lesssim (\|u_1\|_{\mathcal{H}^1} + \|u_2\|_{\mathcal{H}^1})\|u_1 - u_2\|_{\mathcal{B}}\|w_1 - w_2\|_{\mathcal{B}}.$$

Remark 4 We remark that the constant in the continuity estimate is not important, and that the nonlinear estimates ensure a continuous mapping in $\mathcal{B}$ and a bounded mapping in $\mathcal{H}^1$, in preparation for the Schauder fixed-point argument.

Essentially, a quadratic nonlinearity combined with Sobolev embedding will satisfy the above assumptions. These assumptions can be relaxed to incorporate the nonlinearities of other orders.

3.2.3 Main theorem

With the assumptions above, we establish the following result:

Theorem 3 (Existence of exact solutions in the abstract case) *If Assumptions 2 and 5 hold, Assumption 3 holds for sufficiently large n and a sufficiently small ε_1, ensuring:*

$$K_1 - K_0K_2\delta_1(n) - K_0\gamma_1(n)\varepsilon_1 > 0, \tag{3.16}$$

and Assumption 4 holds with a sufficiently small ε_2 such that the determinant

$$M_4 := (K_1 - K_0K_2\delta_1 - K_0\gamma_1\varepsilon_1)^2 - 4\varepsilon_2K_0K_3(1+\gamma_1\gamma_2)^2 \geqslant 0, \tag{3.17}$$

then the equation (3.13) *has a solution w_1 with:*

$$\|w_1\|_{\mathcal{H}^1} \leqslant x^w := \frac{K_1 - K_0K_2\delta_1 - K_0\gamma_1\varepsilon_1 - \sqrt{M_4}}{2K_3(1+\gamma_1\gamma_2)^2}. \tag{3.18}$$

Consequently, there exists a solution $\widetilde{w}$ to equation (3.1) *such that:*

$$\|\overline{w} - \widetilde{w}\|_{\mathcal{H}^1} \leqslant (1+\gamma_1\gamma_2)x^w.$$

Remark 5 The logical sequence for addressing the assumptions in the preceding theorem is as follows: First, Assumptions 2 and 5 describe the qualitative properties of the operators and must initially be verified. Next, we select a sufficiently large n to construct the approximation operator so that Assumption 3 and (3.16) hold. Finally, the residue ε_2 is chosen sufficiently small satisfying Assumption 4 and (3.17).

Proof We employ a Schauder fixed-point argument to establish this theorem.

Well-definedness of the fixed point map. We will first establish that $L_1 + L_{\text{res}}$ induces a coercive and bounded bilinear form.

We begin by quantifying the smallness of the residual operator L_{res}. Recall (3.12) that:

$$L_{\text{res}}f = L_2(I - I_n)f + \sum_{j=1}^{n} s_j(f)r_j.$$

Using the boundedness of L_2 (3.10) and the finite-rank approximation (3.14), we have:

$$\|L_2(I - I_n)f\|_{\mathcal{H}^0} \leqslant K_2\delta_1\|f\|_{\mathcal{H}^1}.$$

For the second term, by applying the Cauchy-Schwarz inequality, we have:

$$\|\sum_{j=1}^{n} s_j(f)r_j\|_{\mathcal{H}^0} \leqslant \sqrt{\sum_{j=1}^{n}|s_j(f)|^2}\sqrt{\sum_{j=1}^{n}\|r_j\|_{\mathcal{H}^0}^2} = |S(f)|\|R\|_{\mathcal{H}^0} \leqslant \gamma_1\varepsilon_1\|f\|_{\mathcal{H}^1},$$

where we use Assumption 3 in the last inequality. We conclude that

$$\|L_{\text{res}}f\|_{\mathcal{H}^0} \leqslant (K_2\delta_1 + \gamma_1\varepsilon_1)\|f\|_{\mathcal{H}^1}. \tag{3.19}$$

We conclude the coercivity of $L_1 + L_{\text{res}}$ using estimates (3.8), (3.19), and the embedding (3.7):

$$\langle (L_1 + L_{\text{res}})f, f\rangle_{\mathcal{H}^0} \geqslant (K_1 - K_0K_2\delta_1 - K_0\gamma_1\varepsilon_1)\|f\|_{\mathcal{H}^1}^2. \tag{3.20}$$

The boundedness is trivial by (3.19), (3.7), and Assumption 2. By the Lax-Milgram theorem, we define the mapping T by setting $T(w_1) = w_1^*$, where w_1^* solves:

$$(L_1 + L_{\text{res}})w_1^* = -\mathrm{E} - N(w_1 + Gw_1). \tag{3.21}$$

A priori estimate in $\mathcal{H}^1$. From Assumption 4 and 5, the residual term and the nonlinear term are respectively controlled by:

$$|\langle \mathrm{E}, w_1^* \rangle_{\mathcal{H}^0}| \leqslant \varepsilon_2 \|w_1^*\|_{\mathcal{H}^0} \leqslant \varepsilon_2 K_0 \|w_1^*\|_{\mathcal{H}^1}, \tag{3.22}$$

$$|\langle N(w_1 + Gw_1), w_1^* \rangle_{\mathcal{H}^0}| \leqslant K_3 \|w_1 + Gw_1\|_{\mathcal{H}^1}^2 \|w_1^*\|_{\mathcal{H}^1} \leqslant K_3 (\|w_1\|_{\mathcal{H}^1} + \|Gw_1\|_{\mathcal{H}^1})^2 \|w_1^*\|_{\mathcal{H}^1}.$$

The estimate of Gw_1 follows from the Cauchy-Schwarz inequality:

$$\|Gw_1\|_{\mathcal{H}^1} \leqslant \sum_{j=1}^{n} |s_j(w_1)| \|\phi_j\|_{\mathcal{H}^1} \leqslant |S(w_1)| \|\Phi\|_{\mathcal{H}^1} \leqslant \gamma_1 \gamma_2 \|w_1\|_{\mathcal{H}^1}, \tag{3.23}$$

where we use (3.15) from Assumption 3. We finally have

$$|\langle N(w_1 + Gw_1), w_1^* \rangle_{\mathcal{H}^0}| \leqslant K_3 (1 + \gamma_1 \gamma_2)^2 \|w_1\|_{\mathcal{H}^1}^2 \|w_1^*\|_{\mathcal{H}^1}. \tag{3.24}$$

By collecting the estimates (3.20), (3.22), and (3.24), we obtain:

$$(K_1 - K_0 K_2 \delta_1 - K_0 \gamma_1 \varepsilon_1) \|w_1^*\|_{\mathcal{H}^1} \leqslant \varepsilon_2 K_0 + K_3 (1 + \gamma_1 \gamma_2)^2 \|w_1\|_{\mathcal{H}^1}^2.$$

Solving the inequality as in (3.18) shows that if $\|w_1\|_{\mathcal{H}^1} \leqslant x^w$, then $\|w_1^*\|_{\mathcal{H}^1} \leqslant x^w$. T maps the ball B_M to itself.

Continuity estimate in $\mathcal{B}$. Next, we establish the continuity of T. Let $w_1^* = T(w_1), \widehat{w}_1^* = T(\widehat{w}_1)$. Subtracting the equation (3.21) that they satisfy, we get:

$$(L_1 + L_{\mathrm{res}})(w_1^* - \widehat{w}_1^*) = N(\widehat{w}_1 + G\widehat{w}_1) - N(w_1 + Gw_1).$$

Instead of the estimate (3.23), we need the gain of regularity in G by (3.15):

$$\|Gf\|_{\mathcal{H}^1} \leqslant |S(f)| \|\Phi\|_{\mathcal{H}^1} \lesssim \|f\|_{\mathcal{H}^0} \lesssim \|f\|_{\mathcal{B}} \lesssim \|f\|_{\mathcal{H}^1},$$

where we use the comparison of the norms $\mathcal{H}^0, \mathcal{B}, \mathcal{H}^1$ in Assumption 2. Combining with the nonlinear estimate in Assumption 5, the difference between the nonlinear term is bounded by

$$\begin{aligned}
&|\langle N(\widehat{w}_1 + G\widehat{w}_1) - N(w_1 + Gw_1), \widehat{w}_1^* - w_1^* \rangle_{\mathcal{H}^0}| \\
&\lesssim (\|w_1 + Gw_1\|_{\mathcal{H}^1} + \|\widehat{w}_1 + G\widehat{w}_1\|_{\mathcal{H}^1}) \|\widehat{w}_1 - w_1 + G\widehat{w}_1 - Gw_1\|_{\mathcal{B}} \|\widehat{w}_1^* - w_1^*\|_{\mathcal{B}} \\
&\lesssim (\|w_1\|_{\mathcal{H}^1} + \|\widehat{w}_1\|_{\mathcal{H}^1}) \|\widehat{w}_1 - w_1\|_{\mathcal{B}} \|\widehat{w}_1^* - w_1^*\|_{\mathcal{B}} \lesssim \|\widehat{w}_1 - w_1\|_{\mathcal{B}} \|\widehat{w}_1^* - w_1^*\|_{\mathcal{B}},
\end{aligned}$$

for $\widehat{w}_1, w_1 \in B_M$. By the coercivity estimate (3.20) and the embedding (3.7), it follows that

$$\|w_1^* - \widehat{w}_1^*\|_{\mathcal{B}}^2 \lesssim \|w_1^* - \widehat{w}_1^*\|_{\mathcal{H}^1}^2 \lesssim \|\widehat{w}_1 - w_1\|_{\mathcal{B}} \|w_1^* - \widehat{w}_1^*\|_{\mathcal{B}}.$$

If $w_1^* \neq \widehat{w}_1^*$, we can cancel the common factor to obtain

$$\|w_1^* - \widehat{w}_1^*\|_{\mathcal{B}} \lesssim \|\widehat{w}_1 - w_1\|_{\mathcal{B}}.$$

Hence T is (Lipschitz) continuous in the weaker norm $\mathcal{B}$.

The ball B_M in $\mathcal{H}^1$ is compact in $\mathcal{B}$ by Assumption 2, and by the Schauder fixed-point theorem, there exists a solution w_1 to equation (3.13) satisfying $\|w_1\|_{\mathcal{H}^1} \leqslant x^w$. By (3.23), we know that

$$\|\overline{w} - \widetilde{w}\|_{\mathcal{H}^1} = \|w_1 + Gw_1\|_{\mathcal{H}^1} \leqslant (1 + \gamma_1 \gamma_2) x^w.$$

This concludes the proof. □

4 Proof of Theorem 2: Analysis Part

In this section, we apply the framework developed in the previous section to establish Theorem 2, whose proof consists of two parts: demonstrating the existence of the profile $\widetilde{U}$, and proving the existence of the eigenpair $(\widetilde{\lambda}, \widetilde{v})$, via Propositions 1 and 2. We will use superscript U and v, such as L^U and L^v, to indicate dependence on the operators associated with Propositions 1 and 2, respectively. The strategies are largely the same, with minor modifications highlighted. From this section onward, we will only work in the self-similar variables, and upon an abuse of notation, we still use x rather than ξ for the spatial variables.

Remark 6 (Key Idea) In order to obtain sharper constants, we choose to verify Assumptions 2 and 4, while replacing Assumptions 3 and 5 by obtaining the key estimates (3.20), (3.24), and (3.25) from the proof of Theorem 3 directly.

We remark that the key challenge lies in the linear estimate (3.20), while the nonlinear and residual estimates are more straightforward. The crucial changes are that the linear operator is no longer bounded due to the term $x\cdot\nabla$, and that H^1 is not compactly embedded into L^2 on the whole space. We truncate the domain so that the associated bilinear form will be bounded, as in Assumption 2 to apply the Lax-Milgram theorem. Moreover, thanks to the gain of regularity, we show that the fixed point map maps a bounded set in H^1 to itself and is continuous in L^4. Therefore, in the truncated domain, we can apply the Schauder fixed-point theorem to obtain a fixed point, and taking weak limits yields the desired solution.

We first discuss the concrete setting and the linear operators in Section 4.1. The finite-rank approximation for a general type of compact perturbations applicable to U and v simultaneously is discussed in Section 4.2. Proposition 1 is addressed in Section 4.3, as Proposition 2 follows a similar verification process in Section 4.4. Section 4.5 briefly presents our numerical results and records the verified numerical constants used in the proof. Implementation details of the numerical algorithm are deferred to Sections 5 and 6, and a roadmap for rigorous computer-assisted proof is in Section 7.

4.1 Setting and decomposition of linear operators

We discuss the setting and the definition of the linear operators.

Setting for U for Proposition 1. For U, we separate the linear and nonlinear components in equation (1.15):

$$\begin{aligned} L^U U &:= -\frac{1}{2}U - \frac{1}{2}x\cdot\nabla U - \Delta U + \Pi(\overline{U}\cdot\nabla U + U\cdot\nabla\overline{U}),\\ N^U(U) &:= \Pi(U\cdot\nabla U). \end{aligned}$$

Our strategy involves decomposing the linear operator L^U into two parts as in Section 3: a coercive operator L_1^U and a compact operator L_2^U. We first specify the Hilbert spaces under consideration: $\mathcal{H}^0 = L^2_\sigma(\mathbb{R}^3), \mathcal{H}^1 = H^1_\sigma(\mathbb{R}^3)$. For numerical purposes, we will later restrict to a subspace with certain symmetries, which does not affect the analysis presented below. Noticing the cancellation via an integration by parts, an initial attempt at this decomposition could be:

$$L_1^U U = -\frac{1}{2}U - \frac{1}{2}x\cdot\nabla U - \Delta U + \Pi(\overline{U}\cdot\nabla U), \quad L_2^U U = \Pi(U\cdot\nabla\overline{U}).$$

While this decomposition is correct, the construction of a finite rank approximation prompts us to ensure the matrix function in L_2^U is compactly supported. To achieve this, we truncate the gradient $\nabla\overline{U}$ as follows. We first decompose $\nabla\overline{U}$ into antisymmetric and symmetric parts:

$$\nabla\overline{U}(x) = Q_a(x) + Q_s(x), \quad Q_a(x) := \frac{\nabla\overline{U}(x) - \nabla^T\overline{U}(x)}{2}, \quad Q_s(x) := \frac{\nabla\overline{U}(x) + \nabla^T\overline{U}(x)}{2}.$$

Note that Q_a is antisymmetric and thus does not contribute to the scalar product $\langle L_2^U U, U\rangle$. Therefore, we focus on truncating the symmetric part Q_s.

To truncate Q_s, we choose a constant $0 < \eta_1 < \frac{1}{4}$. Then, the symmetric matrix function $Q_s + \eta_1 I_3$ (where I_3 is the 3×3 identity matrix) is decomposed into positive and negative parts:

$$Q_s(x) + \eta_1 I_3 = Q_+(x) - Q_-(x), \quad Q_+(x) \geqslant 0, \quad Q_-(x) \geqslant 0.$$

Since $\nabla \overline{U}(x)$ decays at infinity, we observe that:

$$\lim_{|x|\to+\infty} Q_s(x) + \eta_1 I_3 = \eta_1 I_3 \geqslant 0.$$

Therefore, the negative part $Q_-(x)$ of $Q_s(x) + \eta_1 I_3$ has compact support. Using $\nabla \overline{U} = Q_a + Q_+ - \eta_1 I_3 - Q_-$, the operator L_U is finally decomposed as:

$$L_1^U U := (-\eta_1 - \frac{1}{2})U - \frac{1}{2} x \cdot \nabla U - \Delta U + \Pi(\overline{U} \cdot \nabla U + U \cdot (Q_a + Q_+)), \tag{4.1}$$

$$L_2^U U := -\Pi(U \cdot Q), \tag{4.2}$$

where we choose $Q = Q_-$ to ensure the following coercivity:

$$\langle L_1^U U, U\rangle = (\frac{1}{4} - \eta_1)\|U\|_{L^2}^2 + \|\nabla U\|_{L^2}^2 + \langle Q_+ U, U\rangle \geqslant (\frac{1}{4} - \eta_1)\|U\|_{L^2}^2 + \|\nabla U\|_{L^2}^2. \tag{4.3}$$

Since Q is bounded of compact support, L_2^U is a compact operator from $\mathcal{H}^1$ to $\mathcal{H}^0$ and bounded from $\mathcal{H}^0$ to $\mathcal{H}^0$. We have verified Assumption 2: the coercivity of L_U^1 and the compactness of L_U^2.

Setting for v for Proposition 2. For v, the only nonlinear term is λv, and we need to decompose λ appropriately. Starting from the equation (1.17), we take the inner product with $\overline{v}$ to obtain:

$$\begin{aligned}\lambda &= \langle -\frac{1}{2} v - \frac{1}{2} x \cdot \nabla v - \Delta v + \Pi(\widetilde{U} \cdot \nabla v + U \cdot \nabla \overline{v} + v \cdot \nabla \widetilde{U} + \overline{v} \cdot \nabla U) - \overline{\lambda} v - \lambda v + \Pi \mathrm{E}^v, \overline{v}\rangle \\ &= \langle -\frac{1}{2} x \cdot \nabla v - \Delta v + \widetilde{U} \cdot \nabla v + v \cdot \nabla \widetilde{U} + \overline{v} \cdot \nabla U, \overline{v}\rangle,\end{aligned}$$

where we use orthogonalities to $\overline{v}$ and divergence-free assumptions in Assumption 1 combined with an integration by parts. It can be decomposed into:

$$\lambda(v) = \lambda^{\mathrm{lin}}(v) + \lambda^{\mathrm{con}}, \quad \lambda^{\mathrm{lin}}(v) := \langle -\frac{1}{2} x \cdot \nabla v - \Delta v + \widetilde{U} \cdot \nabla v + v \cdot \nabla \widetilde{U}, \overline{v}\rangle, \quad \lambda^{\mathrm{con}} := \langle \overline{v} \cdot \nabla U, \overline{v}\rangle.$$

Here λ^{lin} is linear in v, while λ^{con} is independent of v. Consequently, equation (1.17) can be decomposed as:

$$L^v v = -\widehat{\mathrm{E}}^v - N^v(v),$$

where we define

$$\begin{aligned} L^v v &:= -(\frac{1}{2} + \overline{\lambda} + \lambda^{\mathrm{con}})v - \frac{1}{2} x \cdot \nabla v - \Delta v + \Pi(\widetilde{U} \cdot \nabla v + v \cdot \nabla \widetilde{U}) - \lambda^{\mathrm{lin}}(v)\overline{v}, \\ N^v(v) &:= -\lambda^{\mathrm{lin}}(v) v, \quad \widehat{\mathrm{E}}^v := \Pi \mathrm{E}^v + \Pi(U \cdot \nabla \overline{v} + \overline{v} \cdot \nabla U) - \lambda^{\mathrm{con}} \overline{v}. \end{aligned} \tag{4.4}$$

We observe that L^v resembles L^U, except for a few additional terms in the linear operator. The $(\overline{\lambda} + \lambda^{\mathrm{con}})v$ term provides enhanced coercivity, while the extra terms $U \cdot \nabla v$ and $v \cdot \nabla U$ are treated as perturbations. The term $-\lambda^{\mathrm{lin}}(v)\overline{v}$ can be interpreted as a projection. More explicitly, we define:

$$P_{\overline{v}} f := f - \langle f, \overline{v}\rangle \overline{v}.$$

Since $\overline{v}$ is divergence-free, it follows that $P_{\overline{v}}$ commutes with the Leray projection operator Π. With this projection, the linear operator can be represented as:

$$L^v v = -(\frac{1}{2} + \overline{\lambda} + \lambda^{\mathrm{con}})v - \frac{1}{2} P_{\overline{v}}(x \cdot \nabla v) - P_{\overline{v}} \Delta v + P_{\overline{v}} \Pi(\widetilde{U} \cdot \nabla v + v \cdot \nabla \widetilde{U}).$$

We decompose the linear operator L into a coercive operator L_1^v and a compact perturbation L_2^v.

Recall the definitions of Q_a, Q_+, Q from the decomposition of L^U. Similarly, we split the linear operator L^v into two components:

$$\begin{aligned} L_1^v v &:= (-\eta_1 - \frac{1}{2} - \overline{\lambda} - \lambda^{\text{con}})v - \frac{1}{2}P_{\overline{v}}(x \cdot \nabla v) - P_{\overline{v}}\Delta v + P_{\overline{v}}\Pi(\widetilde{U} \cdot \nabla v + v \cdot \nabla U + v \cdot (Q_a + Q_+)), \\ L_2^v v &:= -P_{\overline{v}}\Pi(v \cdot Q). \end{aligned} \tag{4.5}$$

We choose the relevant Hilbert spaces as follows:

$$\mathcal{H}^0 = \{u \in L^2_\sigma(\mathbb{R}^3) : \langle u, \overline{v}\rangle = 0\}, \quad \mathcal{H}^1 = \{u \in H^1_\sigma(\mathbb{R}^3) : \langle u, \overline{v}\rangle = 0\}. \tag{4.6}$$

Similarly, we will impose symmetries later for numerical purposes. We verify the coercivity of the operator L_1^v. Indeed, recalling that $\overline{\lambda}$ is negative and $|\lambda^{\text{con}}|$ is small, it holds that

$$\langle L_1^v v, v\rangle \geqslant (\frac{1}{4} - \eta_1 - \overline{\lambda} - |\lambda^{\text{con}}|)\|v\|_{L^2}^2 + \|\nabla v\|_{L^2}^2 - |\langle v \cdot \nabla U, v\rangle|.$$

By Holder's inequality with multiple functions and Sobolev embedding in Lemma 6, where we define the sharp Sobolev constant K_4, we have

$$|\langle v \cdot \nabla U, v\rangle| \leqslant \|\nabla U\|_{L^2}\|v\|_{L^4}^2 \leqslant 2K_4\|\nabla U\|_{L^2}(\|v\|_{L^2}^2 + \|\nabla v\|_{L^2}^2), \tag{4.7}$$

we obtain:

$$\langle L_1^v v, v\rangle \geqslant (\frac{1}{4} - \eta_1 - \overline{\lambda} - 2K_4\|\nabla U\|_{L^2} - |\lambda^{\text{con}}|)\|v\|_{L^2}^2 + (1 - 2K_4\|\nabla U\|_{L^2})\|\nabla v\|_{L^2}^2, \tag{4.8}$$

ensuring coercivity for sufficiently small $\|\nabla U\|_{L^2}$ and $|\lambda^{\text{con}}|$. Finally, since Q is bounded of compact support, L_2^v is a compact operator from $\mathcal{H}^1$ to $\mathcal{H}^0$ and bounded from $\mathcal{H}^0$ to $\mathcal{H}^0$. We have verified Assumption 2: the coercivity of L_v^1 and the compactness of L_v^2.

4.2 Finite rank approximation

For a general compact operator in the form of (4.2) and (4.5) as

$$L_2 = -\mathcal{P}(U \cdot Q), \tag{4.9}$$

where Q is compactly supported and positive definite, and $\mathcal{P}$ denotes a projection on L^2 that equals the Leray projection Π for the case of U and $P_{\overline{v}}\Pi$ for the case of v. Here, L_2^U and L_2^v only differ by the projection operator. Notice that L maps the image of the projection operator to itself: for any $f = \mathcal{P}f$, we have $\mathcal{P}Lf = Lf$.

Recall that we want the finite-rank operator to have a number of basis functions as small as possible so that our numerical verification of invertibility on the space can be easier. Ideally, we should choose the eigenspace corresponding to the largest eigenvalues of L_2 so that the residue of the finite-rank approximation is small. This is not tractable in practice, however, since the eigenvectors are not explicit. We instead solve the eigenvalue problem on an explicitly constructed finite-dimensional subspace numerically, and require that L_2 acting outside of the space is small. To be precise, the construction involves three main steps:

1. Choose a domain Ω sufficiently large to encompass the support of Q, and construct a finite-dimensional collection of spectral basis functions on Ω.

2. Compute the eigenvectors corresponding to the largest eigenvalues and construct their spanning eigenspace in the finite-dimensional space.

3. Construct approximations of L_2 and invert L numerically restricted to the eigenspace.

4.2.1 Construction of the finite rank approximation

We first identify a suitable domain Ω that fully encompasses the support of the matrix function $Q(x)$. Now, we introduce spectral approximations for functions defined on Ω. Let V_N denote the finite-dimensional space with the first N spectral basis functions. We remark that the space and thus the eigenpairs associated with U and v will be different due to their respective parity symmetries. Consider the following E-inner product and its induced norm

$$\langle u, v\rangle_E := \lambda(\langle \nabla u, \nabla v\rangle_\Omega + \eta_2 \langle u, v\rangle_\Omega),$$

where we choose the constant η_2 to be 0.005. Notice that by construction of the spectral basis, the L^2-projection I_N defined by (6.5) in Section 6 onto the space V_N is also an H^1-projection, hence an E-projection.

To obtain an efficient finite-rank approximation, we consider the following eigenvalue problem within the space of spectral basis functions V_N:

$$\langle u, Qv\rangle_\Omega = \lambda \langle u, v\rangle_E. \tag{4.10}$$

Specifically, we arrange the eigenvalues as:

$$\lambda_1^Q \geqslant \cdots \geqslant \lambda_k^Q > 0 = \lambda_{k+1}^Q = \cdots = \lambda_N^Q,$$

and denote their corresponding eigenfunctions as $\{\psi_1^Q, \ldots, \psi_N^Q\}$. The eigenfunctions are orthonormal in the E-inner product:

$$\langle \psi_i^Q, \psi_i^Q\rangle_E = 1; \quad \langle \psi_i^Q, \psi_j^Q\rangle_E = \langle \psi_i^Q, Q\psi_j^Q\rangle_\Omega = 0, i \neq j.$$

We retain only eigenfunctions with index $j \leqslant m$, for a small m. For each $j \leqslant m$, we numerically obtain the eigenpair $(\overline{\lambda}_j, \overline{\psi}_j)$, and solve for $\overline{\phi}_j$ as:

$$L\overline{\phi}_j = \mathcal{P}Q\overline{\psi}_j + r_j, \quad \mathcal{P}\overline{\phi}_j = \overline{\phi}_j, \tag{4.11}$$

where r_j denotes a small residual term that satisfies $\mathcal{P}r_j = r_j$ by definition. As in Section 3.2.1, to ensure an exact inversion of L, we define the final finite-rank approximation as:

$$L_{\mathrm{ap}} f := -\sum_{j=1}^{m} \overline{\lambda}_j^{-1} \langle f, Q\overline{\psi}_j\rangle_\Omega \mathcal{P}(Q\overline{\psi}_j + r_j), \tag{4.12}$$

with $Gf := -L^{-1}L_{\mathrm{ap}}$ given by

$$Gf = \sum_{j=1}^{m} \overline{\lambda}_j^{-1} \langle f, Q\overline{\psi}_j\rangle_\Omega \overline{\phi}_j.$$

4.2.2 Estimates of the finite rank approximation

Since our approximate eigensystem incurs numerical errors, we first present a lemma concerning projection onto the eigensystem, whose proof is deferred to Appendix B. We denote the eigenvalues $\overline{\Lambda} = \mathrm{diag}\{\overline{\lambda}_1, \cdots, \overline{\lambda}_m\}$, and the space $V_{\mathrm{lg}} = \mathrm{span}\{\overline{\psi}_j\}_{j=1}^m$. The Gram matrices

$$G_E := (\langle \overline{\psi}_i, \overline{\psi}_j\rangle_E)_{1\leqslant i,j\leqslant m}, \quad G_Q := (\langle \overline{\psi}_i, Q\overline{\psi}_j\rangle_\Omega)_{1\leqslant i,j\leqslant m},$$

are close to the identity matrix $\mathbb{1}_m$ and $\overline{\Lambda}$ respectively.

Lemma 1 (Quasi-orthonormal projection) *For any f with the orthogonal projection $f_{\mathrm{lg}}^{Q,\perp} \in V_{\mathrm{lg}}$ such that $\langle f - f_{\mathrm{lg}}^{Q,\perp}, Q\overline{\psi}_j\rangle_\Omega = 0$, we have the estimates*

$$|\|Q^{\frac{1}{2}} f_{\mathrm{lg}}^{Q,\perp}\|_{L^2}^2 - \sum_{j=1}^{m} \overline{\lambda}_j^{-1} \langle f, Q\overline{\psi}_j\rangle_\Omega^2| \leqslant \varepsilon_3 \|\lambda_{\max}(Q)\|_{L^\infty} \|f\|_{L^2(\Omega)}^2. \tag{4.13}$$

Here we use the notation that

$$\varepsilon_3 := \|\mathbb{1}_m - (G_Q)^{\frac{1}{2}}\overline{\Lambda}^{-1}(G_Q)^{\frac{1}{2}}\|, \tag{4.14}$$

measuring how close the approximate eigenpairs are to satisfying exact orthonormality in the Q-geometry.

We now present a lemma on the quasi-orthogonality in the E-inner product; see its proof in Appendix B.

Lemma 2 (Quasi-orthogonality in Q- and E- inner products) *Denote the residues of the approximate eigenvector problem as $R^e := \{r_j^e\}_{j=1}^m$ defined via*

$$\langle\overline{\psi}_j, Qv\rangle_\Omega = \overline{\lambda}_j\langle\overline{\psi}_j, v\rangle_E + \langle r_j^e, v\rangle_E, \quad \forall v \in V_N.$$

For any $f \in V_{\text{lg}}$ and u orthogonal to V_{lg} in the Q-inner product as $\langle\overline{\psi}_j, Qu\rangle_\Omega = 0$, we have

$$|\langle f, u\rangle_E| \leqslant \varepsilon_4\|f\|_E\|u\|_E.$$

Here we use the notation that

$$\varepsilon_4 := |(G_E)^{\frac{-1}{2}}\overline{\Lambda}^{-1}(\|r_1^e\|_E, \cdots, \|r_m^e\|_E)^T|,$$

where ε_4 is the quasi-orthogonality constant between the "large" subspace V_{lg} and its Q–orthogonal complement, measured in the E–inner product.

Now we work on bounded estimates. The approximation rate associated with V_N is defined as

$$K_5 := \|\lambda_{\max}(Q)\|_{L^\infty}\sup_{u\neq 0, u\perp_{L^2}V_N}\frac{\|u\|_{L^2(\Omega)}^2}{\|u\|_E^2}.$$

K_5 tends to 0 as N increases by our spectral basis construction of V_N, since the Rayleigh quotients are upper bounded by the inverse of eigenvalues of the Laplacian. Defining the L^2-projection on V_N as I_N, we have the estimate

$$\|Q^{\frac{1}{2}}(u - I_N u)\|_{L^2}^2 \leqslant K_5\|(u - I_N u)\|_E^2. \tag{4.15}$$

We define the following constant

$$K_6 := \sup_{u\in V_N, u\neq 0, u\perp_Q V_{\text{lg}}}\frac{\|Q^{\frac{1}{2}}u\|_{L^2}^2}{\|u\|_E^2}, \tag{4.16}$$

the maximal Rayleigh quotient of Q measured in the E–energy on the Q–orthogonal complement of the captured subspace $V_{\text{lg}} = \text{span}\{\psi_1, \ldots, \psi_m\} \subset V_N$, i.e. the top generalized eigenvalue of Q on $V_{\text{lg}}^{\perp_Q}$. Moreover, K_6 can be computed rigorously in the matrix equivalent characterization of

$$K_6 \leqslant \sup_{u\in V_N, u\neq 0}\frac{\langle u, Qu\rangle_\Omega - \sum_{j=1}^m\overline{\lambda}_j^{-1}\langle u, Q\overline{\psi}_j\rangle_\Omega^2}{\|u\|_E^2},$$

which should approximately be the eigenvalue smaller than $\overline{\lambda}_m$. In practice, since we only need to provide an upper bound of K_6, we can increase K_6 a bit and only need to ensure and verify a positive-definiteness in the following sense:

$$\sup_{u\in V_N} K_6\|u\|_E^2 + \sum_{j=1}^m\overline{\lambda}_j^{-1}\langle u, Q\overline{\psi}_j\rangle_\Omega^2 - \langle u, Qu\rangle_\Omega \geq 0, \tag{4.17}$$

which we can verify in the matrix representation via a numerical LDL^T decomposition and by showing the residue is small and diagonal entries are away from 0.

With the bounded estimates in hand, we are in a position to present the following lemma on a rigorous estimate of the approximation error associated with L_{ap}.

Lemma 3 (Finite-rank approximation) *For L_{ap} defined by (4.12) and L_2 defined by (4.9), we have the estimate for any f such that $\mathcal{P}f = f$:*

$$|\langle (L_2 - L_{\mathrm{ap}})f, f\rangle| \leqslant M_1 \|\nabla f\|^2_{L^2(\Omega)} + M_2 \|f\|^2_{L^2(\Omega)},$$

where

$$M_1 := K_5 + \frac{K_6}{(1-\varepsilon_4)^2}, \quad M_2 := \eta_2 M_1 + \varepsilon_3 \|\lambda_{\max}(Q)\|_{L^\infty} + K_7.$$

Here, the constant K_7 is related to the inner product of the Gram matrices

$$K_7 := \sqrt{\mathrm{tr}(G_{Q^2} G_r)}, \quad G_{Q^2} := (\langle \overline{\lambda}_i^{-1} Q\overline{\psi}_i, \overline{\lambda}_j^{-1} Q\overline{\psi}_j\rangle_\Omega)_{1\leqslant i,j\leqslant m}, \quad G_r := (\langle r_i, r_j\rangle_\Omega)_{1\leqslant i,j\leqslant m}. \tag{4.18}$$

Finally, we remark that by construction, $\overline{\phi}_j \in H^2$.

We defer the proof of the lemma to Appendix B. Here, K_7 is related to the cross term resulting from the residue of the finite-rank approximation.

4.3 Proof of Proposition 1

We begin by addressing Proposition 1. We construct a finite-rank approximation L^U_{ap} of L^U_2 by the strategy in Section 4.2 as

$$L^U_{\mathrm{ap}} f := -\sum_{j=1}^m (\overline{\lambda}^U_j)^{-1} \langle f, Q\overline{\psi}^U_j\rangle_\Omega \Pi(Q\overline{\psi}^U_j + r^U_j). \tag{4.19}$$

By Lemma 3 and the coercivity of L^U_1 in (4.3), we have the linear estimate:

$$\langle L^U_1 U_1 + (L^U_2 - L^U_{\mathrm{ap}})U_1, U_1\rangle \geqslant (\frac{1}{4} - \eta_1 - M^U_2)\|U_1\|^2_{L^2} + (1 - M^U_1)\|\nabla U_1\|^2_{L^2}. \tag{4.20}$$

This verifies (3.20). We will subsequently choose the parameters appropriately to ensure that both coefficients on the right-hand side are strictly positive.

This approximation allows us to split the solution $U = U_1 + U_2$ and rewrite equation (1.15) as:

$$L^U_1 U_1 + (L^U_2 - L^U_{\mathrm{ap}})U_1 = -N^U(U_1 + U_2) - \Pi \mathrm{E}^U, \tag{4.21}$$

$$L^U U_2 = -L^U_{\mathrm{ap}} U_1. \tag{4.22}$$

Finally, we define:

$$U_2 = G^U U_1 := \sum_{j=1}^m (\overline{\lambda}^U_j)^{-1} \langle U_1, Q\overline{\psi}^U_j\rangle_\Omega \overline{\phi}^U_j, \tag{4.23}$$

which gives an exact solution to (4.22). By construction, $\overline{\phi}^U_j$ and thus U_2 are divergence-free. We detail our fixed-point approach for (4.21) as follows.

Definition of the fixed point map. Typically, the fixed-point map T^U is defined as:

$$L^U_1 U^*_1 + (L^U_2 - L^U_{\mathrm{ap}})U^*_1 = -\Pi((U_1 + G^U U_1)\cdot\nabla(U_1 + G^U U_1)) - \Pi \mathrm{E}^U,$$

where $U^*_1 := T^U(U_1)$. To simplify nonlinear estimates, we replace ∇U_1 by ∇U^*_1 in the nonlinear term. In the weak form, we slightly modify the map T^U_R to:

$$\langle L^U_1 U^*_1 + (L^U_2 - L^U_{\mathrm{ap}})U^*_1 + (U_1 + G^U U_1)\cdot\nabla U^*_1, g\rangle = \langle -(U_1 + G^U U_1)\cdot\nabla G^U U_1 - \mathrm{E}^U, g\rangle, \tag{4.24}$$

for all $g \in \mathcal{H}^1_R$. Here we denote $U^*_1 := T^U_R(U_1)$, and work in the space $\mathcal{H}^1_R$ consisting of functions in $\mathcal{H}^1$ of compact support in the open ball $B_R(0)$. Recall that $\mathcal{H}^1$ consists of divergence-free functions, so we can remove the Leray projection. We require R sufficiently large so that $\Omega \subset B_R(0)$ in the finite rank approximation.

Well-definedness of the fixed point map. Integration by parts yields:

$$\langle (U_1 + G^U U_1) \cdot \nabla g, g \rangle = 0, \tag{4.25}$$

and thus we know by (4.20) that

$$\langle L_1^U f + (L_2^U - L_{\text{ap}}^U) f + (U_1 + G^U U_1) \cdot \nabla f, g \rangle \tag{4.26}$$

induces a coercive bilinear form for (f, g) on $\mathcal{H}_R^1$.

By definition of the finite rank approximation in (4.19), we compute using the boundedness of Q, $\overline{\psi}_j^U$ and r_j^U that $\|L_{\text{ap}}^U f\|_{L^2} \lesssim \|f\|_{L^2(\Omega)} \lesssim \|f\|_{\mathcal{H}^1}$. Using Sobolev embedding, along with the forms (4.1) and (4.2), we deduce that (4.26) induces a bounded bilinear form for (f, g) in $\mathcal{H}_R^1$.

By definition (4.23) and Lemma 3, $G^U U_1 \in H^2_{\text{loc}}$, and by Sobolev embedding we have

$$-(U_1 + G^U U_1) \cdot \nabla G^U U_1 - \mathrm{E}^U \in L^2 .$$

As a consequence of the Lax-Milgram theorem applied to the bilinear form (4.26), we know that there exists $U_1^* = T_R^U(U_1) \in \mathcal{H}_R^1$ such that (4.24) holds.

A priori estimate in H^1. By (4.24), (4.20), and (4.25), we obtain:

$$(\frac{1}{4} - \eta_1 - M_2^U)\|U_1^*\|_{L^2}^2 + (1 - M_1^U)\|\nabla U_1^*\|_{L^2}^2 \leqslant -\langle (U_1 + G^U U_1) \cdot \nabla G^U U_1 + \mathrm{E}^U, U_1^* \rangle. \tag{4.27}$$

The residual term is bounded by:

$$|\langle \mathrm{E}^U, U_1^* \rangle| \leqslant \|\mathrm{E}^U\|_{L^2} \|U_1^*\|_{L^2} \leqslant \varepsilon^U \|U_1^*\|_{L^2},$$

with ε^U sufficiently small defined in Assumption 1.

To handle the nonlinear term, we establish the following bound:

$$|\langle (U_1 + G^U U_1) \cdot \nabla G^U U_1, U_1^* \rangle| \leqslant \|(U_1 + G^U U_1) \cdot \nabla G^U U_1\|_{L^2} \|U_1^*\|_{L^2} \leqslant M_3^U \|U_1\|_{L^2}^2 \|U_1^*\|_{L^2}, \tag{4.28}$$

where we recall the definition of $G_{Q^2}^U$ in (4.18) and define M_3^U

$$M_3^U := \sqrt{\|G_{Q^2}^U\| \sum_{j=1}^m \|\nabla \overline{\phi}_j^U\|_{L^\infty}^2} + \|G_{Q^2}^U\| \sqrt{\sum_{j=1}^m \sum_{i=1}^m \|\overline{\phi}_i^U \cdot \nabla \overline{\phi}_j^U\|_{L^2}^2}.$$

Proof [Proof of (4.28)] Now we estimate the LHS by the definition in (4.23) as

$$\begin{aligned} \|U_1 \cdot \nabla G^U U_1 + G^U U_1 \cdot \nabla G^U U_1\|_{L^2} &\leqslant \|\sum_{j=1}^m (\overline{\lambda}_j^U)^{-1} \langle U_1, Q\overline{\psi}_j^U \rangle_\Omega U_1 \cdot \nabla \overline{\phi}_j^U\|_{L^2} \\ + \|\sum_{j=1}^m \sum_{i=1}^m (\overline{\lambda}_j^U)^{-1} \langle U_1, Q\overline{\psi}_j^U \rangle_\Omega (\overline{\lambda}_i^U)^{-1} \langle U_1, Q\overline{\psi}_i^U \rangle_\Omega \overline{\phi}_i^U \cdot \nabla \overline{\phi}_j^U\|_{L^2} &=: I_4 + I_5 \end{aligned}$$

The absolute value of the first term is bounded by Cauchy-Schwarz as

$$|I_4| \leqslant \sqrt{\sum_{j=1}^m \langle U_1, (\overline{\lambda}_j^U)^{-1} Q\overline{\psi}_j^U \rangle_\Omega^2} \sqrt{\sum_{j=1}^m \|\nabla \overline{\phi}_j^U\|_{L^\infty}^2} \Big(\|U_1\|_{L^2} \Big).$$

The second term is similarly bounded by

$$|I_5| \leqslant \sqrt{\sum_{j=1}^m \langle U_1, (\overline{\lambda}_j^U)^{-1} Q\overline{\psi}_j^U \rangle_\Omega^2 \sum_{i=1}^m \langle U_1, (\overline{\lambda}_i^U)^{-1} Q\overline{\psi}_i^U \rangle_\Omega^2} \sqrt{\sum_{j=1}^m \sum_{i=1}^m \|\overline{\phi}_i^U \cdot \nabla \overline{\phi}_j^U\|_{L^2}^2}.$$

Relating the projection to the Gram matrix as in (B.1), we conclude the proof of (4.28). □

We collect the estimates in H^1 by (4.27):

$$(\frac{1}{4} - \eta_1 - M_2^U)\|U_1^*\|_{L^2}^2 + (1 - M_1^U)\|\nabla U_1^*\|_{L^2}^2 \leqslant (\varepsilon^U + M_3^U\|U_1\|_{L^2}^2)\|U_1^*\|_{L^2}.$$

We analyze the bounded mapping with the following assumption.

Assumption 6 (Bounded mapping assumption for U) *We assume*

$$M_4^U := (\frac{1}{4} - \eta_1 - M_2^U)^2 - 4M_3^U\varepsilon^U > 0.$$

With Assumption 6, we define

$$x_0^U := \frac{2\varepsilon^U}{\frac{1}{4} - \eta_1 - M_2^U + \sqrt{M_4^U}}, \quad \text{so that} \quad \varepsilon^U + M_3^U(x_0^U)^2 = (\frac{1}{4} - \eta_1 - M_2^U)x_0^U.$$

We can solve the H^1 estimates to see T_R^U maps $B^R_{x_0^U, x_1^U}$ to itself, where

$$B^R_{x_0,x_1} := \{U \in \mathcal{H}_R^1 : \|U\|_{L^2} \leqslant x_0, \|\nabla U\|_{L^2} \leqslant x_1\}, \quad x_1^U := \sqrt{\frac{\frac{1}{4} - \eta_1 - M_2^U}{1 - M_1^U}}\frac{x_0^U}{2}.$$

We will verify Assumption 6 in Subsection 4.5.

Estimates of U_2. In the argument above, we derived an estimate for U_1. However, this does not yet yield a bound for U, since $U = U_1 + U_2$. For U_2, its definition implies the following bounds:

$$\begin{aligned}
\|U_2\|_{L^2} &\leqslant \sum_{j=1}^m |(\overline{\lambda}_j^U)^{-1}\langle U_1, Q\overline{\psi}_j^U\rangle_\Omega| \|\overline{\phi}_j^U\|_{L^2} \\
&\leqslant \sqrt{\sum_{j=1}^m (\overline{\lambda}_j^U)^{-2}|\langle U_1, Q\overline{\psi}_j^U\rangle_\Omega|^2}\sqrt{\sum_{j=1}^m \|\overline{\phi}_j^U\|_{L^2}^2} \\
&\leqslant \|G_{Q^2}^U\|\sqrt{\sum_{j=1}^m \|\overline{\phi}_j^U\|_{L^2}^2}\|U_1\|_{L^2}, \qquad (4.29)
\end{aligned}$$

and similarly,

$$\|\nabla U_2\|_{L^\infty} \leqslant \|G_{Q^2}^U\|\sqrt{\sum_{j=1}^m \|\nabla\overline{\phi}_j^U\|_{L^\infty}^2}\|U_1\|_{L^2}. \qquad (4.30)$$

Here, for convenience, we estimate the L^∞ norm of ∇U_2 rather than the L^2 norm. This allows us to sharpen some of the previous estimates. For instance, (4.7) becomes

$$|\langle v\cdot\nabla U, v\rangle| \leqslant |\langle v\cdot\nabla U_1, v\rangle| + |\langle v\cdot\nabla U_2, v\rangle| \leqslant 2K_4\|\nabla U_1\|_{L^2}(\|v\|_{L^2}^2 + \|\nabla v\|_{L^2}^2) + \|\nabla U_2\|_{L^\infty}\|v\|_{L^2}^2.$$

Accordingly, the coercivity estimate for the linear operator in (4.8) becomes

$$\langle L_1^v v, v\rangle \geqslant \left(\frac{1}{4} - \eta_1 - \overline{\lambda} - 2K_4\|\nabla U_1\|_{L^2} - \|\nabla U_2\|_{L^\infty} - |\lambda^{\mathrm{con}}|\right)\|v\|_{L^2}^2 + (1 - 2K_4\|\nabla U_1\|_{L^2})\|\nabla v\|_{L^2}^2. \qquad (4.31)$$

Similarly, the residual defined in (4.4) satisfies

$$|\langle\hat{\mathrm{E}}^v, v_1^*\rangle| = |\langle\Pi\mathrm{E}^v + \Pi(U\cdot\nabla\overline{v} + \overline{v}\cdot\nabla U) - \lambda^{\mathrm{con}}\overline{v}, v_1^*\rangle| \leqslant (\varepsilon^v + \varepsilon_5)\|v_1^*\|_{L^2}, \qquad (4.32)$$

where via the orthogonality $\langle v_1^*, \overline{v}\rangle = 0$ (4.6), we have

$$\varepsilon_5 := (\|U_1\|_{L^2} + \|U_2\|_{L^2})\|\nabla\overline{v}\|_{L^\infty} + \|\nabla U_1\|_{L^2}\|\overline{v}\|_{L^\infty} + \|\nabla U_2\|_{L^\infty}. \qquad (4.33)$$

Since $\|\overline{v}\|_{L^2} = 1$, the final term does not carry a factor of $\|\overline{v}\|_{L^2}$.

Continuity estimate in L^4. We estimate the difference between $U_1^* := T_R^U(U_1) \in \mathcal{H}_R^1$ and $\widehat{U}_1^* := T_R^U(\widehat{U}_1) \in \mathcal{H}_R^1$. By (4.24), we take differences and plug in $g = U_1^* - \widehat{U}_1^*$, to get

$$\langle L_1^U \delta U^* + (L_2^U - L_{\text{ap}}^U)\delta U^*, \delta U^* \rangle = -\langle (\widehat{U}_1 + G^U \widehat{U}_1) \cdot \nabla (G^U \delta U) + (\delta U + G^U \delta U) \cdot \nabla (U_1^* + G^U U_1), \delta U^* \rangle, \tag{4.34}$$

where we denote $\delta U^* := U_1^* - \widehat{U}_1^*$, $\delta U := U_1 - \widehat{U}_1$, and use the cancellation (4.25).

Notice that for the continuity estimate, we do not require sharp constants, but want to gain some regularity to the extent possible. We first provide some estimates for $G^U f$ by $\|f\|$. Recall the definition (4.23) and notice that $\overline{\phi}_j^U \in H^2$ by Lemma 3. We conclude that

$$\|\nabla^i G^U f\|_{L^2} \leqslant C \|f\|_{L^2}, \tag{4.35}$$

where $i = 0, 1$ and C is a constant depending on $\overline{\phi}_j^U, \overline{\psi}_j^U$.

We estimate the difference of the nonlinear term as follows:

$$\begin{aligned} &|\langle (\widehat{U}_1 + G^U \widehat{U}_1) \cdot \nabla (G^U \delta U) + (\delta U + G^U \delta U) \cdot \nabla (U_1^* + G^U U_1), \delta U^* \rangle| \\ &\leqslant C(\|\widehat{U}_1\|_{H^1} + \|U_1^*\|_{H^1} + \|U_1\|_{H^1}) \|\delta U\|_{L^4} \|\delta U^*\|_{L^4}, \end{aligned} \tag{4.36}$$

where C is some constant only depending on $\overline{\phi}_j^U, \overline{\psi}_j^U, R$.

Proof [Proof of (4.36)] Combining the boundedness of G^U in (4.35) with Holder's inequality with multiple functions and Sobolev embedding, we bound the LHS by

$$\begin{aligned} &\leqslant (\|\widehat{U}_1 + G^U \widehat{U}_1\|_{L^4} \|\nabla (G^U \delta U)\|_{L^2} + \|\delta U + G^U \delta U\|_{L^4} \|\nabla (U_1^* + G^U U_1)\|_{L^2}) \|\delta U^*\|_{L^4} \\ &\lesssim (\|\widehat{U}_1 + G^U \widehat{U}_1\|_{H^1} \|\delta U\|_{L^2} + (\|\delta U\|_{L^4} + \|G^U \delta U\|_{H^1})(\|U_1^*\|_{H^1} + \|U_1\|_{H^1})) \|\delta U^*\|_{L^4} \\ &\lesssim (\|\widehat{U}_1\|_{H^1} + \|U_1^*\|_{H^1} + \|U_1\|_{H^1}) \|\delta U\|_{L^4} \|\delta U^*\|_{L^4}, \end{aligned}$$

where in the last inequality, we use the fact that δU is compactly supported. □

Combined with (4.34), the coercivity (4.20), Sobolev embedding of H^1 into L^4 with $\|f\|_{L^4} \lesssim \|f\|_{H^1}$, and the previous step on the a priori bound of H^1 norm, we conclude that

$$\|\delta U^*\|_{L^4} \lesssim \|\delta U\|_{L^4}.$$

Thus T_R^U is a continuous mapping in L^4, in the space $B^R_{x_0^U, x_1^U}$.

Notice that $B^R_{x_0^U, x_1^U}$ is bounded in $\mathcal{H}_R^1$, and by the Rellich–Kondrachov embedding theorem we know that it is a compact subset of L^4. We apply the Schauder fixed-point theorem to the topology induced by L^4. Since T_R^U is continuous, maps the compact subset $B^R_{x_0^U, x_1^U}$ to itself, there exists a fixed point U_1^R such that by (4.24), for any $g \in \mathcal{H}_R^1$, we have

$$\langle L_1^U U_1^R + (L_2^U - L_{\text{ap}}^U) U_1^R, g \rangle = \langle -(U_1^R + G^U U_1^R) \cdot \nabla (U_1^R + G^U U_1^R) - \mathrm{E}^U, g \rangle. \tag{4.37}$$

Taking weak limits. Notice that the divergence-free condition is preserved in the weak limit, and U_1^R has uniform bounds in H^1 by definition of $B^R_{x_0^U, x_1^U}$. We can thus take weak limits for a subsequence of U_1^R in $\mathcal{H}^1$ for $R \to \infty$. Denote U_1^∞ as the weak limit.

Now fix any test function $\varphi \in C_c^\infty$ that is divergence free, for sufficiently large R, $B_R(0)$ contains the support of φ. We compute by taking limits of (4.37) to get

$$\langle L_1^U U_1^\infty + (L_2^U - L_{\text{ap}}^U) U_1^\infty, \varphi \rangle = \langle -(U_1^\infty + G^U U_1^\infty) \cdot \nabla (U_1^\infty + G^U U_1^\infty) - \mathrm{E}^U, \varphi \rangle,$$

where we use an integration by parts for the diffusion term on the left-hand side. For the convergence of the right-hand side, we use the fact that in L^2, $\nabla^i G^U U_1^R \to \nabla^i G^U U_1^\infty$ by definition (4.23), $i = 0, 1$, and $(U_1^R + G^U U_1^R)\varphi \to (U_1^\infty + G^U U_1^\infty)\varphi$ due to the compact support of φ upon taking a subsequence by Rellich–Kondrachov again, and $\langle f_R, g_R \rangle \to \langle f_\infty, g_\infty \rangle$ for $f_R \to f_\infty$ and $g_R \rightharpoonup g_\infty$. Since the test function φ is arbitrary, we conclude that (4.21) holds for our U_1^∞ and we conclude Proposition 1.

4.4 Proof of Proposition 2

We work on Proposition 2 following an argument similar to the previous subsection by assuming that Proposition 1 holds, and we only highlight the key changes. We construct the finite-rank approximation operator $L^v_{\rm ap}$ of L^v_2 as:

$$L^v_{\rm ap} f := -\sum_{j=1}^{m} (\overline{\lambda}^v_j)^{-1} \langle f, Q\overline{\psi}^v_j \rangle_\Omega P_{\overline{v}} \Pi (Q\overline{\psi}^v_j + r^v_j).$$

Similarly, Lemma 3 and the coercivity of L^v_1 in (4.31) indicate the estimate:

$$\begin{aligned} \langle L^v_1 v_1 + (L^v_2 - L^v_{\rm ap}) v_1, v_1 \rangle \geqslant (\frac{1}{4} - \eta_1 - \overline{\lambda} - 2K_4 \|\nabla U_1\|_{L^2} - \|\nabla U_2\|_{L^\infty} - |\lambda^{\rm con}| - M^v_2) \|v_1\|^2_{L^2} \\ + (1 - 2K_4 \|\nabla U_1\|_{L^2} - M^v_1) \|\nabla v_1\|^2_{L^2}. \end{aligned} \tag{4.38}$$

We choose parameters to ensure that both coefficients on the right-hand side are strictly positive.

Consequently, equation (1.17) can be rewritten as:

$$\begin{aligned} & L^v_1 v_1 + (L^v_2 - L^v_{\rm ap}) v_1 = -N^v(v_1 + v_2) - \widehat{\mathrm{E}}^v, \\ & L^v v_2 = -L^v_{\rm ap} v_1. \end{aligned}$$

Finally, we define v_2 as follows:

$$v_2 = G^v v_1 := \sum_{j=1}^{m} (\overline{\lambda}^v_j)^{-1} \langle v_1, Q\overline{\psi}^v_j \rangle_\Omega \overline{\phi}^v_j. \tag{4.39}$$

Well-definedness of the fixed point map. Define T^v_R via the weak form:

$$\langle L^v_1 v^*_1 + (L^v_2 - L^v_{\rm ap}) v^*_1, g \rangle = \langle -N^v(v_1 + G^v v_1) - \widehat{\mathrm{E}}^v, g \rangle, \tag{4.40}$$

for all $g \in \mathcal{H}^1_R$. We know by (4.38) that the left-hand side induces a coercive bilinear form on $\mathcal{H}^1_R$. As in the case for U, we know it is a bounded bilinear form. We can show $N^v(v_1 + G^v v_1) - \widehat{\mathrm{E}}^v \in L^2$ easily and by Lax-Milgram, we know that there exists $v^*_1 := T^v_R(v_1) \in \mathcal{H}^1_R$ such that (4.40) holds.

A priori estimate in H^1. We first estimate of $\lambda^{\rm lin}$ and $\lambda^{\rm con}$, in a way similar to (4.31):

$$|\lambda^{\rm con}| \leqslant \|\overline{v} \cdot \nabla U\|_{L^2} \leqslant \|\nabla U_1\|_{L^2} \|\overline{v}\|_{L^\infty} + \|\nabla U_2\|_{L^\infty}.$$

For $\lambda^{\rm lin}$, we derive the following bound by integration by parts:

$$\begin{aligned} |\lambda^{\rm lin}(v)| &= |\langle \frac{1}{2} x \cdot \nabla \bar{v} - \Delta \bar{v} - \tilde{U} \cdot \nabla \bar{v} + \bar{v} \cdot \nabla^T \tilde{U}, v \rangle| \leqslant M_0 \|v\|_{L^2} \\ M_0 &:= \left\| P_{\bar{v}} (\frac{1}{2} x \cdot \nabla \bar{v} - \Delta \bar{v} - \bar{U} \cdot \nabla \bar{v} + \bar{v} \cdot \nabla^T \bar{U}) \right\|_{L^2} + \varepsilon_5, \end{aligned} \tag{4.41}$$

where we use the orthogonality of v to $\bar{v}$ and the definition of $P_{\bar{v}}$ and ε_5 is defined by (4.33). By the same argument as U_2, v_2 is bounded by

$$\|v_2\|_{L^2} \leqslant \|v_1\|_{L^2} \|G^v_{Q^2}\| \sqrt{\sum_{j=1}^{m} \|\overline{\phi}^v_j\|^2_{L^2}}.$$

Then we have the following nonlinear estimate by (4.41), (4.39), the Cauchy-Schwarz inequality, and relating the projection to the Gram matrix as in the proof of (4.28):

$$|\langle N^v(v_1 + G^v v_1), v^*_1 \rangle| = |\langle \lambda^{\rm lin}(v_1 + v_2)(v_1 + v_2), v^*_1 \rangle| \leqslant M_0 (\|v_1\|_{L^2} + \|v_2\|_{L^2})^2 \|v^*_1\|_{L^2} \leqslant M^v_3 \|v_1\|^2_{L^2} \|v^*_1\|_{L^2}, \tag{4.42}$$

where we define

$$M_3^v := M_0(1+\sqrt{\|G_{Q^2}^v\|\sum_{j=1}^m \|\overline{\phi}_j^v\|_{L^2}^2})^2.$$

We thus collect the following H^1 estimate by (4.32), (4.38), (4.40) and (4.42):

$$(\frac{1}{4}-\eta_1-\overline{\lambda}-2K_4\|\nabla U_1\|_{L^2}-\|\nabla U_2\|_{L^\infty}-|\lambda^{\mathrm{con}}|-M_2^v)\|v_1\|_{L^2}^2+(1-2K_4\|\nabla U_1\|_{L^2}-M_1^v)\|\nabla v_1\|_{L^2}^2$$
$$\leqslant(\varepsilon^v+\varepsilon_5+M_3^v\|v_1\|_{L^2}^2)\|v_1^*\|_{L^2}.$$

As in the case of U, we prepare the following assumption.

Assumption 7 (Bounded mapping assumption for v) *Recall from Proposition 1 that*

$$\|U_1\|_{L^2}\leqslant x_0^U,\quad \|\nabla U_1\|_{L^2}\leqslant x_1^U.$$

We also denote the bound of U_2 as

$$\|U_2\|_{L^2}\leqslant y_0^U,\quad \|\nabla U_2\|_{L^\infty}\leqslant y_1^U.$$

We assume

$$M_4^v := (M_5)^2-4M_3^v(\varepsilon^v+\varepsilon_5)>0.\quad M_5:=\frac{1}{4}-\eta_1-\overline{\lambda}-2K_4x_1^U-y_1^U-|\lambda^{\mathrm{con}}|-M_2^v.$$

We see that the map T_R^v maps the ball $B_{x_0^v,x_1^v}^R$ to itself, where

$$x_0^v := \frac{2(\varepsilon^v+\varepsilon_5)}{M_5+\sqrt{M_4^v}},$$

$$x_1^v := \sqrt{\frac{M_5}{1-2K_4x_1^U-M_1^v}}\frac{x_0^v}{2}.$$

We will verify Assumption 7 in Subsection 4.5.

Continuity estimate in L^4. For $v_1^* := T_R^v(v_1), \widehat{v}_1^* := T_R^v(\widehat{v}_1)$, we denote $\delta v^* := v_1^*-\widehat{v}_1^*$, $\delta v := v_1-\widehat{v}_1$. By (4.40), we have

$$\langle L_1^v\delta v^*+(L_2^v-L_{\mathrm{ap}}^v)\delta v^*,\delta v^*\rangle = -\langle\lambda^{\mathrm{lin}}(\widehat{v}_1+G^v\widehat{v}_1)(\delta v+G^v\delta v)+\lambda^{\mathrm{lin}}(\delta v+G^v\delta v)(v_1+G^vv_1),\delta v^*\rangle. \tag{4.43}$$

Recalling (4.39) and noticing that $\overline{\phi}_j^v\in H^2$, we conclude similarly $\|G^vf\|_{L^2}\leqslant C\|f\|_{L^2}$. Using (4.41) to estimate the right-hand side of (4.43), we get the upper bound

$$M_0(C+1)^2(\|v_1\|_{L^2}+\|\widehat{v}_1\|_{L^2})\|\delta v\|_{L^2}\|\delta v^*\|_{L^2}.$$

By (4.43), (4.38), the Sobolev embedding of H^1 into L^4 into L^2, and the a priori bound of the H^1 norm, we conclude that

$$\|\delta v^*\|_{L^4}\lesssim\|\delta v\|_{L^4}.$$

Thus T_R^v is a continuous mapping in L^4 in the space $B_{x_0^v,x_1^v}^R$. By the Schauder fixed-point theorem, there exists a fixed point v_1^R such that by (4.40), for any $g\in\mathcal{H}_R^1$, we have

$$\langle L_1^vv_1^R+(L_2^v-L_{\mathrm{ap}}^v)v_1^R,g\rangle=\langle -N^v(v_1^R+G^vv_1^R)-\widehat{\mathrm{E}}^v,g\rangle.$$

Taking weak limits. Notice that the divergence-free condition and orthogonality condition are preserved in the weak limit. Denote $v_1^\infty \in \mathcal{H}^1$ as the weak limit for a subsequence of v_1^R as R tends to infinity. For any test function $\varphi \in C_c^\infty \cap \mathcal{H}^1$, we have

$$\langle L_1^v v_1^\infty + (L_2^v - L_{\rm ap}^v) v_1^\infty, \varphi\rangle = \langle -N^v(v_1^\infty + G^v v_1^\infty) - \widehat{\mathrm{E}}^v, \varphi\rangle,$$

where the only change is to show $\lambda^{\rm lin}(v_1^R + G^v v_1^R) \to \lambda^{\rm lin}(v_1^\infty + G^v v_1^\infty)$, this is true by definition of the linear operator $\lambda^{\rm lin}$ in (4.41). Since the test function φ is arbitrary, we conclude Proposition 2.

4.5 Numerical results

Although comprehensive numerical details are presented in subsequent sections, we summarize the key results here for convenience. In particular, we complete the proofs of the propositions by verifying Assumptions 6 and 7. We remark that our verifications are carried out effectively in a subspace of H^1_σ, leveraging axissymmetry and parities, to reduce the number of basis functions in our finite-rank approximation. We begin by listing all quantities verified by numerics:

$$\|\mathrm{E}^U\|_{L^2} \leqslant \varepsilon^U = 6.5\times 10^{-7}, \tag{4.44}$$

$$\frac{\nabla\bar{U} + \nabla^T\bar{U}}{2} + \eta_1 I + Q \succeq 0, \quad \eta_1 = 0.199, \tag{4.45}$$

$$\|\lambda_{\max}(Q)\|_{L^\infty} \leqslant 4.5, \tag{4.46}$$

$$\|\mathrm{E}^v\|_{L^2} \leqslant \varepsilon^v = 1.9\times 10^{-5}, \tag{4.47}$$

$$\overline{\lambda} \approx -0.11314203274385938 \leqslant -0.113, \tag{4.48}$$

$$\|\overline{v}\|_{L^\infty} \leqslant 2.52, \tag{4.49}$$

$$\|\nabla\overline{v}\|_{L^\infty} \leqslant 3.4, \tag{4.50}$$

$$\|P_{\bar{v}}(\frac{1}{2}x\cdot\nabla\bar{v} - \Delta\bar{v} - \bar{U}\cdot\nabla\bar{v} + \bar{v}\cdot\nabla^T\bar{U})\|_{L^2} \leqslant 6.38, \tag{4.51}$$

$$\sup_{u\neq 0, u\perp_{L^2} V_N^U} \frac{\|u\|^2_{L^2(\Omega)}}{\|u\|_E^2}, \sup_{u\neq 0, u\perp_{L^2} V_N^v} \frac{\|u\|^2_{L^2(\Omega)}}{\|u\|_E^2} \leqslant 0.1024, \tag{4.52}$$

$$\sup_{u\in V_N^U, u\neq 0} \frac{\langle u, Qu\rangle_\Omega - \sum_{j=1}^m \overline{\lambda}_j^{-1}\langle u, Q\overline{\psi}_j^U\rangle_\Omega^2}{\|u\|_E^2} \leqslant 0.46, \tag{4.53}$$

$$\sup_{u\in V_N^v, u\neq 0} \frac{\langle u, Qu\rangle_\Omega - \sum_{j=1}^m \overline{\lambda}_j^{-1}\langle u, Q\overline{\psi}_j^v\rangle_\Omega^2}{\|u\|_E^2} \leqslant 0.46, \tag{4.54}$$

$$\varepsilon_3^U, \varepsilon_4^U, \varepsilon_3^v, \varepsilon_4^v \leqslant 5.3\times 10^{-5}, \tag{4.55}$$

$$\sqrt{\mathrm{tr}(G^U_{Q^2} G^U_r)} \leqslant 0.0012, \tag{4.56}$$

$$\|G^U_{Q^2}\|_F \leqslant 0.025, \tag{4.57}$$

$$\sqrt{\sum_{j=1}^m\sum_{l=1}^m \|\overline{\phi}_l^U\cdot\nabla\overline{\phi}_j^U\|^2_{L^2}} \leqslant 0.12, \tag{4.58}$$

$$\sqrt{\sum_{j=1}^m \|\nabla\overline{\phi}_j^U\|^2_{L^\infty}} \leqslant 1.33, \tag{4.59}$$

$$\sqrt{\sum_{j=1}^m \|\overline{\phi}_j^U\|^2_{L^2}} \leqslant 0.36, \tag{4.60}$$

$$\sqrt{\mathrm{tr}(G^v_{Q^2} G^v_r)} \leqslant 0.004, \tag{4.61}$$

$$\|G^v_{Q^2}\|_F \leqslant 0.029, \tag{4.62}$$

$$\sqrt{\sum_{j=1}^{m} \|\overline{\phi}^v_j\|^2_{L^2}} \leqslant 1.02\,. \tag{4.63}$$

4.5.1 Verification of Proposition 1

To verify Proposition 1, we need to check that

$$M^U_4 = (\frac{1}{4} - \eta_1 - M^U_2)^2 - 4M^U_3\varepsilon^U > 0.$$

Since the residual satisfies

$$\varepsilon^U \leqslant 6.5 \times 10^{-7},$$

and we take $\eta_1 = 0.199$, M^U_4 reduces to

$$M^U_4 \geqslant (0.051 - M^U_2)^2 - 2.8 \times 10^{-6} \times M^U_3.$$

We still need to estimate M^U_2 and M^U_3.

Step 1: Estimate of M^U_2. M^U_2 is defined as

$$M^U_2 = \eta_2 M^U_1 + \varepsilon^U_3 \|\lambda_{\max}(Q)\|_{L^\infty} + K^U_7\,,$$

where $\eta_2 = 0.005$ is the L^2 coefficient of E-norm in (4.10). The term M_1 is given by

$$M^U_1 = K^U_5 + \frac{K^U_6}{(1-\varepsilon^U_4)^2},$$

where

$$K^U_6 = \sup_{u\in V^U_N, u\neq 0} \frac{\langle u, Qu\rangle_\Omega - \sum_{j=1}^m \overline{\lambda}_j^{-1}\langle u, Q\overline{\psi}^U_j\rangle^2_\Omega}{\|u\|^2_E} \leqslant 0.46,$$

and

$$K^U_5 = \|\lambda_{\max}(Q)\|_{L^\infty} \sup_{u\neq 0, u\perp_{L^2} V^U_N} \frac{\|u\|^2_{L^2(\Omega)}}{\|u\|^2_E} \leqslant 0.47$$

Therefore, we get

$$M^U_1 \leqslant 0.47 + \frac{0.46}{(1-5.3\times 10^{-5})^2} \leqslant 0.9301.$$

By the definition of the constant K^U_7, we can bound it as follows:

$$K^U_7 = \sqrt{\mathrm{tr}(G^U_{Q^2} G^U_r)} \leqslant 0.0012.$$

Therefore, we obtain

$$M^U_2 \leqslant 0.005 \times 0.9301 + 5.3 \times 10^{-5} \times 4.5 + 0.0012 \leqslant 0.0061.$$

Step 2: Estimate of M^U_3 and M^U_4. M^U_3 is defined and bounded by

$$M^U_3 = \sqrt{\|G^U_{Q^2}\| \sum_{j=1}^m \|\nabla\overline{\phi}^U_j\|^2_{L^\infty}} + \|G^U_{Q^2}\| \sqrt{\sum_{j=1}^m\sum_{i=1}^m \|\overline{\phi}^U_i \cdot \nabla\overline{\phi}^U_j\|^2_{L^2}} \leqslant \sqrt{0.025}\times 1.33 + 0.025\times 0.12 \leqslant 0.22.$$

Therefore, M^U_4 has the following lower bound:

$$M^U_4 \geqslant (\frac{1}{4} - 0.199 - 0.0061)^2 - 4\times 0.22 \times 6.5 \times 10^{-7} \geqslant 0.002.$$

Step 3: Estimate of x_0^U and x_1^U. Finally, we conclude that

$$x_0^U = \frac{2\varepsilon^U}{\left(\frac{1}{4} - \eta_1 - M_2^U + \sqrt{M_4^U}\right)} \leqslant \frac{2 \times 6.5 \times 10^{-7}}{0.25 - 0.199 - 0.005 + \sqrt{0.002}} \leqslant 1.44 \times 10^{-5},$$

and

$$x_1^U = \sqrt{\frac{\frac{1}{4} - \eta_1 - M_2^U}{1 - M_1^U}} \frac{x_0^U}{2} \leqslant \sqrt{\frac{\frac{1}{4} - 0.199}{1 - 0.9301}} \times \frac{1.44 \times 10^{-5}}{2} \leqslant 6.2 \times 10^{-6}.$$

By the estimates (4.29) and (4.30), U_2 is bounded by:

$$y_0^U := \|U_2\|_{L^2} \leqslant \|U_1\|_{L^2} \|G_{Q^2}^U\|_F \sqrt{\sum_{j=1}^m \|\overline{\phi}_j^U\|_{L^2}^2} \leqslant 1.44 \times 10^{-5} \times 0.025 \times 0.36 \leqslant 1.3 \times 10^{-7},$$

$$y_1^U := \|\nabla U_2\|_{L^\infty} \leqslant \|U_1\|_{L^2} \|G_{Q^2}^U\|_F \sqrt{\sum_{j=1}^m \|\nabla \overline{\phi}_j^U\|_{L^\infty}^2} \leqslant 1.44 \times 10^{-5} \times 0.025 \times 1.33 \leqslant 4.8 \times 10^{-7}.$$

This finishes the proof of Proposition 1.

4.5.2 Verification of Proposition 2

For Proposition 2, similarly, we need to verify

$$M_4^v = (M_5)^2 - 4M_3^v(\varepsilon^v + \varepsilon_5) > 0,$$

where we recall

$$M_5 := \frac{1}{4} - \eta_1 - \overline{\lambda} - 2K_4 x_1^U - y_1^U - |\lambda^{\mathrm{con}}| - M_2^v.$$

Step 1: Estimate of ε_5 and $|\lambda^{\mathrm{con}}|$. Therefore, ε_5 and λ^{con} are bounded by

$$|\lambda^{\mathrm{con}}| \leqslant \|\nabla U_1\|_{L^2} \|\overline{v}\|_{L^\infty} + \|\nabla U_2\|_{L^\infty} \leqslant 6.2 \times 10^{-6} \times 2.52 + 4.8 \times 10^{-7} \leqslant 1.62 \times 10^{-5},$$
$$\varepsilon_5 \leqslant (1.44 \times 10^{-5} + 1.3 \times 10^{-7}) \times 3.4 + 6.2 \times 10^{-6} \times 2.52 + 4.8 \times 10^{-7} \leqslant 6.6 \times 10^{-5}.$$

We have verified that the residuals satisfy

$$\varepsilon^v + \varepsilon_5 \leqslant 1.9 \times 10^{-5} + 6.6 \times 10^{-5} \leqslant 8.5 \times 10^{-5}.$$

Step 2: Estimate of M_5. Recall that $K_4 \leqslant 0.091$ is introduced in Lemma 6. We can simplify M_5 as follows:

$$M_5 \geqslant \frac{1}{4} - 0.199 + 0.113 - 2 \times 0.091 \times 6.2 \times 10^{-6} - 4.8 \times 10^{-7} - 1.62 \times 10^{-5} - M_2^v \geqslant 0.1639 - M_2^v.$$

M_2^v is defined by

$$M_2^v = \eta_2 M_1^v + \varepsilon_3^v \|\lambda_{\max}(Q)\|_{L^\infty} + K_7^v.$$

Since M_1^v is bounded by

$$M_1^v = K_5^v + \frac{K_6^v}{(1 - \varepsilon_4^v)^2} \leqslant 0.47 + \frac{0.46}{(1 - 5.3 \times 10^{-5})^2} \leqslant 0.9301,$$

we obtain the following upper bound for M_2^v:

$$M_2^v \leqslant 0.005 \times 0.9301 + 4.5 \times 5.3 \times 10^{-5} + 0.004 \leqslant 0.0089.$$

M_5 thus has the following lower bound:

$$M_5 \geqslant 0.1639 - 0.0089 = 0.155.$$

Step 3: Estimate of M_3^v and M_4^v. Recall that M_3^v is defined by

$$M_3^v = M_0(1 + \sqrt{\|G_{Q^2}^v\| \sum_{j=1}^{m} \|\overline{\phi}_j^v\|_{L^2}^2})^2,$$

where

$$\begin{aligned} M_0 &= \|P_{\overline{v}}(\frac{1}{2}x \cdot \nabla \overline{v} - \Delta \overline{v} - \overline{U} \cdot \nabla \overline{v} + \overline{v} \cdot \nabla^T \overline{U})\|_{L^2} + \varepsilon_5 \\ &\leqslant 6.38 + 6.6 \times 10^{-5} \\ &\leqslant 6.4, \end{aligned}$$

which yields the following approximate values:

$$\begin{aligned} M_3^v &\leqslant 6.4 \times (1 + 1.02 \times \sqrt{0.029})^2 \leqslant 8.82, \\ M_4^v &\geqslant 0.155^2 - 4 \times 8.82 \times 8.5 \times 10^{-5} \geqslant 0.021. \end{aligned}$$

Step 4: Estimate of $\|v\|$ and $|\lambda|$. We collect all estimates above and obtain:

$$\begin{aligned} x_0^v &= \frac{2(\varepsilon^v + \varepsilon_5)}{M_5 + \sqrt{M_4^v}} \leqslant \frac{2 \times 8.5 \times 10^{-5}}{0.155 + \sqrt{0.021}} \leqslant 5.67 \times 10^{-4}, \\ x_1^v &= \sqrt{\frac{M_5}{1 - 2K_4\|\nabla U\|_{L^2} - M_1^v}} \frac{x_0^v}{2} \leqslant \sqrt{\frac{0.155}{1 - 2 \times 0.091 \times 6.2 \times 10^{-6} - 0.9301}} \times \frac{5.67 \times 10^{-4}}{2} \leqslant 4.3 \times 10^{-4}. \end{aligned}$$

Hence, we have verified the existence of v. The estimate of $\lambda^{\mathrm{lin}}(v)$ follows:

$$|\lambda^{\mathrm{lin}}(v)| \leqslant M_0\|v\|_{L^2} \leqslant M_0(1 + \sqrt{\sum_{j=1}^{m} \|G_{Q^2}^v\| \|\overline{\phi}_j^v\|_{L^2}^2}) x_0^v \leqslant 6.4 \times (1 + 0.18) \times 5.67 \times 10^{-4} \leqslant 0.0044.$$

Finally, we confirm that:

$$|\lambda| \leqslant |\lambda^{\mathrm{lin}}(v)| + |\lambda^{\mathrm{con}}| \leqslant 0.0045 \ll |\overline{\lambda}| \approx 0.113.$$

This concludes the numerical verification and thus completes the proof of the proposition 2.

5 Numerical Construction of Approximate Solutions

In this section, we detail the numerical procedures used to solve the equation (1.12). In prior research [27], boundary conditions of the form:

$$A_\alpha(\theta) = \alpha(0, 0, e^{-4\cot^2\theta}),$$

were used, where α is a parameter. As α increased, the eigenvalue associated with the linear operator $\mathcal{L}(\overline{U})$ crossed the imaginary axis at approximately $\alpha \approx 292$. However, the finite-rank approximation in Section 4.2 for solutions with such large values of boundary conditions will be inefficient, rendering the numerical verification challenging. To overcome this, we introduce an alternative numerical strategy aimed at obtaining a smaller solution associated with a negative eigenvalue. Instead of tuning α and tracking eigenvalue crossings, we optimize the field $\overline{U}$ directly: we compute $\nabla\lambda(\overline{U})$ and run a projected gradient descent to obtain a small solution with a negative eigenvalue. Then, we interpolate the approximate solution to enforce exact divergence-free conditions.

This section is structured as follows. In Section 5.1, we derive the gradient descent method for the eigenvalue $\lambda(\widetilde{U})$. Section 5.2 simplifies the problem by leveraging symmetries (axisymmetry in

spherical coordinates). In Section 5.3, we discretize the equations using the finite element method. Section 5.4 details the computation of the eigenvalue. The first four subsections produce a finite-element candidate; we then refine it to a high-precision candidate using a spectral basis, which is divergence-free and smooth away from the origin. In Section 5.5, we extend the obtained solutions to the entire space. Section 5.6 presents the construction of a divergence-free basis. In Section 5.7, we interpolate our numerical solutions onto this basis and reduce residuals. Finally, Section 5.8 summarizes our numerical approach and provides pseudo-code for the implemented algorithm.

5.1 Gradient descent for eigenvalue

To compute the desired eigenvalue, we adopt a gradient descent approach. The iterative update from $\bar{U}_n$ to $\bar{U}_{n+1}$ is defined as follows. Recall that $\lambda(\tilde{U})$, as a functional of $\tilde{U}$, is the eigenvalue of $\mathcal{L}(\tilde{U})$ with the smallest real part. First, we calculate the Fréchet derivative of $\lambda(\tilde{U})$. Throughout, we assume that $\lambda(\tilde{U})$ is simple (thus real) and isolated, which guarantees that it is also a simple and isolated eigenvalue for $\mathcal{L}(\tilde{U})^*$. Let $v^l(\tilde{U}), v^r(\tilde{U})$ denote the left and right eigenvectors associated with the eigenvalue $\lambda(\tilde{U})$, respectively satisfying:

$$\mathcal{L}(\tilde{U})v^r(\tilde{U}) = \lambda(\tilde{U})v^r(\tilde{U}), \quad \mathcal{L}(\tilde{U})^* v^l(\tilde{U}) = \lambda(\tilde{U})v^l(\tilde{U}).$$

Denoting $v_n^r = v^r(\bar{U}_n)$ and $v_n^l = v^l(\bar{U}_n)$ respectively, the gradient of $\lambda(\bar{U}_n)$ is explicitly given by:

$$\frac{\delta\lambda(\bar{U}_n)}{\delta\tilde{U}} = \frac{v_n^l \cdot \nabla^T v_n^r - v_n^r \cdot \nabla v_n^l}{\langle v_n^l, v_n^r \rangle}. \tag{5.1}$$

A formal derivation of the above equation is provided in Appendix C. This is also known as the non-self-adjoint Hellmann–Feynman formula:

$$\partial\lambda = \langle v^l, (\partial\mathcal{L})v^r \rangle / \langle v^l, v^r \rangle, \quad \partial\mathcal{L}(\delta U) := -(\delta U)\cdot\nabla\,(\cdot) + (\cdot)\cdot\nabla(\delta U).$$

Without additional constraints, the increment g_n would ideally be given by

$$g_n = -k_n \frac{\delta\lambda(\bar{U}_n)}{\delta\tilde{U}},$$

where k_n denotes step size. In practice, k_n can be chosen by different strategies; we use the Barzilai–Borwein method [4] for efficiency.

However, since $\tilde{U}$ is constrained to lie on the solution manifold defined by equation (1.6), the increment g_n must belong to the tangent space of this manifold at the current iterate $\bar{U}_n$:

$$T_{\bar{U}_n} := \{\, g : \mathrm{div} g = 0, \mathcal{L}(\bar{U}_n)\, g = 0 \,\}.$$

Moreover, the boundary condition $A_n(\omega)$ with $\omega = \frac{x}{|x|}$ is updated together with $\bar{U}_n$. In addition to the tangent-space constraint, we impose conditions on $A(\omega)$ that governs the far-field behavior of $\tilde{U}$. The key motivation is to ensure that the most negative eigenvalue of the symmetric gradient

$$Q_s(x) = \frac{1}{2}(\nabla U(x) + \nabla^T U(x)),$$

decays as rapidly as possible in the far field. Using the ansatz $\bar{U}_n \approx \frac{A_n(\omega)}{|x|}$, we obtain

$$Q_{s,n} \approx \frac{Q_{s,n}^A(\omega)}{|x|^2},$$

so the radial decay rate is fixed at $|x|^{-2}$, while the prefactor $Q_{s,n}^A(\omega)$ depends on $A_n(\omega)$ and controls the size of the most negative eigenvalue. To control this prefactor and to ensure numerical stability, we introduce a positive constant $\gamma_U > 0$ and impose two boundary constraints on A_{n+1}:

1. Regularity bound (to sufficient smoothness of $A(\omega)$):

$$\|\nabla^2 A(\omega)\|_{L^\infty} \leqslant \gamma_U, \tag{5.2}$$

2. Spectral bound (to suppress the most negative eigenvalue in the far field):

$$\lambda_{\max}(-Q^A_{s,n}(\omega)) \leqslant \gamma_U. \tag{5.3}$$

Combining these requirements, we determine the increment by solving the convex problem:

$$\min_{g_n} \|g_n + k_n \frac{\delta\lambda(\bar{U}_n)}{\delta\tilde{U}}\|_{L^2}, \quad \text{s.t. } g_n \in T_{\bar{U}_n},\ A_{n+1} \text{ satisfies (5.2) and (5.3).}$$

This problem can be solved efficiently in MATLAB. With the increment g_n determined by solving the constrained optimization problem, we obtain the tentative update

$$\bar{U}^*_{n+1} = \bar{U}_n + g_n.$$

Since $\bar{U}^*_{n+1}$ is not yet a solution to equation (1.6), we project it onto the solution manifold while fixing the boundary condition $A_{n+1}(\omega)$, yielding the updated solution $\bar{U}_{n+1}$. In practice, we discretize the system (1.6) using the finite element method, resulting in a nonlinear equation for the numerical solution $\bar{U}$. We then fix the boundary condition A_{n+1} and apply Newton's method with initial guess $\bar{U}^*_{n+1}$ to solve the discretized version of equation (1.6), thereby obtaining $\bar{U}_{n+1}$. A few Newton steps suffice; we stop once the discrete residual falls below a prescribed tolerance.

We iterate this procedure until convergence. If the eigenvalue satisfies $\lambda < -0.1$, the iteration terminates. Otherwise, we incrementally increase γ_U and repeat the above steps.

5.2 Axisymmetry, parity and boundary conditions

We consider the axisymmetric case throughout the computations and denote the cylindrical coordinates as (ρ, z, ϕ). We also impose symmetry conditions in z: even for the profile problem (U, P) and odd for the eigenvalue problem (v, q). In the Euclidean coordinates, a vector field (u_x, u_y, u_z) is *even in z* if

$$u_x(x, y, -z) = u_x(x, y, z), \quad u_y(x, y, -z) = u_y(x, y, z), \quad u_z(x, y, -z) = -u_z(x, y, z).$$

In other words, the horizontal components are even functions of z, while the vertical component is odd. In spherical coordinates (r, θ, ϕ), the reflection $z \mapsto -z$ corresponds to $\theta \mapsto \pi - \theta$. The condition of being even in z then reads

$$u_r(r, \pi - \theta, \phi) = u_r(r, \theta, \phi), \quad u_\phi(r, \pi - \theta, \phi) = u_\phi(r, \theta, \phi), \quad u_\theta(r, \pi - \theta, \phi) = -u_\theta(r, \theta, \phi).$$

The definition of *odd in z* is the opposite.

We note that if $\widetilde{\lambda}$ is a simple eigenvalue, since $\widetilde{U}$ is even in z, $\widetilde{v}$ must be either even or odd. Numerical evidence indicates that eigenvalues associated with odd eigenvectors decrease more rapidly. Therefore, we assume $\widetilde{v}$ is odd with respect to z.

In practice, for the construction of accurate approximate solutions in this section, we adopt spherical coordinates (r, θ, ϕ). Due to the axisymmetry and parity, the computational domain reduces to $r \in \mathbb{R}_+$ and $\theta \in \left[0, \frac{\pi}{2}\right]$. Since the spherical coordinates (r, θ) correspond to a polar representation of the cylindrical coordinates (ρ, z), boundary conditions in the spherical coordinates are thus given by:

- At $\theta = 0$, which corresponds to $\rho = 0$, we have $e_r = e_z$ and $e_\theta = e_\rho$. To ensure $\Delta U, \Delta v \in L^2$ and smoothness of the pressure, we impose a Dirichlet zero condition on the ρ and ϕ components of the velocity field and a Neumann zero condition on the z component and the pressure. This implies $\widetilde{U}_\theta(r, 0) = \widetilde{U}_\phi(r, 0) = 0$ and $\partial_\theta \widetilde{U}_r(r, 0) = \partial_\theta \widetilde{P}(r, 0) = 0$. Likewise, $\widetilde{v}_\theta(r, 0) = \widetilde{v}_\phi(r, 0) = 0$ and $\partial_\theta \widetilde{v}_r(r, 0) = \partial_\theta \widetilde{q}(r, 0) = 0$.

- At $\theta = \frac{\pi}{2}$, which corresponds to $z = 0$, we have $e_r = e_\rho$ and $e_\theta = -e_z$, implying $\partial_\theta \widetilde{U}_r\left(r, \frac{\pi}{2}\right) = \widetilde{U}_\theta\left(r, \frac{\pi}{2}\right) = \partial_\theta \widetilde{U}_\phi\left(r, \frac{\pi}{2}\right) = \partial_\theta \widetilde{P}\left(r, \frac{\pi}{2}\right) = 0$ by even symmetry. Conversely, by odd symmetry, we have $\widetilde{v}_r\left(r, \frac{\pi}{2}\right) = \partial_\theta \widetilde{v}_\theta\left(r, \frac{\pi}{2}\right) = \widetilde{v}_\phi\left(r, \frac{\pi}{2}\right) = \widetilde{q}\left(r, \frac{\pi}{2}\right) = 0$.

- At $r = 0$, which corresponds to the origin in the cylindrical coordinates, the even symmetry in z and the Dirichlet zero condition in ρ directly lead to $\widetilde{U}(0, \theta) = (0, 0, 0)$. Similarly, we impose $\partial_r \widetilde{P}(0, \theta) = 0$ and $\widetilde{q}(0, \theta) = 0$. Finally, since at the origin in cylindrical coordinates, $\widetilde{v}$ must align with the direction e_z, we know that $\widetilde{v}$ takes the following form for a constant C:

$$\widetilde{v} = C(\cos\theta, -\sin\theta, 0). \tag{5.4}$$

  Another reason why we need to impose this boundary condition at $r = 0$ is because we have to cancel the two terms that contain the singular factor $\frac{1}{r^2}$ in the Laplacian operator Δ in the spherical coordinates, see Appendix D. If we do not enforce this boundary condition and allow $\widetilde{v}$ to have modes $\sin(m\theta)$ or $\cos(m\theta)$ with $m \geqslant 2$, then the equation for $\widetilde{v}$ will generate some singular terms that do not cancel each other, rendering $\widetilde{v} \notin H^2$.

- At the far-field boundary, the condition is given by the function $A(\theta)$: $\lim_{r\to+\infty} r\widetilde{U}(r, \theta) = A(\theta)$. We require $\widetilde{v}$ to decay faster than $\widetilde{U}$ by imposing $\lim_{r\to+\infty} r\widetilde{v}(r, \theta) = 0$. In [27], the authors estimate the decay rate as approximately $O(r^{-4})$.

Here, $A(\theta)$ satisfies the consistency condition derived from the incompressibility constraint (1.8):

$$A_r(\theta) + \frac{1}{\sin\theta}\partial_\theta(A_\theta(\theta)\sin\theta) = 0. \tag{5.5}$$

5.3 Spherical coordinates and finite element method

In this section, we detail our setting for finite element approximation. The incompressible Navier–Stokes equations in the spherical coordinates read:

$$\begin{cases} -\frac{1}{2}\widetilde{U} - \frac{1}{2}r\partial_r\widetilde{U} + \widetilde{U}\cdot\nabla_{\text{sph}}\widetilde{U} + \nabla_{\text{sph}}\widetilde{P} - \Delta_{\text{sph}}\widetilde{U} = 0, \\ \operatorname{div}_{\text{sph}}\widetilde{U} = 0, \end{cases} \tag{5.6}$$

where ∇_{sph}, $\operatorname{div}_{\text{sph}}$, and Δ_{sph} are the gradient, divergence, and Laplacian operators in the spherical coordinates, respectively (see Appendix D for explicit expressions). The weak form of (5.6) is:

$$\langle\widetilde{U}\cdot\nabla\widetilde{U}, V\rangle - \frac{1}{2}\langle x\cdot\nabla\widetilde{U}, V\rangle - \frac{1}{2}\langle\widetilde{U}, V\rangle - \langle\widetilde{P}, \operatorname{div} V\rangle - \langle Q, \operatorname{div}\widetilde{U}\rangle + \langle\nabla\widetilde{U}, \nabla V\rangle = 0,$$

for all test functions $V \in H_0^1(\mathbb{R}^3)^3, Q \in L^2(\mathbb{R}^3)$. In the spherical coordinates, the weak form reads:

$$\begin{aligned} &\langle\widetilde{U}\cdot\nabla_{\text{sph}}\widetilde{U}, V\rangle_{\text{sph}} - \tfrac{1}{2}\langle r\partial_r\widetilde{U}, V\rangle_{\text{sph}} - \tfrac{1}{2}\langle\widetilde{U}, V\rangle_{\text{sph}} - \langle\widetilde{P}, \operatorname{div}_{\text{sph}} V\rangle_{\text{sph}} \\ &-\langle Q, \operatorname{div}_{\text{sph}}\widetilde{U}\rangle_{\text{sph}} + \langle\nabla_{\text{sph}}\widetilde{U}, \nabla_{\text{sph}} V\rangle_{\text{sph}} = 0, \end{aligned}$$

for all test functions $V \in H^1_{0,\text{sph}}(\mathbb{R}_+ \times [0, \frac{\pi}{2}])^3, Q \in L^2_{\text{sph}}(\mathbb{R}_+ \times [0, \frac{\pi}{2}])$. The inner product is

$$\langle f, g\rangle_{\text{sph}} = \int_{[0,\frac{\pi}{2}]}\int_{[0,\infty]} f^T(r, \theta)g(r, \theta)r^2\sin\theta\mathrm{d}r\mathrm{d}\theta.$$

In practice, we truncate the domain to a finite domain $B(0, R)$ with $R = 20$. The far-field boundary condition $\lim_{r\to+\infty} r\widetilde{U}(r, \theta) = A(\theta)$ is approximated by the Dirichlet boundary condition:

$$\widetilde{U}(r = R, \theta) = \frac{1}{R}A(\theta),$$

where $A(\theta)$ must satisfy the consistency constraint (5.5) derived from incompressibility. We impose a Neumann boundary condition for the pressure: $\partial_r\widetilde{P}(R, \theta) = 0$.

We discretize the domain using finite elements, following closely the method detailed in [27]. Specifically, the computational domain is divided into $N_r \times N_\theta$ squares, with $N_r = 128$ and $N_\theta = 64$. Each square is subdivided into two triangles. As the parameter γ_U increases, a larger computational domain is required to ensure that truncation errors remain negligible. To efficiently handle this domain expansion without modifying the finite element mesh, we adopt a spatial rescaling strategy following the approach described in [27]. Specifically, we fix the computational domain radius at $R = 20$ and introduce a spatial rescaling given by:

$$\widetilde{U}_\kappa(x) = \widetilde{U}(\kappa x).$$

This rescaling is equivalent to expanding the computational domain from $B(0, R)$ to $B(0, \kappa R)$, while allowing the reuse of the same finite element mesh for varying values of γ_U. The scaling factor κ is chosen to be:

$$\kappa = \sqrt{1 + \frac{\gamma_U}{4}}.$$

Thus, the rescaled equations are given by:

$$\begin{aligned} &\kappa^{-1}\langle \widetilde{U} \cdot \nabla_{\mathrm{sph}} \widetilde{U}, V\rangle_{\mathrm{sph}} - \tfrac{1}{2}\langle r\partial_r \widetilde{U}, V\rangle_{\mathrm{sph}} - \tfrac{1}{2}\langle \widetilde{U}, V\rangle_{\mathrm{sph}} - \kappa^{-1}\langle \widetilde{P}, \mathrm{div}_{\mathrm{sph}}\, V\rangle_{\mathrm{sph}} \\ &-\kappa^{-1}\langle Q, \mathrm{div}_{\mathrm{sph}}\, \widetilde{U}\rangle_{\mathrm{sph}} + \kappa^{-2}\langle \nabla_{\mathrm{sph}} \widetilde{U}, \nabla_{\mathrm{sph}} V\rangle_{\mathrm{sph}} = 0, \end{aligned} \tag{5.7}$$

with boundary conditions:

$$\widetilde{U}(r = R, \theta) = \frac{1}{\kappa R} A(\theta).$$

Here, we omit the subscript κ for simplicity. Finally, we discretize the weak form (5.7) using Lagrange quadratic polynomials (P2 elements) for $\widetilde{U}$ and linear polynomials (P1 elements) for $\widetilde{P}$. The discretization involves assembling not only bilinear forms but trilinear forms, such as the convection term $\langle \widetilde{U} \cdot \nabla_{\mathrm{sph}} \widetilde{U}, V\rangle_{\mathrm{sph}}$, which require handling third-order tensors. For this reason, we implement our finite element discretization using the Python package *scikit-fem* rather than the more commonly used *FEniCS*.

5.4 Eigenvalue solver

Suppose we have obtained a solution $\widetilde{U}$. Our next step is to compute the eigenvalues of the linearized operator $\mathcal{L}(\widetilde{U})$. The eigenvalue problem in the spherical coordinates reads:

$$\begin{cases} -\frac{1}{2}\widetilde{v} - \frac{1}{2} r\partial_r \widetilde{v} + \widetilde{U} \cdot \nabla_{\mathrm{sph}} \widetilde{v} + \widetilde{v} \cdot \nabla_{\mathrm{sph}} \widetilde{U} + \nabla_{\mathrm{sph}} \widetilde{q} - \Delta_{\mathrm{sph}} \widetilde{v} = \widetilde{\lambda} \widetilde{v}, \\ \mathrm{div}_{\mathrm{sph}}\, \widetilde{v} = 0. \end{cases}$$

We start by truncating the domain to a ball $B(0, R)$. The same spatial rescaling by κ discussed earlier is then applied. Consequently, the weak form of the eigenvalue problem is expressed as:

$$\begin{aligned} &\kappa^{-1}\langle \widetilde{U} \cdot \nabla_{\mathrm{sph}} v, u\rangle_{\mathrm{sph}} + \kappa^{-1}\langle v \cdot \nabla_{\mathrm{sph}} \widetilde{U}, u\rangle_{\mathrm{sph}} - \tfrac{1}{2}\langle r\partial_r v, u\rangle_{\mathrm{sph}} - \tfrac{1}{2}\langle v, u\rangle_{\mathrm{sph}} - \kappa^{-1}\langle q, \mathrm{div}_{\mathrm{sph}}\, u\rangle_{\mathrm{sph}} \\ &-\kappa^{-1}\langle p, \mathrm{div}_{\mathrm{sph}}\, v\rangle_{\mathrm{sph}} + \kappa^{-2}\langle \nabla_{\mathrm{sph}} v, \nabla_{\mathrm{sph}} u\rangle_{\mathrm{sph}} = \lambda \langle v, u\rangle_{\mathrm{sph}}, \end{aligned} \tag{5.8}$$

for all test functions $u \in H^1_{0,\mathrm{sph}}(\mathbb{R}_+ \times [0, \frac{\pi}{2}])^3, p \in L^2_{\mathrm{sph}}(\mathbb{R}_+ \times [0, \frac{\pi}{2}])$. We impose a homogeneous Dirichlet boundary condition at the truncation radius $r = R$: $\widetilde{v}(R, \theta) = (0, 0, 0)$ and a Neumann boundary condition for the pressure: $\partial_r \widetilde{q}(R, \theta) = 0$.

We discretize this weak form using the finite element method described in the previous section, which yields a generalized matrix eigenvalue problem of the form:

$$Ax = \lambda Bx,$$

where A corresponds to the discretization of the left-hand side of equation (5.8), and B represents the discretization of the inner product term on the right-hand side. The resulting eigenvalue problem is solved numerically using MATLAB.

Remark 7 In [27], the authors noted that directly imposing Dirichlet boundary conditions at a finite radius R might slightly distort the computed solutions. For this reason, the numerical settings described in this subsection and the previous section are employed only within the gradient descent iterations for obtaining coarse solutions $\overline{U}$ and $\overline{v}$, rather than for rigorous numerical analysis. To minimize potential distortions and obtain accurate numerical solutions, we adopt an interpolation-based extension technique, as detailed in the subsequent section.

5.5 Extension to whole space

After obtaining a numerical solution $(\overline{U}, \overline{P})$ on the bounded domain, we need to extend it to the entire space. To achieve this, we introduce the coordinate transformation:

$$r = \tan\beta.$$

Under this transformation, we define new variables to capture the decay at the far field:

$$\widehat{U}(\beta,\theta) = \frac{\widetilde{U}(\tan\beta,\theta)}{\cos\beta}, \quad \widehat{P}(\beta,\theta) = \frac{\widetilde{P}(\tan\beta,\theta)}{\cos\beta}.$$

In these new variables, equation (5.6) takes the following form:

$$\begin{cases} -\frac{1}{2}\cos^2\beta(\cos\beta\widehat{U} + \sin\beta\partial_\beta\widehat{U}) + \cos\beta\widehat{U}\cdot\widetilde{\nabla}_{\text{sph}}\widehat{U} + \widetilde{\nabla}_{\text{sph}}\widehat{P} - \widetilde{\Delta}_{\text{sph}}\widehat{U} = 0, \\ \widetilde{\text{div}}_{\text{sph}}\widehat{U} = 0, \end{cases}$$

where the definitions of $\widetilde{\nabla}_{\text{sph}}$, $\widetilde{\Delta}_{\text{sph}}$ and $\widetilde{\text{div}}_{\text{sph}}$ are listed in Appendix D. The corresponding weak form can be expressed similarly as:

$$\begin{aligned} &\kappa^{-1}\langle\cos\beta\widehat{U}\cdot\widetilde{\nabla}_{\text{sph}}\widehat{U}, V\rangle_{\text{sphcv}} - \tfrac{1}{2}\langle\cos^2\beta(\cos\beta\widehat{U} + \sin\beta\partial_\beta\widehat{U}), V\rangle_{\text{sphcv}} - \kappa^{-1}\langle\widehat{P}, \widetilde{\text{div}}_{\text{sph}}V\rangle_{\text{sphcv}} \\ &-\kappa^{-1}\langle Q, \widetilde{\text{div}}_{\text{sph}}\widehat{U}\rangle_{\text{sphcv}} + \kappa^{-2}\langle\widetilde{\nabla}_{\text{sph}}\widehat{U}, \widetilde{\nabla}_{\text{sph}}V\rangle_{\text{sphcv}} = 0, \end{aligned} \tag{5.9}$$

for all test functions $V \in H^1_{0,\text{sphcv}}([0,\frac{\pi}{2}]^2)^3, Q \in L^2_{\text{sphcv}}([0,\frac{\pi}{2}]^2)$, with the inner product

$$\langle f, g\rangle_{\text{sphcv}} = \int_{[0,\frac{\pi}{2}]^2} f^T(\beta,\theta)g(\beta,\theta)\frac{\tan^2\beta}{\cos^2\beta}\sin\theta\mathrm{d}\beta\mathrm{d}\theta.$$

The far-field boundary condition transforms into:

$$\widehat{U}\left(\frac{\pi}{2},\theta\right) = \frac{A(\theta)}{\kappa}.$$

When numerically solving the weak form (5.9), it is beneficial to select a larger scaling factor κ:

$$\kappa = 2\sqrt{1+\gamma_U/4}.$$

We employ the same discretization method as before to solve this weak form numerically. Given a solution $\overline{U}$ defined on $\mathbb{R}_+ \times \left[0,\frac{\pi}{2}\right]$, we first interpolate it onto the finite element basis corresponding to the new mesh. Although the interpolated function generally does not exactly satisfy equation (5.9), it provides a sufficiently accurate initial guess. Consequently, by applying Newton's iteration with fixed boundary conditions, we can efficiently solve the transformed system within a few steps, obtaining a good approximation over the entire spatial domain.

Next, we linearize the operator at the solution profile $\overline{U}$ obtained from equation (5.9) and compute the corresponding eigenvectors. We note that the computed solution profile $\overline{U}$ and eigenvector $\overline{v}$ are close to being divergence-free, though not exactly so. In the next subsections, we introduce a procedure to enforce the divergence-free condition exactly.

Remark 8 Numerical instabilities occasionally lead to spurious eigenvalues with highly oscillatory eigenvectors, which do not correspond to the actual eigenmodes of the operator. However, despite these numerical artifacts, the method still enables us to approximate the genuine eigenvectors accurately.

5.6 Construction of divergence-free basis

To exactly enforce the divergence-free condition, we construct a divergence-free basis. We first expand the vector $\widetilde{U}$ using axisymmetric vector spherical harmonics X_l, Y_l, Z_l, defined later in (5.10):

$$\widetilde{U}(r,\theta) = \sum_{l=0}^{+\infty} (\widetilde{U}_l^Y(r) Y_l(\theta) + \widetilde{U}_l^X(r) X_l(\theta) + \widetilde{U}_l^Z(r) Z_l(\theta)).$$

Here, for a scalar function p, we can expand p with the scalar spherical harmonics:

$$p(r,\omega) = \sum_{l=0}^{+\infty} \sum_{m=-l}^{l} p_{lm}(r) S_{lm}(\omega), \quad r \geqslant 0, \quad \omega \in \mathbb{S}^2,$$

where $S_{lm}(\omega)$ is the spherical harmonics. For a vector field u, we can also expand u with the vector spherical harmonics:

$$u(r,\omega) = \sum_{l=0}^{+\infty} \sum_{m=-l}^{l} (u_{lm}^Y(r) Y_{lm}(\omega) + u_{lm}^X(r) X_{lm}(\omega) + u_{lm}^Z(r) Z_{lm}(\omega)),$$

where

$$Y_{lm}(\omega) = S_{lm}(\omega)\vec{e}_r, \quad X_{lm}(\omega) = \nabla_{\mathbb{S}^2} S_{lm}(\omega), \quad Z_{lm}(\omega) = \vec{e}_r \times \nabla_{\mathbb{S}^2} S_{lm}(\omega).$$

Since we only consider axisymmetric functions, we choose $m = 0$ and ω reduces to θ:

$$Y_l(\theta) = S_l(\theta)\vec{e}_r, \quad X_l(\theta) = S_l'(\theta)\vec{e}_\theta, \quad Z_l(\theta) = \vec{e}_\phi S_l'(\theta), \quad S_l(\theta) = P_l(\cos\theta), \tag{5.10}$$

where P_l denotes the Legendre polynomial. Here we drop the subscript $m = 0$ for simplicity.

We have the reduced expansions

$$p(r,\theta) = \sum_{l=0}^{+\infty} p_l(r) S_l(\theta), \quad u(r,\theta) = \sum_{l=0}^{+\infty} (u_l^Y(r) Y_l(\theta) + u_l^X(r) X_l(\theta) + u_l^Z(r) Z_l(\theta)).$$

We note that X_l, Y_m, Z_n are mutually orthogonal for all indices l, m, n. Furthermore, they are normalized in the L^2 inner product:

$$\int_0^\pi Y_l(\theta) Y_m(\theta) \sin\theta \mathrm{d}\theta = \frac{2\delta_{lm}}{2l+1}, \quad \int_0^\pi X_l(\theta) X_m(\theta) \sin\theta \mathrm{d}\theta = \int_0^\pi Z_l(\theta) Z_m(\theta) \sin\theta \mathrm{d}\theta = \frac{2l(l+1)\delta_{lm}}{2l+1}.$$

The gradients of p and u have the following forms, by Appendix D and the eigenvector properties of the spherical harmonics and the Legendre polynomials:

$$\nabla_{\mathrm{sph}} p = \sum_{l=0}^{+\infty} \left(p_l'(r) Y_l(\theta) + \frac{1}{r} p_l(r) X_l(\theta) \right), \tag{5.11}$$

$$\Delta_{\mathrm{sph}} p = \sum_{l=0}^{+\infty} \left(\Delta_r p_l(r) - \frac{\mu_l}{r^2} p_l(r) \right) S_l(\theta), \tag{5.12}$$

$$\mathrm{div}_{\mathrm{sph}}\, u = \sum_{l=0}^{+\infty} \left(\frac{\mathrm{d}}{\mathrm{d}r} u_l^Y + \frac{2}{r} u_l^Y - \frac{\mu_l}{r} u_l^X \right) S_l, \tag{5.13}$$

$$\begin{aligned} \Delta_{\mathrm{sph}} u &= \sum_{l=0}^{+\infty} (\Delta_r u_l^Y Y_l + \Delta_r u_l^X X_l + \Delta_r u_l^Z Z_l) \\ &+ \frac{1}{r^2} \sum_{l=0}^{+\infty} ((2\mu_l u_l^X - (\mu_l + 2) u_l^Y) Y_l + (2u_l^Y - \mu_l u_l^X) X_l - \mu_l u_l^Z Z_l), \end{aligned} \tag{5.14}$$

where we define

$$\mu_l = l(l+1), \quad \Delta_r = \frac{1}{r^2}\frac{\mathrm{d}}{\mathrm{d}r}r^2\frac{\mathrm{d}}{\mathrm{d}r}.$$

We note that the superscripts X, Y, Z refer to the spherical harmonics and have nothing to do with Cartesian coordinates. We note that when l is even, the vector field $(Y_l, X_l, 0)$ is even with respect to z while $(0, 0, Z_l)$ is odd. When l is odd, they have the opposite parities. Therefore, for the even $\widetilde{U}$, we choose even l for Y_l, X_l and odd l for Z_l. For the odd $\widetilde{v}$, it is the other way around. Therefore, we modify our expansion to:

$$\begin{aligned}\widetilde{U}(r,\theta) &= \sum_{l=0}^{+\infty}(\widetilde{U}_l^Y(r)Y_{2l}(\theta) + \widetilde{U}_l^X(r)X_{2l}(\theta)) + \sum_{l=1}^{+\infty}\widetilde{U}_l^Z(r)Z_{2l-1}(\theta), \\ \widetilde{v}(r,\theta) &= \sum_{l=1}^{+\infty}(\widetilde{v}_l^Y(r)Y_{2l-1}(\theta) + \widetilde{v}_l^X(r)X_{2l-1}(\theta) + \widetilde{v}_l^Z(r)Z_{2l}(\theta)).\end{aligned} \tag{5.15}$$

We compute the divergence of $\widetilde{U}$ by (5.13) as

$$\operatorname{div}\widetilde{U} = \sum_{l=0}^{+\infty}\left(\frac{\mathrm{d}}{\mathrm{d}r}\widetilde{U}_l^Y + \frac{2}{r}\widetilde{U}_l^Y - \frac{\mu_{2l}}{r}\widetilde{U}_l^X\right)S_l, \quad \mu_{2l} = 2l(2l+1).$$

Therefore, the divergence-free condition is

$$r\frac{\mathrm{d}}{\mathrm{d}r}\widetilde{U}_l^Y + 2\widetilde{U}_l^Y - \mu_{2l}\widetilde{U}_l^X = 0.$$

Under the previously introduced coordinate transformation, the divergence-free condition becomes:

$$\frac{1}{2}\sin 2\beta\frac{\mathrm{d}}{\mathrm{d}\beta}\widehat{U}_l^Y + \frac{1}{2}(3+\cos 2\beta)\widehat{U}_l^Y - \mu_{2l}\widehat{U}_l^X = 0, \quad \forall l \geqslant 0. \tag{5.16}$$

For each mode l, since both $\widehat{U}_l^Y$ terms are multiplied with $\sin 2\beta$ or $\cos 2\beta$, we need one more Fourier mode in β for $\widehat{U}_l^X$ to make sure (5.16) holds. In practice, we truncate the series in (5.15) up to L terms. Therefore, the divergence free condition splits into L equations relating the β coefficient functions $\widehat{U}_l^Y$ and $\widehat{U}_l^X$.

In order to expand the coefficient functions into trigonometric series, we first examine the boundary behavior. Specifically, we recall the boundary conditions in Section 5.2 as $\widehat{U}(\beta = 0, \theta) = (0, 0, 0)$ at the origin. The far field behavior (1.13) in Assumption 1 implies that

$$\widehat{U} = \frac{\widetilde{U}}{\cos\beta} = (\frac{A(\theta)}{r} + O(\frac{1}{r^3}))/O((\frac{\pi}{2} - \beta)) = A(\theta) + O((\frac{\pi}{2} - \beta)^2),$$

where we have used the change of variable $r = \tan\beta = O((\frac{\pi}{2} - \beta)^{-1})$. These conditions lead naturally to the following expansion of $\widehat{U}_l^Y(\beta)$ and $\widehat{U}_l^X(\beta)$ as:

$$\widehat{U}_l^Y(\beta) = \sum_{m=1}^{M}\mathrm{B}_{m,l}^{U,Y}\sin((2m-1)\beta), \quad \widehat{U}_l^X(\beta) = \sum_{m=1}^{M+1}\mathrm{B}_{m,l}^{U,X}\sin((2m-1)\beta), \tag{5.17}$$

since

$$\sin((2m-1)\beta = (-1)^{m-1} + O((\frac{\pi}{2} - \beta)^2).$$

It should be noted, however, that this expansion lacks smoothness at the origin $\beta = 0$. Substituting these into the divergence-free constraint (5.16) yields the algebraic relations:

$$\mathrm{B}_{m,l}^{U,X} = -\frac{1}{\mu_{2l}}\left(\frac{m}{2}\mathrm{B}_{m+1,l}^{U,Y} - \frac{3}{2}\mathrm{B}_{m,l}^{U,Y} - \frac{m-1}{2}\mathrm{B}_{m-1,l}^{U,Y}\right), \quad \forall m \geqslant 1, l \in \mathbb{Z}^+ \tag{5.18}$$

with boundary conditions: $\mathrm{B}_{0,l}^{U,Y} = \mathrm{B}_{M+1,l}^{U,Y} = \mathrm{B}_{M+2,l}^{U,Y} = 0$. Now we have solved the coefficients $\mathrm{B}^{U,X}$ from $\mathrm{B}^{U,Y}$ to enforce the divergence-free condition.

When $l = 0$, we have $\mathrm{B}_{m,l}^{U,Y} = 0$, and hence $\widehat{U}_l^Y(\beta)$ becomes trivial. Moreover, since $X_0(\theta) = 0$, the first term $\widetilde{U}_0^Y(r)Y_0(\theta) + \widetilde{U}_0^X(r)X_0(\theta)$ vanishes. Consequently, in the first series of (5.15), the summation effectively starts from 1.

For the eigenvector $\overline{v}$, the boundary conditions are given by: $\overline{v}(\beta = 0, \theta) = C(\cos\theta, -\sin\theta, 0)$ and $\overline{v}\left(\beta = \frac{\pi}{2}, \theta\right) = (0, 0, 0)$. Consequently, only the functions $\widehat{v}_1^X$ and $\widehat{v}_1^Y$ remain nonzero at $\beta = 0$. To satisfy these boundary conditions, we adopt the following expansions:

$$\widehat{v}_1^Y(\beta) = \sum_{m=1}^{M} \mathrm{B}_{m,1}^{v,Y} \cos((2m-1)\beta), \quad \widehat{v}_1^X(\beta) = \sum_{m=1}^{M+1} \mathrm{B}_{m,1}^{v,X} \cos((2m-1)\beta), \quad \text{for } l = 1,$$

and

$$\widehat{v}_l^Y(\beta) = \sum_{m=1}^{M} \mathrm{B}_{m,l}^{v,Y} \sin(2m\beta), \quad \widehat{v}_l^X(\beta) = \sum_{m=1}^{M+1} \mathrm{B}_{m,l}^{v,X} \sin(2m\beta). \quad \text{for } l \geqslant 2.$$

The coefficients must satisfy the algebraic relations:

$$\begin{aligned} \mathrm{B}_{m,1}^{v,X} &= -\frac{1}{\mu_{2l-1}} \left(\frac{m}{2} \mathrm{B}_{m+1,1}^{v,Y} - \frac{3}{2} \mathrm{B}_{m,1}^{v,Y} - \frac{m-1}{2} \mathrm{B}_{m-1,1}^{v,Y} \right), \\ \mathrm{B}_{m,l}^{v,X} &= -\frac{1}{\mu_{2l-1}} \left(\frac{2m+1}{4} \mathrm{B}_{m+1,l}^{v,Y} - \frac{3}{2} \mathrm{B}_{m,l}^{v,Y} - \frac{2m-1}{4} \mathrm{B}_{m-1,l}^{v,Y} \right), \quad \forall l \in \mathbb{Z}^+, \end{aligned} \tag{5.19}$$

with boundary conditions: $\mathrm{B}_{0,l}^{v,Y} = \mathrm{B}_{M+1,l}^{v,Y} = \mathrm{B}_{M+2,l}^{v,Y} = 0$. These algebraic constraints ensure strict divergence-freeness of $\overline{U}$ and $\overline{v}$. From (5.18) and (5.19), we can construct a divergence-free basis from any trigonometric basis of U_r and U_ϕ. For example, we take the coefficients $\mathrm{B}^{U,Y}, \mathrm{B}^{U,Z}$ as independent variables, and define $\mathrm{B}^{U,X}$ by the divergence-free constraint (5.18). This defines a linear reconstruction map from the space of free coefficients into the truncated vector-field space. Its image is precisely the truncated exactly divergence-free subspace. Therefore, by applying this reconstruction map to the standard coordinate basis in the free coefficient space, we obtain a basis of the truncated exactly divergence-free subspace. In the next subsection, we demonstrate how to interpolate our solutions onto this basis.

5.7 Divergence-free interpolation

In the preceding subsections, we obtained numerical approximations for the profile $\overline{U}$ and the eigenvector $\overline{v}$ using the finite element method. To ensure strict adherence to the divergence-free condition, we now interpolate these solutions onto the carefully structured divergence-free basis developed in the previous subsection.

We remark that $\overline{U}_\theta$, $\overline{U}_r$, $\overline{U}_\phi$ corresponds to the X, Y and Z family coefficients in the harmonic expansions respectively, and we enforce the divergence-free condition in a mode-by-mode fashion, to be precise, via the algebraic relations (5.18) and (5.19). We use $\overline{U}_r$ as an example. We select a computational mesh defined by $\beta_j = \frac{j\pi}{2M}, \theta_k = \frac{k\pi}{2L}$, and evaluate $\overline{U}_r$ at each grid point (β_j, θ_k). We apply discrete Fourier transforms in θ to obtain expansions:

$$\overline{U}_r(\beta_j, \theta) = \sum_{l=1}^{L} \mathcal{F}_\theta \overline{U}_r^l(\beta_j) \sin(2l\theta), \quad j = 1, \ldots, M,$$

where $\mathcal{F}_\theta$ denotes the discrete Fourier transform with respect to θ. We then convert the resulting Fourier expansion in θ into the eigenfunction basis Y_{2l}, which amounts to a finite change of basis in the angular variable θ. Therefore, we get the value of $\widehat{U}_l^Y$ at each β_j. Applying another discrete Fourier transform in β, we derive the coefficients $\mathrm{B}_{m,l}^{U,Y}$. Similarly we obtain $\mathrm{B}_{m,l}^{v,Y}$.We explicitly enforce the divergence-free conditions by setting coefficients $\mathrm{B}_{m,l}^{U,X}$ and $\mathrm{B}_{m,l}^{v,X}$ according to

the derived algebraic constraints (5.18) and (5.19). In practice, we observe only small deviations from the original values.

Typically, the initial interpolation yields residuals insufficiently small for rigorous numerical analysis. To address this, we further refine our solutions. Defining the residual:

$$R^U_{\mathrm{sph}}(\overline{U},\overline{P}) = -\frac{1}{2}\overline{U} - \frac{1}{2}r\partial_r\overline{U} + \overline{U}\cdot\nabla_{\mathrm{sph}}\overline{U} + \nabla_{\mathrm{sph}}\overline{P} - \Delta_{\mathrm{sph}}\overline{U}.$$

We want to find a correction $\delta\overline{U}, \delta\overline{P}$ to minimize $\|R^U_{\mathrm{sph}}(\overline{U}+\delta\overline{U}, \overline{P}+\delta\overline{P})\|$. We approximate $\delta\overline{U}$ within the structured divergence-free basis as follows:

$$\delta\overline{U}_r(\beta,\theta) = \sum_{l=1}^{L}\sum_{m=1}^{M} \delta \mathrm{B}^{U,Y}_{ml} \sin((2m-1)\beta) Y_{2l}(\theta). \tag{5.20}$$

For the other entries, we adopt similar ansatz expansions. Motivated by Newton's method, we linearize R^U_{sph} around $(\overline{U},\overline{P})$, yielding the following equation:

$$-\frac{1}{2}\delta\overline{U} - \frac{1}{2}r\partial_r\delta\overline{U} + \overline{U}\cdot\nabla_{\mathrm{sph}}\delta\overline{U} + \delta\overline{U}\cdot\nabla_{\mathrm{sph}}\overline{U} + \nabla_{\mathrm{sph}}\delta\overline{P} - \Delta_{\mathrm{sph}}\delta\overline{U} = R^U_{\mathrm{sph}}(\overline{U},\overline{P}), \tag{5.21}$$

which cannot be solved precisely by the approximated $\delta\overline{U}$. Hence, we solve the resulting optimization problem:

$$\min_{\delta\overline{U}} \left| -\frac{1}{2}\delta\overline{U} - \frac{1}{2}r\partial_r\delta\overline{U} + \overline{U}\cdot\nabla_{\mathrm{sph}}\delta\overline{U} + \delta\overline{U}\cdot\nabla_{\mathrm{sph}}\overline{U} + \nabla_{\mathrm{sph}}\delta\overline{P} - \Delta_{\mathrm{sph}}\delta\overline{U} - R^U_{\mathrm{sph}}(\overline{U},\overline{P}) \right|. \tag{5.22}$$

The above optimization problem is essentially a least squares problem for the coefficients of δU and δP and can be efficiently solved using the conjugate gradient method without the need to construct the matrix corresponding to the bilinear form. The updated profile $(\overline{U}+\delta\overline{U}, \overline{P}+\delta\overline{P})$ exhibits a smaller residual. We iterate this refinement process until the residual is sufficiently small for precise numerical analysis. This iterative refinement method is similarly applied to refine the eigenvector $\overline{v}$. Notice that by Assumption 1, the residue is orthogonal to $\overline{v}$ and λ is uniquely determined given $\overline{v}$, and we thus update $\overline{v}$ and $\overline{q}$ before updating $\overline{\lambda}$.

5.8 Summary

For clarity, we distinguish four stages of the numerical approximation. We denote by $(\overline{U}_n, \overline{P}_n)$ the finite-element solution computed on the bounded computational domain using n-steps of Newton iterations. After applying the coordinate transformation described above, we obtain the whole-space candidate $(\overline{U}^{\mathrm{tr}}, \overline{P}^{\mathrm{tr}})$. Interpolating this field into the truncated exactly divergence-free spectral representation yields $(\overline{U}^{\mathrm{df}}, \overline{P}^{\mathrm{df}})$. Finally, we use $(\overline{U}^{(k)}, \overline{P}^{(k)})$ for the iteratively refined approximations produced by the residual correction procedure at iteration k. The converged output of this residual correction procedure is denoted by $(\overline{U}^{\mathrm{cv}}, \overline{P}^{\mathrm{cv}})$ and $(\overline{\lambda}, \overline{v}^{\mathrm{cv}}, \overline{q}^{\mathrm{cv}})$.

We summarize below the four-stage numerical pipeline, from the finite-element approximation on the bounded computational domain to the final corrected profile and associated eigenpair.

Algorithm 1: Gradient descent for eigenvalue

Input: Initial bound γ_λ and boundary condition A_0
Output: Profile $\overline{U}^{\mathrm{cv}}$ and eigenpair $(\overline{\lambda}, \overline{v}^{\mathrm{cv}})$
Construct a mesh on the computational domain $[0, R] \times \left[0, \frac{\pi}{2}\right]$;
Assemble the weak form and obtain the corresponding matrices and tensors;
Set initial bound γ_U, ε;
Initialize iteration index $n = 0$ and eigenvalue $\lambda_0 = 2$;
while $\lambda_n > -\gamma_\lambda$ **do**
  Update scaling factor $\kappa = \sqrt{1 + \gamma_U/4}$ and adjust boundary condition A_n;
  while $n = 0$ *or* $|\lambda_n - \lambda_{n-1}| > \varepsilon$ **do**
    Solve equation (5.7) under boundary condition A_n using Newton's method;
    Compute the smallest eigenvalue λ_n of the linearized operator $\mathcal{L}(\overline{U}_n)$;
    Evaluate the gradient $\frac{\delta\lambda}{\delta U}$ using (5.1);
    Solve the projected gradient problem to determine descent direction;
    Update solution and boundary condition: $\overline{U}_n, A_n \to \overline{U}^*_{n+1}, A_{n+1}$; `// Note` $\overline{U}^*_{n+1}$ `is not yet on the solution manifold and will be corrected in the next iteration of the loop.`
    Increment the iteration index $n \leftarrow n + 1$;
  end
  Increase γ_U;
end
Construct a new mesh on the extended domain $\left[0, \frac{\pi}{2}\right]^2$;
Transform the computed solution $\overline{U}_n$ onto the new mesh;
Solve equation (5.9) using Newton's method: $\overline{U}_n \to \overline{U}^{\mathrm{tr}}$;
Compute eigenpair $(\overline{\lambda}, \overline{v}^{\mathrm{tr}})$;
Interpolate the solutions onto a divergence-free basis: $\overline{U}^{\mathrm{tr}}, \overline{v}^{\mathrm{tr}} \to \overline{U}^{\mathrm{df}}, \overline{v}^{\mathrm{df}}$;
Initialize iteration index $k = 0$, with initialization $\overline{U}^{(0)}, \overline{v}^{(0)} = \overline{U}^{\mathrm{df}}, \overline{v}^{\mathrm{df}}$;
Set the bound for residual $\varepsilon_{\mathrm{res}}$;
while $\|R^U_{\mathrm{sph}}(\overline{U}^{(k)}, \overline{P}^{(k)})\| > \varepsilon_{\mathrm{res}}$ *or* $\|R^v_{\mathrm{sph}}(\overline{v}^{(k)}, \overline{q}^{(k)})\| > \varepsilon_{\mathrm{res}}$ **do**
  Solve (5.22) to obtain $(\delta\overline{U}^{(k)}, \delta\overline{P}^{(k)}$ and an analogous problem for $(\delta\overline{v}^{(k)}, \delta\overline{q}^{(k)})$;
  Update
  $\overline{U}^{(k+1)}, \overline{P}^{(k+1)}, \overline{v}^{(k+1)}, \overline{q}^{(k+1)} \leftarrow \overline{U}^{(k)} + \delta\overline{U}^{(k)}, \overline{P}^{(k)} + \delta\overline{P}^{(k)}, \overline{v}^{(k)} + \delta\overline{v}^{(k)}, \overline{q}^{(k)} + \delta\overline{q}^{(k)}$;
  Update $\overline{\lambda}^{(k+1)}$ based on orthogonality by Assumption 1;
  Increment the iteration index $k \leftarrow k + 1$;
end
return *Profile* $\overline{U}^{cv} = \overline{U}^{(k)}$ *and eigenpair* $(\overline{\lambda}, \overline{v}^{cv}) = (\overline{\lambda}^{(k)}, \overline{v}^{(k)})$;

We also present our numerical results in cylindrical coordinates. Figure 1 shows the three components of $\overline{U}$ together with the streamlines, while Figure 2 displays the corresponding components of $\overline{v}$. Compared with the results of Guillod and Sverak [27], our profile $\overline{U}$ exhibits relatively larger components in the ρ- and z-directions and resembles a hyperbolic flow. The azimuthal component of the eigenvector $\overline{v}$ is comparatively small, indicating that the bifurcation primarily occurs in the ρ-z plane, where it disrupts the hyperbolic structure. Figure 3 illustrates $\overline{U} + \sigma\overline{v}$ for $\sigma = 10, 20, 30, 50$, which can be interpreted as the flow at different times τ after the bifurcation has taken place. As σ increases, the parity symmetry with respect to z is broken, and small swirls emerge near the ρ-axis. In figure 4, we display the vorticity ω_ϕ of $\overline{U}, \overline{v}$ and $\overline{U} + 10\overline{v}$. The results show that the vorticity is concentrated along the ρ-axis, where $z = 0$.

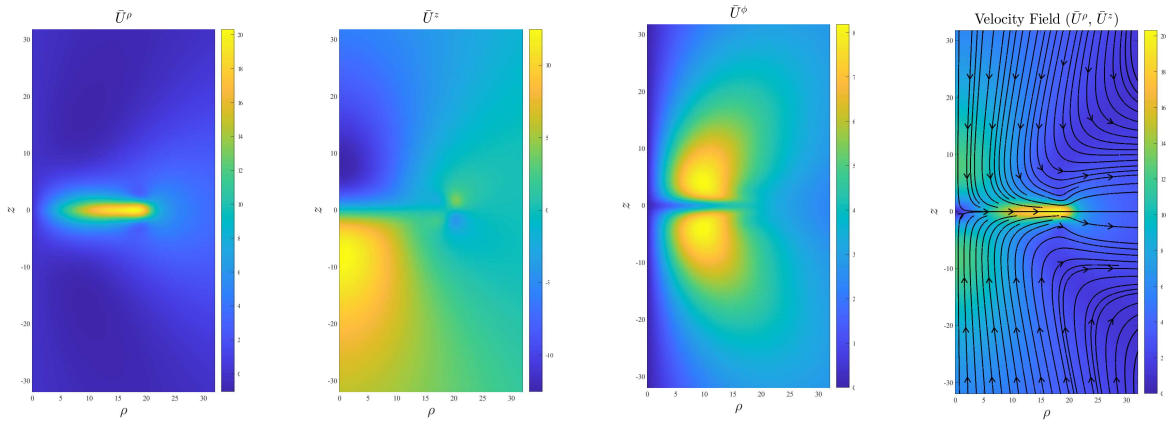

(a) $\overline{U}^{\rho}$ (b) $\overline{U}^{z}$ (c) $\overline{U}^{\phi}$ (d) $\overline{U}$ on the $\rho - z$ plane

Figure 1: Figures of $\overline{U}$

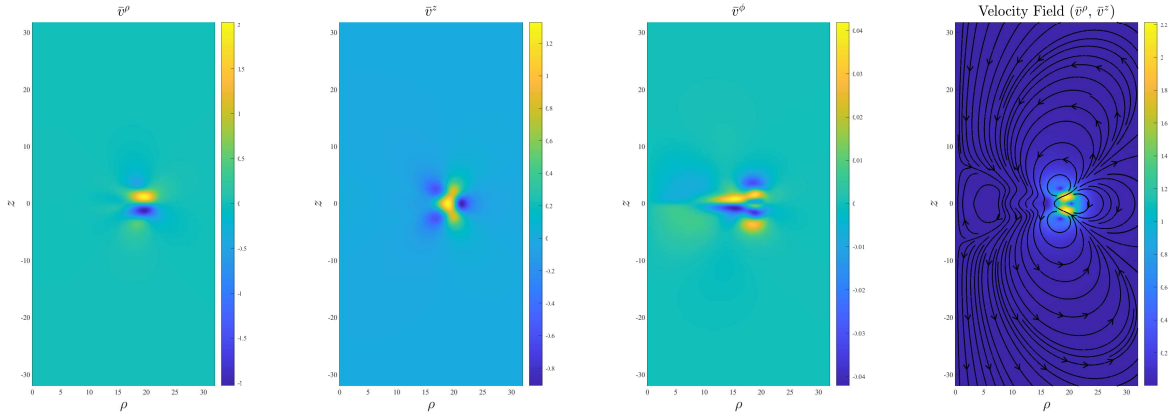

(a) $\overline{v}^{\rho}$ (b) $\overline{v}^{z}$ (c) $\overline{v}^{\phi}$ (d) $\overline{v}$ on the $\rho - z$ plane

Figure 2: Figures of $\overline{v}$

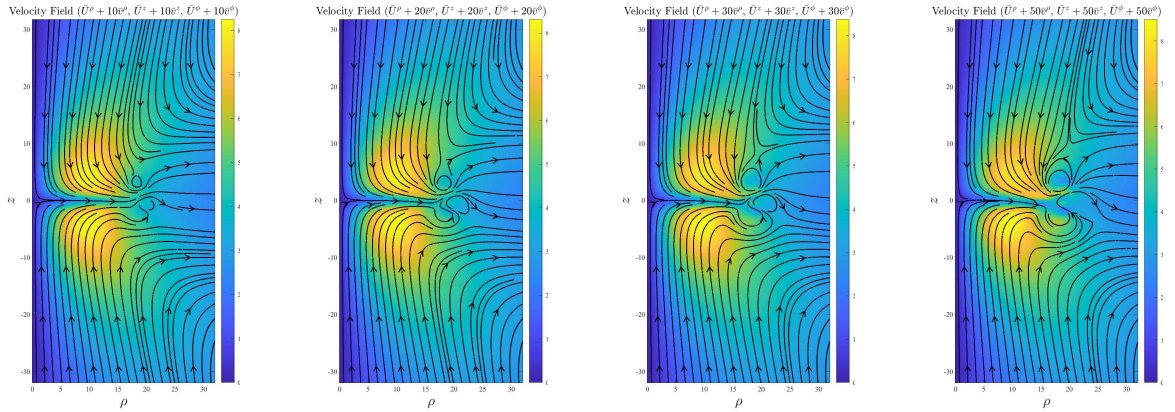

(a) $\overline{U} + 10\overline{v}$ (b) $\overline{U} + 20\overline{v}$ (c) $\overline{U} + 30\overline{v}$ (d) $\overline{U} + 50\overline{v}$

Figure 3: Figures of $\overline{U} + \sigma\overline{v}$ with different σ

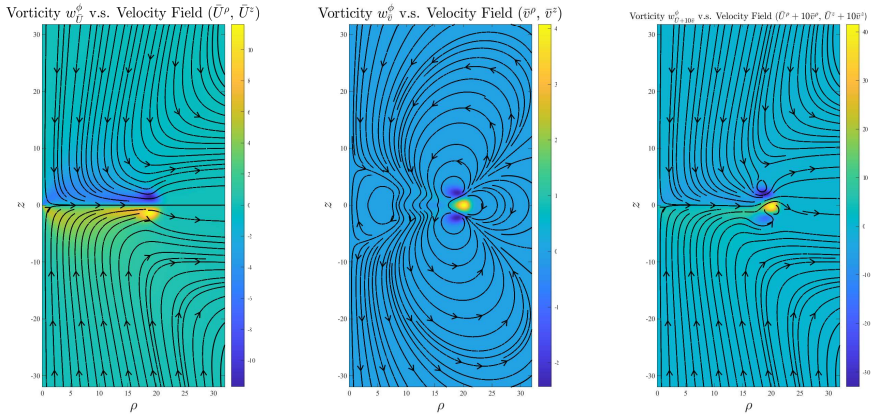

(a) ω_ϕ^U (b) ω_ϕ^v (c) $\omega_\phi^U + 10\omega_\phi^v$

Figure 4: Vorticity of $\overline{U}, \overline{v}$ and $\overline{U} + 10\overline{v}$

6 Finite Rank Approximation

In this section, we construct the finite rank approximation for $L_2 = -\Pi(U \cdot Q)$. Recall the decomposition of $\nabla \overline{U}$:

$$Q_s = \frac{\nabla \overline{U} + \nabla^T \overline{U}}{2}, \quad Q_s + \eta_1 I = Q_+ - Q_-, \quad Q_+ \succeq 0, \quad Q_- \succeq 0.$$

Here, Q_- is the negative part of $Q_s + \eta_1 I$. In previous sections, we choose $Q = Q_-$. We truncate the domain $\Omega = [0, R_0] \times \left[0, \frac{\pi}{2}\right]$ with $R_0 = 32$ and verify that outside Ω, we have $\lambda_{\max}(Q_s) < 0.199$. Thus, we set $\eta_1 = 0.199$ so that the support of Q_- is fully contained in Ω.

Although it is natural to take $Q = Q_-$, this choice has the drawback that Q is not smooth, which complicates the future error analysis of numerical integrals. Fortunately, we only need Q to satisfy

$$Q_s + \eta_1 I + Q \succeq 0. \tag{6.1}$$

Therefore, we design a smooth matrix function $Q(x)$ on Ω that meets this condition. The algorithm is described in Section 6.1. Next, we construct an appropriate basis to approximate functions defined on Ω in Section 6.2 and solve an eigenvalue problem to build L_{ap} in Section 6.3. Finally, in Section 6.4, we solve

$$L\phi_i = Q\psi_i,$$

to define the operator G.

6.1 Construction of Q

We first construct Q. Since Q is a symmetric matrix function, it has 6 independent entries: $Q_{11}, Q_{12}, Q_{13}, Q_{22}, Q_{23}, Q_{33}$. Each entry satisfies the same boundary conditions as the corresponding entry of Q_s on the three sides of the domain boundary:

$$\theta = 0, \frac{\pi}{2} \text{ and } r = 0.$$

Specifically, if $Q_{s,ij} = 0$ on a particular part of the boundary (say, $r = 0$), then we impose the Dirichlet boundary condition $Q_{ij} = 0$ on that same boundary segment. On the remaining boundary segments, where $Q_{s,ij}$ does not vanish, we instead impose the Neumann boundary condition $\partial_n Q = 0$. Consequently, Q satisfies:

$$\begin{aligned}
&\partial_r Q_{11}(0,\theta) = \partial_r Q_{12}(0,\theta) = Q_{13}(0,\theta) = \partial_r Q_{22}(0,\theta) = Q_{23}(0,\theta) = Q_{33}(0,\theta) = 0,\\
&\partial_\theta Q_{11}(r,0) = Q_{12}(r,0) = Q_{13}(r,0) = \partial_\theta Q_{22}(r,0) = Q_{23}(r,0) = \partial_\theta Q_{33}(r,0) = 0,\\
&\partial_\theta Q_{11}\left(r,\tfrac{\pi}{2}\right) = Q_{12}\left(r,\tfrac{\pi}{2}\right) = \partial_\theta Q_{13}\left(r,\tfrac{\pi}{2}\right) = \partial_\theta Q_{22}\left(r,\tfrac{\pi}{2}\right) = Q_{23}\left(r,\tfrac{\pi}{2}\right) = \partial_\theta Q_{33}\left(r,\tfrac{\pi}{2}\right) = 0.
\end{aligned}$$

On $r = R_0$, we need to impose the Dirichlet boundary condition $Q = 0$ since the support of Q is fully contained in Ω. Guided by these boundary conditions, we select the corresponding trigonometric basis to approximate each entry. For instance, Q_{11} is approximated by

$$Q_{11} = \sum_{l=1}^{L} \sum_{m=1}^{M} q_{11,lm} \cos\left(\frac{(2m+1)\pi r}{2R_0}\right) \cos(2l\theta).$$

A naïve approach would be to apply the discrete Fourier transform to Q_- and truncate the series. However, this does not ensure $Q_s + \eta_1 I + Q \succeq 0$. To address this, we first select a slightly smaller $\eta_0 = 0.19$ and reconstruct Q using the same idea of a truncation of Fourier series. As long as L, M are sufficiently large, we obtain (6.1).

This method, however, typically requires very large L, M, which is undesirable. To improve efficiency, we fix $L = 150, M = 300$ and use an iterative method. We initialize $Q_0 = 0$ with $\eta_0 = 0.19$. For every iteration Q_i, we calculate

$$\delta Q_{-,i} := \text{negative part of}\,(Q_s + \eta_0 I + Q_i).$$

If $\|\lambda_{\max}(\delta Q_{-,i})\|_{L^\infty} < \delta_\eta := \eta_1 - \eta_0$, we terminate the iteration.

Otherwise, we approximate $\delta Q_{-,i}$ by a trigonometric polynomial, denoted δQ_i. Specifically, to guarantee that δQ_i is positive, we take δQ_i to be the Fejér transform of $\delta Q_{-,i}$ in both r and θ, which is equivalent to convolving with the kernel:

$$K_N(x) = \frac{1}{N}\left(\frac{1-\cos(Nx)}{1-\cos(x)}\right).$$

This algorithm is particularly easy to implement because convolution acts as a Fourier multiplier. Thus, it suffices to compute the Fourier transform of the kernel, whose coefficients are given by

$$\mathcal{F}_x K_N^j = \left(1 - \frac{|j|}{N}\right), \quad |j| < N,$$

and vanish for $|j| \geqslant N$. We then update Q_i by

$$Q_{i+1} = Q_i + \delta Q_i.$$

Finally, we can obtain a smooth function Q satisfying (6.1) within 5 iterations.

6.2 Construction of spectral basis

Since the Q-norm $\|\cdot\|_Q$ is controlled by the standard L^2-norm, we begin by considering the following eigenvalue problem in the Rayleigh quotient form:

$$\lambda_n^s = \sup_{\dim(V_n)=n-1} \inf_{u\neq 0, u\in V, u\perp V_n} \frac{\|\nabla u\|_\Omega^2}{\|u\|_\Omega^2}, \tag{6.2}$$

where V is the space of admissible functions, namely divergence-free axisymmetric functions. We obtain a sequence of λ_n^s in ascending order with associated eigenfunctions ψ_n^s. These eigenfunctions will constitute our spectral basis.

The solutions to this eigenvalue problem admit explicit representations in terms of Bessel functions and spherical harmonics, as established in the following lemma.

Lemma 4 *Consider the eigenvalue problem* (6.2) *with* Ω *being the unit ball in 3D. The first eigenpair is*

$$\lambda_0^s = 0, \quad \psi_0^s = (\cos\theta, -\sin\theta, 0).$$

For $s \geqslant 1$*, the remaining eigenvalues can be written as*

$$\lambda_n^s = (\alpha_{l,m}^i)^2, \quad l \geqslant 1, \quad m \geqslant 1, \quad i = Y \text{ or } Z.$$

Case 1: $i = Z$

Here, $\alpha^Z_{l,m} > 0$ denotes the m-th zero of the equation for r:

$$rJ'_{l+\frac{1}{2}}(r) - \frac{1}{2}J_{l+\frac{1}{2}}(r) = 0, \tag{6.3}$$

where J_ν is the Bessel function of the first kind. The corresponding eigenfunction is

$$\psi^s_n = \psi^Z_{ml} = \frac{J_{l+\frac{1}{2}}(\alpha^Z_{ml}r)}{\sqrt{r}} Z_l(\theta).$$

Case 2: $i = Y$

Here, $\alpha^Y_{l,m} > 0$ denotes the m-th zero of the equation for r:

$$(r^2 - l(l-1)(l+2))r\tilde{j}'_l(r) + (r^2 - l(l-1))(r^2 - (l-1)(l+2))\tilde{j}_l(r) = 0, \tag{6.4}$$

where

$$\tilde{j}_l(r) := \frac{J_{l+\frac{1}{2}}(r)}{r^{\frac{3}{2}}}.$$

The corresponding eigenfunction is

$$\psi^s_n = \psi^Y_{ml} = (B_{ml}\tilde{j}_l(\alpha^Y_{ml}r) + lA_{ml}r^{l-1})Y_l(\theta) + \left(\frac{B_l}{\mu_l}(r\alpha^Y_{ml}\tilde{j}'_l(\alpha^Y_{ml}r) + 2\tilde{j}_l(\alpha^Y_{ml}r)) + A_l r^{l-1}\right) X_l(\theta),$$

with

$$A_{ml} = -((\alpha^Y_{ml})^2 - (l-1)(l+2))\tilde{j}_l(\alpha^Y_{ml}), \quad B_{ml} = (\alpha^Y_{ml})^2 - l(l-1)(l+2).$$

The proof of the lemma is given in Appendix E.

Remark 9 (Scaling and Parity) In our setting, $\Omega = B_0(R_0)$ with $R_0 = 32$. The eigenvalues and eigenfunctions can be obtained by rescaling with respect to R_0. Specifically, the eigenvalues are $\frac{\lambda^s_n}{R_0^2}$ and the eigenvectors are $\psi^s_n\left(\frac{r}{R_0}, \theta\right)$. Recall that, since U and v also satisfy different boundary conditions, in the vector spherical harmonics expansion as in Section 5.6, only even l or only odd l appear. Hence, we retain only eigenpairs of certain parities in the construction. We denote by $\lambda^{s,U}_k$ the k-th smallest eigenvalue among all $\frac{\lambda^s_n}{R_0^2}$ with even eigenfunctions $\psi^{s,U}_k = \psi^s_n\left(\frac{r}{R_0}, \theta\right)$, and similarly define $\lambda^{s,v}_k$ and $\psi^{s,v}_k$.

Let V^i_N denote the space spanned by the first N eigenvectors $\psi^{s,i}_n$ for $i = U, v$ respectively. We define the projection I^i_N as

$$I^i_N\psi = \sum_{k=1}^{N} \langle \psi, \psi^{s,i}_k \rangle \psi^{s,i}_k. \tag{6.5}$$

It is both the L^2 and H^1 projection onto V^i_N. By (6.2), it satisfies

$$\|\psi - I^i_N\psi\|_{L^2} \leqslant \frac{1}{\lambda^{c,i}_{N+1}}\|\psi\|_{H^1}, \quad \|\psi - I^i_N\psi\|_{L^2} \leqslant \|\psi\|_{L^2}, \quad \forall \psi \in V.$$

Recall the constant K^i_5 from (4.15), we can set

$$K^i_5 = \frac{\|\lambda_{\max}(Q)\|_\infty}{\eta_2 + \lambda^{s,i}_{N+1}}.$$

Numerically, we find $\|\lambda_{\max}(Q)\|_\infty \leqslant 4.5$. Since we hope $K^i_5 \leqslant 0.45$, we need to choose N such that $\lambda^{s,i}_{N+1} > 10$. Thus, we take $N = 1257$ for U and $N = 1260$ for v to ensure the required bound.

Finally, note that it is necessary to compute all eigenvectors corresponding to eigenvalues smaller than 10. In particular, we need the following estimate to guarantee that all eigenvalues below 10 have been identified: (This lemma is still for the unscaled eigenvalue λ^s_n).

Lemma 5 *Let* $0 = \beta_{l,0} < \beta_{l,1} < \beta_{l,2} < \cdots$ *denote the zeros of* $J_{l+\frac{1}{2}}(k)$ *and* $\gamma = \sqrt{l(l-1)(l+2)}$.

- *If* $l = 1$, *define* $\tilde{\beta}_{1,j} = \beta_{1,j}$;
- *If* $l \geqslant 2$ *and* $\gamma \neq \beta_{l,j}$ *for any* $j > 0$, *denote* $\tilde{\beta}_{l,j}$ *as the sequence obtained by sorting* $\{\beta_{l,j}, \gamma\}$ *in an ascending order.*

Let s_l *be the unique positive root of:*

$$Q_l(s) = s^3 - 4l^2s^2 + l(l-1)(6l^2 + 11l + 7)s - 3l(l-1)^2(l+1)^2(l+2),$$

and $t_l = \sqrt{l(l+1)}$. *Assume that* $\sqrt{s_l}$ *is not a root of* (6.4) *and that* t_l *is not a root of* (6.3).

Then the following statements hold:

1. *The equation* (6.4) *has exactly one root on every interval* $(\tilde{\beta}_{l,j}, \tilde{\beta}_{l,j+1})$ *for* $j \geqslant 0$.
2. *The equation* (6.3) *has exactly one root on every interval* $(\beta_{l,j}, \beta_{l,j+1})$ *for* $j \geqslant 0$.
3. *The first zeros* $\alpha^Y_{l,1}$ *and* $\alpha^Z_{l,1}$ *satisfy the lower bounds:*

$$\alpha^Y_{l,1} \geqslant \sqrt{s_l}, \quad \alpha^Z_{l,1} \geqslant t_l.$$

The proof of the lemma is given in Appendix E. In practice, we use the lower bounds of $\alpha^Y_{l,1}$ and $\alpha^Z_{l,1}$ to determine the largerst index l required, denoted by $l_{\max}$. For every $1 \leqslant l \leqslant l_{\max}$, we then search all the intervals $(\beta_{l,j}, \beta_{l,j+1})$ and $(\widetilde{\beta}_{l,j}, \widetilde{\beta}_{l,j+1})$ for $\alpha^Z_{l,1}$ and $\alpha^Y_{l,1}$, respectively, until the left endpoint of the interval exceeds the prescribed threshold.

6.3 Eigenvalue problem

We subsequently solve the finite-dimensional eigenvalue problem numerically:

$$\langle \psi, Q\psi^{Q,i}_n \rangle_\Omega = \lambda^{Q,i}_n \langle \psi, \psi^{Q,i}_n \rangle_E, \quad \forall \psi \in V^i_N,$$

on the space V^i_N. Recall that $\psi^{s,i}_k$ are orthogonal in L^2 and H^1. We will normalize them to obtain an orthonormal basis in E as $\widetilde{\psi}^{s,i}_k$ and compute the matrix:

$$(A^i_Q)_{k,j} = \langle \widetilde{\psi}^{s,i}_k, Q\widetilde{\psi}^{s,i}_j \rangle_\Omega, \tag{6.6}$$

using numerical integration, and solve the resulting eigenvalue problem:

$$A^i_Q \psi^{Q,i}_n = \lambda^{Q,i}_n \psi^{Q,i}_n.$$

Here, by an abuse of notation, we use $\psi^{Q,i}_n$ to denote both the eigenvector and its coordinates in the basis $\widetilde{\psi}^{s,i}_k$.

We solve the matrix eigenvalue problem numerically to determine all eigenvalues $\lambda^{Q,i}_n \geqslant 0.46$. Numerical computations yield:

$$\lambda^U_{20} \approx 0.456 < 0.46, \quad \lambda^v_{25} \approx 0.453 < 0.46.$$

These numerics determine the rank used in the finite-rank operator. The computed eigenvectors provide the foundation for a finite-rank approximation of L_2, which corresponds to the second step in Section 4.2.

6.4 Inversion on the subspace

Finally, we invert the operator L on the subspace spanned by the finitely many of eigenfunctions, as in the last step in Section 4.2. We numerically solve equation (4.11) by employing the finite element method described in Section 5.5, using the (β, θ) coordinates. We remark that for ϕ_n^v, since $\widetilde{\lambda}$ is not explicit in (4.1), we invert instead the operator $P_{\overline{v}}(L^v - \overline{\lambda})v$ and leave the small term $\lambda\psi_n^v$ in the residue r_n^v. Additionally, we must impose the orthogonality constraint:

$$\langle \phi_n^v, \overline{v} \rangle = 0,$$

which is numerically enforced by solving the following modified linear system:

$$\begin{pmatrix} A & y \\ y^T & 0 \end{pmatrix} \begin{pmatrix} x \\ \mu \end{pmatrix} = \begin{pmatrix} b \\ 0 \end{pmatrix},$$

where the matrix A stands for the discretization of the linear operator $L^v - \overline{\lambda} I$, and the vector x, y, b stands for $\phi_n^v, \overline{v}, Q\overline{\psi}_n^v$ respectively. μ is a scalar Lagrange multiplier ensuring the orthogonality constraint.

The numerical solutions Φ are then interpolated onto the explicitly constructed divergence-free basis presented in Section 5.6. To maintain accuracy, we subsequently refine our solutions using iterative correction techniques detailed in Section 5.7, until sufficiently small residuals are obtained. Specifically, we iteratively minimize the residual:

$$\left| -\frac{1}{2}\phi_n^U - \frac{1}{2} r \partial_r \phi_n^U + \overline{U} \cdot \nabla_{\mathrm{sph}} \phi_n^U + \phi_n^U \cdot \nabla_{\mathrm{sph}} \overline{U} + \nabla_{\mathrm{sph}} P_n - \Delta_{\mathrm{sph}} \phi_n^U - Q\psi_n^U \right|,$$

for U and

$$\left| -\left(\frac{1}{2} + \overline{\lambda}\right) \phi_n^v - \frac{1}{2} r \partial_r \phi_n^v + \overline{U} \cdot \nabla_{\mathrm{sph}} \phi_n^v + \phi_n^v \cdot \nabla_{\mathrm{sph}} \overline{U} + \nabla_{\mathrm{sph}} q_n - \Delta_{\mathrm{sph}} \phi_n^v - Q\psi_n^v - \mu\overline{v} \right|,$$

where μ should be again understood as the scalar Lagrange multiplier ensuring the orthogonality constraint. Finally, we obtain exactly divergence-free functions $\overline{\phi}_n^U$, $\overline{\phi}_n^v$, and we have to modify $\overline{\phi}_n^v$ by a projection to ensure orthogonality to $\overline{v}$.

Remark 10 Since we require ϕ_n^U belongs to L^2, the boundary condition at $\beta = \frac{\pi}{2}$ becomes

$$\phi_n^U(\frac{\pi}{2}, \theta) = 0.$$

When solving for ϕ_n^U with a finite element method, we must impose the homogeneous Dirichlet boundary condition, which differs from the condition for $\overline{U}$. Moreover, in the expansion (5.17), the basis functions $\sin((2m-1)\beta)$ must be replaced by $\sin(2m\beta)$. Consequently, the coefficients $\mathrm{B}_{m,l}$-s are required to satisfy a modified condition.

7 On Rigorous Numerical Verification

In this section, we outline the framework we use for rigorous computer-assisted validation; in particular, the rigorous justification for the constants in Section 4.5. We release the code and reproducibility scripts in a public GitHub repository. Throughout, we work in the spherical coordinates and employ the change of variables

$$r = \tan\beta, \qquad (\beta, \theta) \in [0, \tfrac{\pi}{2}) \times [0, \tfrac{\pi}{2}],$$

so that all fields are expanded on trigonometric basis functions in (β, θ). The items below detail how we bound the residuals, L^∞-norms, eigenvalue envelopes, and quadrature errors appearing in our verification, in a way that is fully compatible with the verifications in Section 4.5. We remark

that verifications concerning the finite-dimensional matrices are much simpler, already sketched in Section 4 and referenced in detail in the codes.

The high-level idea and organization of this section are as follows: we first discuss estimates of numerical integration and, in particular, L^2-residues in Section 7.1 and 7.2. We leverage the trigonometric representation in the profiles and use exact analytic integration if possible in Section 7.1, and discuss how we perform numerical quadrature with certified error bounds using L^∞ bounds on higher-order derivatives in Section 7.2. Then we detail in the remaining part of this section on how to build L^∞ estimates. We discuss the classical linear interpolation bound in 2D using higher-order derivatives in Section 7.3 and discuss in particular the use of the Bernstein inequality for trigonometric functions on bounds for these higher-order derivatives. Concerning the construction and the finite-rank approximation of Q and its associated spectral bound estimate, we need to use a coordinate transform on top of the linear interpolation bound in Section 7.4. Finally, for Bessel functions associated with the eigenpairs constructed from the finite-rank approximation, we derive L^∞ estimates based on the known spherical Bessel integral representation and plane-wave expansions via Legendre polynomials in Section 7.5.

7.1 Analytic L^2 residuals via a trigonometric representation

We expand the approximate self-similar profile $\overline{U}$ and the eigenfunction $\overline{v}$ as finite trigonometric sums

$$\overline{U}(\beta,\theta) = \sum_{p\in\mathcal{P}_\beta}\sum_{q\in\mathcal{P}_\theta}\Big(\mathbf{A}^{ss}_{pq}\sin(p\beta)\sin(q\theta)+\mathbf{A}^{sc}_{pq}\sin(p\beta)\cos(q\theta)+\mathbf{A}^{cs}_{pq}\cos(p\beta)\sin(q\theta)+\mathbf{A}^{cc}_{pq}\cos(p\beta)\cos(q\theta)\Big),$$

where each coefficient $\mathbf{A}^{\star}_{pq}\in\mathbb{R}^3$ collects the three components of $\overline{U}$, and $\mathcal{P}_\beta,\mathcal{P}_\theta\subset\mathbb{N}$ are finite index sets. Similarly, we have an expansion for $\overline{v}$. Because sums, products, and derivatives of sines/cosines remain finite trigonometric sums, every term in the residuals E^U and E^v stays in the same class. The only division introduced arises from the Jacobian in the change of variables $r=\tan\beta$, which produces factors of the form either $\sin(n\beta)/\sin(\beta)$ or $\cos((2m+1)\beta)/\cos(\beta)$. Note that we never have $\cos((2m)\beta)/\cos(\beta)$ in our equations: such terms will be unbounded for $\beta\approx\pi/2$. For $\sin(n\beta)/\sin(\beta)$, we know that this ratio admits an exact trigonometric expansion, so no true division remains. Indeed, recalling that

$$\frac{\sin(n\beta)}{\sin(\beta)} = U_{n-1}(\cos\beta),$$

where U_{n-1} denotes the Chebyshev polynomial of the second kind, we obtain the explicit cosine series

$$\frac{\sin(n\beta)}{\sin(\beta)} = \begin{cases} 1+2\displaystyle\sum_{k=1}^{m}\cos(2k\beta), & n=2m+1,\\ 2\displaystyle\sum_{k=1}^{m}\cos\big((2k-1)\beta\big), & n=2m. \end{cases}$$

For $\frac{\cos\left((2m+1)\beta\right)}{\cos\beta}$, we have for any integer $m\geqslant 0$ and $\beta\not\equiv\frac{\pi}{2}\pmod{\pi}$,

$$\frac{\cos\big((2m+1)\beta\big)}{\cos\beta} = (-1)^m\left(1+2\sum_{k=1}^{m}(-1)^k\cos(2k\,\beta)\right).$$

In particular, the ratio is a finite cosine polynomial in β. Hence, every such Jacobian factor can be represented exactly as a finite trigonometric sum, and we can evaluate certain integrals analytically. We remark that while in principle, inner products for $\|E^U\|_{L^2},\|E^v\|_{L^2}$ could be evaluated analytically, we choose to use numerical integration for the sake of simplicity; see the next subsection.

Finally we note that we need to keep track of the max frequency. Only products of two trigonometric polynomial increase the max frequency. Therefore, the term with the largest frequency is the transport term $\overline{U}\cdot\nabla\overline{U}$ with max frequency smaller than $2M+10$, where we include a constant wavenumber to account for Jacobians. Here, M stands for the largest frequency of $\overline{U}$. The benefit is that we can easily use the Bernstein inequality to estimate the L^∞ bound of any derivative of a trigonometric polynomial, which brings huge convenience for the error estimate of numerical integrals in the following sections.

7.2 Quadrature for numerical integrals and its error

Now we deal with numerical integrals. In contrast to Section 7.1, due to a multiplication of Q, the integrals related to the finite rank approximation cannot be evaluated analytically, and we use numerical integrations. For a function f, we use the composite Newton–Cotes 7-point rule in each direction, denoted by $\mathrm{Quad}(f)$. A 1D version can be written with an error estimate as

$$\int_a^b f(x) = \frac{h}{140}\Big(41f(x_0)+216f(x_1)+27f(x_2)+272f(x_3)+27f(x_4)+216f(x_5)+41f(x_6)\Big)-\frac{9}{1400}\,h^9\,f^{(8)}(\xi),$$

where $\xi\in(a,b), h=\frac{b-a}{6}, x_i=a+ih\ \ (i=0,\dots,6)$. Let h_β and h_θ denote the step size in β and θ directions, respectively. We know that the error is controlled by

$$\left|\int_0^{\frac{\pi}{2}}\int_0^{\frac{\pi}{2}} f(\beta,\theta)\mathrm{d}\beta\mathrm{d}\theta - \mathrm{Quad}(f)\right| \leqslant \frac{3\pi^2}{11200}(\|\partial_\beta^8 f\|_{L^\infty}h_\beta^8+\|\partial_\theta^8 f\|_{L^\infty}h_\theta^8).$$

In many cases, we need to calculate the L^2 inner product of two functions f and g, given by

$$\left|\int_0^{\frac{\pi}{2}}\int_0^{\frac{\pi}{2}} f(\beta,\theta)g(\beta,\theta)\sin\theta\mathrm{d}\beta\mathrm{d}\theta - \mathrm{Quad}(fg\sin\theta)\right| \leqslant \frac{3\pi^2}{11200}(F_\beta(f,g)h_\beta^8+F_\theta(f,g,\sin\theta)h_\theta^8),$$

where the bound of $\|\partial_t^8(f_1f_2\cdots f_n)\|, t=\beta,\theta$ can be derived via Leibniz's rule as

$$F_t(f_1,f_2,\dots,f_n)\leqslant \sum_{i_1+\cdots+i_n=8}\binom{8}{i_1,\dots,i_n}\prod_{j=1}^n\|\partial_t^{i_j}f_j\|_{L^\infty}.$$

In the subsequent subsections, we will detail how to obtain tight L^∞ estimates on the functions and their derivatives.

7.3 Certified L^∞ bounds on trigonometric polynomials

Let f be any scalar component of $\bar{\phi}_j$, $\bar{v}$, or $\bar{U}$. Partition the β (and similarly for θ) interval into N_β subintervals $[\beta_i,\beta_{i+1}]$ of uniform mesh size $h_\beta:=\beta_{i+1}-\beta_i$, and denote $f_{i,j}=f(\beta_i,\theta_j)$. In each square $I_{i,j}:=[\beta_i,\beta_{i+1}]\times[\theta_j,\theta_{j+1}]$, using the classical error bound for linear interpolation with the Lagrange (Cauchy) form of the remainder, we obtain the following estimate:

$$|f(\beta,\theta)|\leqslant\max\{f_{i,j},f_{i+1,j},f_{i,j+1},f_{i+1,j+1}\}+\frac{h_\beta^2\|f_{\beta\beta}\|_{L^\infty(I_{i,j})}+h_\theta^2\|f_{\theta\theta}\|_{L^\infty(I_{i,j})}}{8},\tag{7.1}$$

for all $(\beta,\theta)\in I_{i,j}$, where $f_{i,j}=f(\beta_i,\theta_j)$.

For a 1D trigonometric polynomial with the highest wavenumber M we have the classical bound via Bernstein's inequality that $\|f''\|_\infty\leqslant M^2\|f\|_\infty$. Taking the supremum and using Bernstein's inequality, we arrive at

$$\|f\|_\infty\leqslant\Big(\max_{0\leqslant i\leqslant N_\beta,0\leqslant j\leqslant N_\theta}f_{i,j}\Big)/\left(1-\tfrac{(M_\beta h_\beta)^2+(M_\theta h_\theta)^2}{8}\right).\tag{7.2}$$

Taking $M_\beta h_\beta, M_\theta h_\theta\ll 1$ makes the amplification factor close to 1.

To evaluate the upper bound of derivatives of f, we can use similar techniques via finite differences. We take f_θ as an example. We first evaluate f on the mesh grids. Then we know that for every i, j, there exists a $\xi_{i,j} \in [\theta_j, \theta_{j+1}]$ such that

$$f_\theta(\beta_i, \xi_{i,j}) = \frac{f_{i,j+1} - f_{i,j}}{h_\theta}.$$

Although we do not know the exact value of $\xi_{i,j}$, since $|\xi_{i,j+1} - \xi_{i,j}| < 2h_\theta$, we can still use the same argument to estimate $\|f_\theta\|_{L^\infty}$. In fact, as in the previous subsection, we need to obtain sharp estimates of as high as 8th-order derivatives of functions. We can use Bernstein's inequality to get a crude estimate of the 12th-order derivatives before applying (7.1) to get, recursively, a tighter estimate of 10th-order and 8th-order derivatives.

Recall that in our run, we use a 300×150 grid in (β, θ) for the numerical construction of the approximate solutions. So with a fixed spectral cutoff M, we pick N as the finer *certification* grid (N_β, N_θ) used to obtain rigorous L^∞ bounds for trigonometric polynomials via the interpolation/Bernstein enclosure, large enough that $h = \frac{\pi}{2N} \ll M^{-1}$. In our computation, we take $M_\beta = 600$ and $M_\theta = 300$, and choose $N_\beta = 4096$ for β and $N_\theta = 2048$ for θ. All pointwise evaluations $f_{i,j}$ are computed with interval arithmetic to enclose round-off.

7.4 Largest eigenvalue estimate: L^∞-estimate via coordinate transform

We also need to estimate $\|\lambda_{\max}(Q(x))\|_{L^\infty}$, where a key difference is that we need to use the r coordinate instead via its construction. Recall that the 3×3 symmetric positive definite matrix Q has compact support in r. We interpolate Q by a trigonometric polynomial in r for $0 \leqslant r = \tan(\beta) \leqslant R = 32$, and set $Q(\beta, \theta) = 0$ whenever $r \geqslant R$. In this way, both positivity and compact support are preserved, since the support is enforced exactly by truncating Q outside the ball $B_0(R)$. On each grid node $x_{i,j} = (r_i, \theta_j)$ we compute closed-form eigenvalues of $Q(x_{i,j})$ and take the largest, $\lambda_{\max}(Q(x_{i,j}))$, with interval arithmetic capturing floating-point uncertainty. To control the error of the eigenvalue $\lambda_{\max}(Q(x))$ within each subdomain $I_{i,j}$ of size h, we use the formula

$$\lambda_{\max}(Q(x)) = \sup_{|v|=1} v^T Q(x) v.$$

Since Q is expressed in terms of trigonometric polynomials, applying the same envelope argument as (7.2) yields a certified global bound on $\|v^T Q(x) v\|_\infty$ as follows:

$$\|v^T Q(x) v\|_{L^\infty} \leqslant \Big(\max_{0 \leqslant i \leqslant N_r, 0 \leqslant j \leqslant N_\theta} v^T Q_{i,j} v\Big) \Big/ \left(1 - \tfrac{(M_r h_r)^2 + (M_\theta h_\theta)^2}{8}\right).$$

Thus, we obtain

$$\|\lambda_{\max}(Q(x))\|_{L^\infty} \leqslant \Big(\max_{0 \leqslant i \leqslant N_r, 0 \leqslant j \leqslant N_\theta} \lambda_{\max}(Q_{i,j})\Big) \Big/ \left(1 - \tfrac{(M_r h_r)^2 + (M_\theta h_\theta)^2}{8}\right),$$

for some computable absolute constant. By taking h_r, h_θ small enough, we can essentially bound $\|\lambda_{\max}(Q)\|_{L^\infty}$ by $\max_{i,j} \lambda_{\max}(Q_{i,j})$ up to a very small error. The numerical results show that

$$\|\lambda_{\max}(Q)\|_{L^\infty} \leqslant 4.5.$$

Next, we need to verify that

$$Q_{\mathrm{res}} := \frac{\nabla \overline{U} + \nabla^T \overline{U}}{2} + \eta_1 I + Q \succeq 0.$$

We need to emphasize that $\frac{\nabla \overline{U} + \nabla^T \overline{U}}{2}$ is trigonometric entrywise in the coordinate β while Q is trigonometric entrywise in the coordinate r. Therefore, Q_{res} is not trigonometric entrywise in either coordinate. We estimate the L^∞ norm via interpolation as in (7.1) and then control the

derivatives via Bernstein's inequality in β or r respectively. Finally, we perform a change of coordinates via

$$\partial_{\beta\beta}Q = (1+r^2)^2\partial_{rr}Q + 2r(1+r^2)\partial_r Q,$$

and we can control $\|\partial_{\beta\beta}Q\|_{L^\infty}$ by $\|\partial_{rr}Q\|_{L^\infty}$ and $\|\partial_r Q\|_{L^\infty}$. Thus, we can conclude the pointwise estimate in this mixture of coordinates. Lastly, we note that Q_{res} is not smooth at $\beta = \arctan R$. Therefore, we should include $\arctan R$ as a mesh point.

7.5 L^∞ bounds for Bessel functions

Now we deal with Bessel functions arising from the finite-rank approximation, whose L^∞ bounds are trickier than trigonometric functions. We recall the construction of our finite-rank approximation in detail in Lemma 4, where the basis ψ^Y_{ml} and ψ^Z_{ml} are of the form:

$$\begin{aligned}
\psi^Y_{ml} &= (U^Y_{ml}(r)Y_l(\theta), U^X_{ml}(r)X_l(\theta), 0),\\
U^Y_{ml} &= B_{ml}\frac{J_{l+\frac12}(\alpha^Y_{ml}r)}{r^{\frac32}} + lA_{ml}r^{l-1},\\
U^X_{ml} &= \frac{B_{ml}}{\mu_l\sqrt{r}}\left(\alpha^Y_{ml}J_{l-\frac12}(\alpha^Y_{ml}r) - \frac{lJ_{l+\frac12}(\alpha^Y_{ml}r)}{r}\right) + A_{ml}r^{l-1},\\
A_{ml} &= -((\alpha^Y_{ml})^2 - (l-1)(l+2))\frac{J_{l+\frac12}(\alpha^Y_{ml})}{(\alpha^Y_{ml})^{\frac32}},\\
B_{ml} &= \frac{(\alpha^Y_{ml})^2 - l(l-1)(l+2)}{(\alpha^Y_{ml})^{\frac32}},\\
\psi^Z_{ml} &= (0,0,U^Z_{ml}(r)Z_l(\theta)),\\
U^Z_{ml} &= \frac{J_{l+\frac12}(\alpha^Z_{ml}r)}{\sqrt{r}}.
\end{aligned}$$

The quantities α^Y_{ml}, α^Z_{ml}, A_{ml}, and B_{ml} are themselves computed with rigorous interval enclosures. In particular, these constants are not treated as floating point inputs; instead, all subsequent bounds for the basis functions ψ^Y_{ml}, ψ^Z_{ml} and their derivatives are propagated from these validated enclosures.

In a similar spirit to the two previous subsections, we would like to give L^∞ estimates on $\frac{J_{l+\frac12}(r)}{r^{\frac12}}$ and its derivatives before using a finer linear interpolation estimate like (7.1). From that, we can derive L^∞ estimates on $\frac{\mathrm{d}^k}{\mathrm{d}r^k}U^i_{ml}(r)$ and consequently ψ^Y_{ml} and ψ^Z_{ml}.

We work with $\frac{J_{l+\frac12}(r)}{r^{\frac12}}$ since it relates to the spherical Bessel functions, which admit an integral expression via plane-wave expansions; see (7.3) and we can further differentiate under the integrand. To be specific, from the plane-wave expansion with $t = \cos\theta \in [-1,1]$, we have

$$e^{izt} = \sum_{n\geq 0}(2n+1)i^n j_n(z)P_n(t),$$

where P_n are Legendre polynomials, $j_n(z) = \sqrt{\frac{\pi}{2z}}J_{n+\frac12}(z)$ are spherical Bessel functions. Using the orthogonality of the Legendre polynomials, we compute

$$\int_{-1}^{1} e^{izt}P_l(t)\mathrm{d}t = 2i^l j_l(z).$$

As a consequence, we derive

$$\frac{J_{l+\frac12}(r)}{r^{\frac12}} = \frac{i^{-l}}{\sqrt{2\pi}}\int_{-1}^{1} e^{irt}P_l(t)\mathrm{d}t, \tag{7.3}$$

and we know that from Cauchy-Schwarz

$$\left\| \frac{\mathrm{d}^k}{\mathrm{d}r^k} \left(\frac{J_{l+\frac{1}{2}}(r)}{r^{\frac{1}{2}}} \right) \right\|_{L^\infty} \leqslant \frac{1}{\sqrt{2\pi}} \int_{-1}^{1} t^k |P_l(t)| \mathrm{d}t \leqslant \frac{\sqrt{2}}{\sqrt{\pi(2k+1)(2l+1)}},$$

where we have used the fact that $|e^{irt}| = 1$ and the normalization of the Legendre polynomials.

Therefore, we have

$$\left\| \frac{\mathrm{d}^k}{\mathrm{d}r^k} U^Z_{ml}(r) \right\|_{L^\infty([0,1])} \leqslant \frac{\sqrt{2}(\alpha^Z_{ml})^k}{\sqrt{\pi(2k+1)(2l+1)}}.$$

We use a recursion formula for the Bessel functions to relate U^Y_{ml} and U^X_{ml} again to $\frac{J_{l+\frac{1}{2}}(r)}{r^{\frac{1}{2}}}$:

$$(2l+1)\ \frac{J_{l+\frac{1}{2}}(r)}{r^{\frac{3}{2}}} = \frac{J_{l-\frac{1}{2}}(r)}{r^{\frac{1}{2}}} + \frac{J_{l+\frac{3}{2}}(r)}{r^{\frac{1}{2}}},$$

and we get

$$\begin{aligned} U^Y_{ml} &= \frac{\alpha^Y_{ml} B_{ml}}{(2l+1)\sqrt{r}} \left(J_{l-\frac{1}{2}}(\alpha^Y_{ml} r) + J_{l+\frac{3}{2}}(\alpha^Y_{ml} r) \right) + l A_{ml} r^{l-1}, \\ U^X_{ml} &= \frac{B_{ml} \alpha^Y_{ml}}{\mu_l \sqrt{r}} \left(\frac{l+1}{2l+1} J_{l-\frac{1}{2}}(\alpha^Y_{ml} r) - \frac{l}{2l+1} J_{l+\frac{3}{2}}(\alpha^Y_{ml} r) \right) + A_{ml} r^{l-1}. \end{aligned}$$

From the above formula, we yield

$$\begin{aligned} \left\| \frac{\mathrm{d}^k}{\mathrm{d}r^k} U^Y_{ml}(r) \right\|_{L^\infty([0,1])} &\leqslant \frac{\sqrt{2}(\alpha^Y_{ml})^{\frac{3}{2}+k} B_{ml}}{\sqrt{\pi(2k+1)}(2l+1)} \left(\frac{1}{\sqrt{(2l-1)}} + \frac{1}{\sqrt{(2l+3)}} \right) + \frac{l! A_{ml}}{(l-1-k)!}, \\ \left\| \frac{\mathrm{d}^k}{\mathrm{d}r^k} U^X_{ml}(r) \right\|_{L^\infty([0,1])} &\leqslant \frac{\sqrt{2}(\alpha^Y_{ml})^{\frac{3}{2}+k} B_{ml}}{\sqrt{\pi(2k+1)}(2l+1)\mu_l} \left(\frac{l+1}{\sqrt{(2l-1)}} + \frac{l}{\sqrt{(2l+3)}} \right) + \frac{(l-1)! A_{ml}}{(l-1-k)!}. \end{aligned}$$

Suppose we have the bound

$$\left\| \frac{\mathrm{d}^k}{\mathrm{d}r^k} U^i_{ml}(r) \right\|_{L^\infty} \leqslant M^i_{kml}, \quad i = X, Y, Z.$$

By Bernstein's inequality of spherical harmonics defined in Section 5.6, we also have

$$\left\| \frac{\mathrm{d}^k}{\mathrm{d}\theta^k} S_l(\theta) \right\|_{L^\infty} \leqslant l^k.$$

Therefore, we obtain

$$\|\partial_r^j \partial_\theta^k \psi^Y_{ml}\|_{L^\infty} \leqslant l^k M^Y_{jml} + l^{k+1} M^X_{jml}, \quad \|\partial_r^j \partial_\theta^k \psi^Z_{ml}\|_{L^\infty} \leqslant l^{k+1} M^Z_{jml}.$$

Since

$$\psi^{Q,i} = \sum_{m,l} \kappa^{i,Y}_{ml} \psi^Y_{ml}(r,\theta) + \sum_{m,l} \kappa^{i,Z}_{ml} \psi^Z_{ml}(r,\theta), \quad i = U, v,$$

we have

$$\|\partial_r^j \partial_\theta^k \psi^{Q,i}\|_{L^\infty} \leqslant \sum_{m,l} \kappa^{i,Y}_{ml} (l^k M^Y_{jml} + l^{k+1} M^X_{jml}) + \sum_{m,l} \kappa^{i,Z}_{ml} l^{k+1} M^Z_{jml}.$$

In a similar fashion, when we want to give estimates on the Bessel functions $J_{l+\frac{1}{2}}(r)$ directly instead of via spherical harmonics, for example, when we want to give a point value estimate of J, we can proceed using the integral representation (7.3) similarly as follows. For an interval

$[a,b]$, to compute $J_{l+\frac{1}{2}}([a,b])$, we first use the package Arblib to compute the end point values $J_{l+\frac{1}{2}}(a)$ and $J_{l+\frac{1}{2}}(b)$ rigorously, and then perform continuum enclosure between endpoints via a second-derivative remainder bound. Since for any $x \in [a,b]$, we know similar to (7.1) that

$$\min\left(|J_{l+\frac{1}{2}}(a) - J_{l+\frac{1}{2}}(x)|, |J_{l+\frac{1}{2}}(b) - J_{l+\frac{1}{2}}(x)|\right) \leqslant \frac{(b-a)^2}{8} \sup_{z\in[a,b]} ||J''_{l+\frac{1}{2}}(z)||_{L^\infty([a,b])}.$$

To get a rigorous enclosure of $J_{l+\frac{1}{2}}([a,b])$, we only need to bound $||J''_{l+\frac{1}{2}}(z)||_{L^\infty([a,b])}$, which follows from the following bound, obtained from (7.3) and Cauchy-Schwarz

$$\left|J''_{l+\frac{1}{2}}(z)\right| \leqslant \sqrt{\frac{2}{(2l+1)\pi}}\left(\frac{1}{4z^{3/2}} + \frac{1}{\sqrt{3}z^{1/2}} + \frac{z^{1/2}}{\sqrt{5}}\right).$$

Acknowledgements: The research was in part supported by the NSF grants DMS-2205590 and DMS-2512878. We would like to thank Jiajie Chen, Joel Dahne, Jia Hao, Xuefeng Liu, Xiang Qin, and Vladimir Sverak for a number of stimulating discussions.

A Sharp Sobolev Constant

We provide a sharp Sobolev constant in the following lemma.

Lemma 6 (Sobolev embedding) *For any vector function $u = (u_1, \dots, u_m) \in L^2(\mathbb{R}^3)$, we have:*

$$\|u\|_{L^4}^2 \leqslant K_4(\|u\|_{L^2} + \|\nabla u\|_{L^2})^2, \quad K_4 := \frac{3^{\frac{3}{4}}}{2^3\pi} \approx 0.0907.$$

Proof By [47], we know that for each u_i,

$$\|u_i\|_{L^6} \leqslant K_s\|\nabla u_i\|_{L^2}, \quad K_s := \frac{2^{\frac{2}{3}}}{3^{\frac{1}{2}}\pi^{\frac{2}{3}}}.$$

Now we consider the vector function $u = (u_1, \dots, u_m)$:

$$\|u\|_{L^6} = \|(\sum_{i=1}^m |u_i|^2)^{\frac{1}{2}}\|_{L^6} \leqslant K_s\|\nabla(\sum_{i=1}^m |u_i|^2)^{\frac{1}{2}}\|_{L^2}.$$

By the Cauchy-Schwarz inequality, we have

$$|\nabla(\sum_{i=1}^m |u_i|^2)^{\frac{1}{2}}| = \frac{|\sum_{i=1}^m u_i\nabla u_i|}{(\sum_{i=1}^m |u_i|^2)^{\frac{1}{2}}} \leqslant (\sum_{i=1}^m |\nabla u_i|^2)^{\frac{1}{2}},$$

and we get

$$\|u\|_{L^6} \leqslant K_s\|\nabla u\|_{L^2}.$$

It follows from the Cauchy-Schwarz inequality that

$$\|u\|_{L^4} \leqslant \|u\|_{L^2}^{\frac{1}{4}}\|u\|_{L^6}^{\frac{3}{4}} \leqslant K_s^{\frac{3}{4}}\|u\|_{L^2}^{\frac{1}{4}}\|\nabla u\|_{L^2}^{\frac{3}{4}} \leqslant \frac{3^{\frac{3}{4}}}{4}K_s^{\frac{3}{4}}(\|u\|_{L^2} + \|\nabla u\|_{L^2}),$$

and we conclude the proof. □

B Estimates of Finite Rank Approximation

We prove Lemmas 1 and 2 on estimates of quasi-orthonormal projection, and then prove Lemma 3 on estimates of finite-rank approximation. We recall that $\langle\cdot,\cdot\rangle_E$ is the energy inner product induced by the norm $\|u\|_E^2 = \|\nabla u\|_{L^2}^2 + \eta_2\|u\|_{L^2}^2$, the diagonal matrix for approximate eigenvalues is $\overline{\Lambda} = \mathrm{diag}(\overline{\lambda}_1, \ldots, \overline{\lambda}_m)$, and the Gram matrix is $G_Q = (\langle\psi_i, Q\psi_j\rangle_\Omega)_{1\leqslant i,j\leqslant m}$.

Proof [Proof of Lemma 1] We assume the representation

$$f_{\mathrm{lg}}^{Q,\perp} = \sum_{j=1}^m d_j\overline{\psi}_j = \overline{\Psi}D\,,$$

where $D := (d_1, \cdots, d_m)^T$, and $\overline{\Psi} := (\overline{\psi}_1, \cdots, \overline{\psi}_m)$. By definition, we have

$$\|Q^{\frac{1}{2}}f_{\mathrm{lg}}^{Q,\perp}\|_{L^2}^2 = |(G_Q)^{\frac{1}{2}}D|^2, \quad \sum_{j=1}^m \overline{\lambda}_j^{-1}\langle f, Q\overline{\psi}_j\rangle_\Omega^2 = |\overline{\Lambda}^{\frac{-1}{2}}G_QD|^2. \tag{B.1}$$

Hence we have

$$|\|Q^{\frac{1}{2}}f_{\mathrm{lg}}^{Q,\perp}\|_{L^2}^2 - \sum_{j=1}^m \overline{\lambda}_j^{-1}\langle f, Q\overline{\psi}_j\rangle_\Omega^2| \leqslant \|\mathbb{1}_m - (G_Q)^{\frac{1}{2}}\overline{\Lambda}^{-1}(G_Q)^{\frac{1}{2}}\|\|Q^{\frac{1}{2}}f_{\mathrm{lg}}^{Q,\perp}\|_{L^2}^2.$$

This is the "Gram mismatch" constant ε_3 defined in (4.14) in Section 4. We thus conclude the proof of (4.13) using the definition of projections. □

Proof [Proof of Lemma 2] Similar to the proof above, we assume the representation $f = \overline{\Psi}B$. By definition of r_j^e and orthogonality of u to V_{lg} in the Q-inner product, we have

$$\langle f, u\rangle_E = -B^T\overline{\Lambda}^{-1}\langle R^e, u\rangle_E, \quad \langle f, f\rangle_E = B^TG_EB,$$

and we thus conclude the proof by the Cauchy-Schwarz inequality. □

Proof [Proof of Lemma 3] We decompose V_N into $V_{\mathrm{lg}} = \mathrm{span}\{\overline{\psi}_j\}_{j=1}^m$ and its orthogonal complement in the Q-inner product V_{sm}. For any f, due to the orthogonality of V_{sm} and V_{lg}, we can write an orthogonal decomposition in the Q-inner product as

$$f = f_{\mathrm{or}}^Q + f^Q = f_{\mathrm{or}}^Q + f_{\mathrm{sm}}^Q + f_{\mathrm{lg}}^Q,$$

where $f_{\mathrm{or}}^Q \perp V_N$, $f_{\mathrm{sm}}^Q \in V_{\mathrm{sm}}$, $f_{\mathrm{lg}}^Q \in V_{\mathrm{lg}}$ hence they are mutually orthogonal. In particular f_{lg}^Q coincides with the orthogonal projection $f_{\mathrm{lg}}^{Q,\perp}$.

Step 1: Quasi-orthogonal projection in E. We invoke another orthogonal decomposition in the E-inner product as

$$f = f_{\mathrm{or}}^E + f^E = f_{\mathrm{or}}^E + f_{\mathrm{sm}}^E + f_{\mathrm{lg}}^E,$$

where $f_{\mathrm{or}}^E \perp V_N$, $f_{\mathrm{sm}}^E \in V_{\mathrm{sm}}$, $f_{\mathrm{lg}}^E \in V_{\mathrm{lg}}$. Notice that $f - f_{\mathrm{or}}^E$ is the E-projection of f onto the space V_N, which coincides with I_Nf. Thus $f_{\mathrm{or}}^E = f - I_Nf$, and from (4.15) we have

$$\|Q^{\frac{1}{2}}f_{\mathrm{or}}^E\|_{L^2}^2 \leqslant K_5\|f_{\mathrm{or}}^E\|_E^2. \tag{B.2}$$

V_{sm} and V_{lg} are not orthogonal in the E-inner product, so f_{lg}^E does not coincide with $f_{\mathrm{lg}}^{E,\perp}$, the orthogonal projection of f^E in the E-inner product in V_{lg}, but we show that they are close. In fact

$$0 = \langle f^E - f_{\mathrm{lg}}^{E,\perp}, f_{\mathrm{lg}}^E - f_{\mathrm{lg}}^{E,\perp}\rangle_E = \|f_{\mathrm{lg}}^E - f_{\mathrm{lg}}^{E,\perp}\|_E^2 + \langle f_{\mathrm{sm}}^E, f_{\mathrm{lg}}^E - f_{\mathrm{lg}}^{E,\perp}\rangle_E.$$

As a consequence of Lemma 2, we have

$$\|f_{\mathrm{lg}}^E - f_{\mathrm{lg}}^{E,\perp}\|_E \leqslant \varepsilon_4\|f_{\mathrm{sm}}^E\|_E \leqslant \varepsilon_4\|f_{\mathrm{lg}}^E - f_{\mathrm{lg}}^{E,\perp}\|_E + \varepsilon_4\|f^E - f_{\mathrm{lg}}^{E,\perp}\|_E,$$

and we solve that

$$\|f_{\mathrm{lg}}^E - f_{\mathrm{lg}}^{E,\perp}\|_E \leqslant \frac{\varepsilon_4}{1-\varepsilon_4}\|f^E - f_{\mathrm{lg}}^{E,\perp}\|_E, \quad \|f_{\mathrm{sm}}^E\|_E \leqslant \frac{1}{1-\varepsilon_4}\|f^E - f_{\mathrm{lg}}^{E,\perp}\|_E \leqslant \frac{1}{1-\varepsilon_4}\|f^E\|_E. \tag{B.3}$$

Step 2: Conclusion of the estimate. Now for $\mathcal{P}f = f$, the difference consists of three parts thanks to the orthogonal decomposition,

$$\langle -(L_2 - L_{\text{ap}})f, f\rangle =: I_1 + I_2 + I_3, \quad I_1 := \|Q^{\frac{1}{2}}(f - f_{\text{lg}}^Q)\|_{L^2}^2,$$
$$I_2 := \|Q^{\frac{1}{2}} f_{\text{lg}}^Q\|_{L^2}^2 - \sum_{j=1}^m \overline{\lambda}_j^{-1}\langle f, Q\overline{\psi}_j\rangle_\Omega^2, \quad I_3 := -\sum_{j=1}^m \overline{\lambda}_j^{-1}\langle f, Q\overline{\psi}_j\rangle_\Omega \langle f, r_j\rangle_\Omega.$$

By the Q-orthogonality, we have the estimate using (B.2), (4.16), and (B.3) that

$$\begin{aligned}|I_1| &\leqslant \|Q^{\frac{1}{2}}(f - f_{\text{lg}}^Q + f_{\text{lg}}^Q - f_{\text{lg}}^E)\|_{L^2}^2 = \|Q^{\frac{1}{2}}(f_{\text{or}}^E + f_{\text{sm}}^E)\|_{L^2}^2 \leqslant (1+\mu)\|Q^{\frac{1}{2}} f_{\text{or}}^E\|_{L^2}^2 + (1 + \frac{1}{\mu})\|Q^{\frac{1}{2}} f_{\text{sm}}^E\|_{L^2}^2 \\ &\leqslant (1+\mu)K_5\|f_{\text{or}}^E\|_E^2 + (1+\frac{1}{\mu})\frac{K_6}{(1-\varepsilon_4)^2}\|f^E\|_E^2 = (K_5 + \frac{K_6}{(1-\varepsilon_4)^2})\|f\|_E^2,\end{aligned} \tag{B.4}$$

where $\mu = \frac{K_6}{K_5(1-\varepsilon_4)^2}$ is chosen to balance the coefficients of the two terms using the E-orthogonality, leveraging the weighted AM-GM inequality.

For I_3, we expand it into double integrals and use the Cauchy-Schwarz inequality to get

$$\begin{aligned}|I_3| &= |\iint_\Omega \sum_{j=1}^m f(x)f(y)\overline{\lambda}_j^{-1} Q\overline{\psi}_j(x) r_j(y) dxdy| \\ &\leqslant \sqrt{\iint_\Omega f^2(x)f^2(y)dxdy}\sqrt{\iint_\Omega \sum_{j=1}^m\sum_{i=1}^m \overline{\lambda}_j^{-1} Q\overline{\psi}_j(x) r_j(y)\overline{\lambda}_i^{-1} Q\overline{\psi}_i(x) r_i(y) dxdy} = K_7\|f\|_{L^2(\Omega)}^2.\end{aligned} \tag{B.5}$$

Combining the estimates (B.4) and (B.5) with (4.13) on I_2, we have

$$|\langle (L_2 - L_{\text{ap}})f, f\rangle| \leqslant (K_5 + \frac{K_6}{(1-\varepsilon_4)^2})\|f\|_E^2 + (\varepsilon_3\|\lambda_{\max}(Q)\|_{L^\infty} + K_7)\|f\|_\Omega^2.$$

Here ε_3 is the "Gram mismatch" constant from Lemma 1, and $K_5, \varepsilon_4, K_6, K_7$ are the constants from Section 4. We thus conclude the proof of the lemma. □

C Derivation of Gradient

We derive the gradient of $\lambda(\widetilde{U})$ by differentiating the eigenvalue equation with respect to $\widetilde{U}$:

$$\frac{\delta\mathcal{L}(\widetilde{U})}{\delta\widetilde{U}} g v^r(\widetilde{U}) + \mathcal{L}(\widetilde{U})\frac{\delta v^r(\widetilde{U})}{\delta\widetilde{U}} g = \frac{\delta\lambda(\widetilde{U})}{\delta\widetilde{U}} g v^r(\widetilde{U}) + \lambda(\widetilde{U})\frac{\delta v^r(\widetilde{U})}{\delta\widetilde{U}} g,$$

where g represents the descent direction. Taking the inner product with $v^l(\widetilde{U})$, we have:

$$\left\langle v^l, \frac{\delta\mathcal{L}(\widetilde{U})}{\delta\widetilde{U}} g v^r\right\rangle + \left\langle v^l, \mathcal{L}(\widetilde{U})\frac{\delta v^r(\widetilde{U})}{\delta\widetilde{U}} g\right\rangle = \langle v^l, v^r\rangle\frac{\delta\lambda(\widetilde{U})}{\delta\widetilde{U}} g + \lambda(\widetilde{U})\left\langle v^l, \frac{\delta v^r(\widetilde{U})}{\delta\widetilde{U}} g\right\rangle.$$

Since

$$\left\langle v^l, \mathcal{L}(\widetilde{U})\frac{\delta v^r(\widetilde{U})}{\delta\widetilde{U}} g\right\rangle = \left\langle \mathcal{L}(\widetilde{U})^* v^l, \frac{\delta v^r(\widetilde{U})}{\delta\widetilde{U}} g\right\rangle = \lambda(\widetilde{U})\left\langle v^l, \frac{\delta v^r(\widetilde{U})}{\delta\widetilde{U}} g\right\rangle,$$

we simplify the expression by assuming $\langle v^l, v^r\rangle \neq 0$:

$$\frac{\delta\lambda(\widetilde{U})}{\delta\widetilde{U}} g = \frac{\left\langle v^l, \frac{\delta\mathcal{L}(\widetilde{U})}{\delta\widetilde{U}} g v^r\right\rangle}{\langle v^l, v^r\rangle}.$$

Additionally, we note that

$$\frac{\delta \mathcal{L}(\widetilde{U})}{\delta \widetilde{U}} g v^r = \Pi(g \cdot \nabla v^r + v^r \cdot \nabla g).$$

It follows via an integration by parts that

$$\frac{\delta \lambda(\widetilde{U})}{\delta \widetilde{U}} g = \frac{\langle g \cdot \nabla v^r + v^r \cdot \nabla g, v^l \rangle}{\langle v^l, v^r \rangle} = \frac{\langle g \cdot \nabla v^r, v^l \rangle - \langle v^r \cdot \nabla v^l, g \rangle}{\langle v^l, v^r \rangle}.$$

We thus conclude the proof of (5.1).

D Expression of Operators in Spherical Coordinates

For axisymmetric scalar f, our velocity vector $\widetilde{U}$, and pressure $\widetilde{P}$, we know we have the following operators in the spherical coordinates:

$$\begin{aligned}
\Delta_{\text{sph}} f &= \frac{1}{r^2}\partial_r(r^2 \partial_r f) + \frac{1}{r^2 \sin\theta}\partial_\theta(\sin\theta \partial_\theta f), \\
\nabla_{\text{sph}} \widetilde{U} &= \begin{pmatrix} \partial_r \widetilde{U}_r & \partial_r \widetilde{U}_\theta & \partial_r \widetilde{U}_\phi \\ \frac{1}{r}\partial_\theta \widetilde{U}_r - \frac{\widetilde{U}_\theta}{r} & \frac{1}{r}\partial_\theta \widetilde{U}_\theta + \frac{\widetilde{U}_r}{r} & \frac{1}{r}\partial_\theta \widetilde{U}_\phi \\ -\frac{\widetilde{U}_\phi}{r} & -\frac{\widetilde{U}_\phi \cot\theta}{r} & \frac{\widetilde{U}_\theta \cot\theta}{r} + \frac{\widetilde{U}_r}{r} \end{pmatrix}, \\
\Delta_{\text{sph}} \widetilde{U} &= \left(\Delta \widetilde{U}_r - \frac{2\widetilde{U}_r}{r^2} - \frac{2\partial_\theta \widetilde{U}_\theta}{r^2} - \frac{2\widetilde{U}_\theta \cot\theta}{r^2}, \Delta \widetilde{U}_\theta + \frac{2\partial_\theta \widetilde{U}_r}{r^2} - \frac{\widetilde{U}_\theta}{r^2 \sin^2\theta}, \Delta \widetilde{U}_\phi - \frac{\widetilde{U}_\phi}{r^2 \sin^2\theta} \right), \\
\nabla_{\text{sph}} \widetilde{P} &= \left(\partial_r \widetilde{P}, \frac{1}{r}\partial_\theta \widetilde{P}, 0 \right), \\
\text{div}_{\text{sph}}\, \widetilde{U} &= \frac{1}{r^2}\partial_r(r^2 \widetilde{U}_r) + \frac{1}{r \sin\theta}\partial_\theta(\widetilde{U}_\theta \sin\theta).
\end{aligned}$$

And in variables of Section 5.5, we compute:

$$\begin{aligned}
\widehat{\partial}_\beta f &:= \sin\beta(\cos\beta \partial_\beta f - \sin\beta f), \\
\widehat{\nabla}_{\text{sph}} \widehat{U} &:= \frac{\cos^2\beta}{\sin\beta} \begin{pmatrix} \widehat{\partial}_\beta \widehat{U}_r & \widehat{\partial}_\beta \widehat{U}_\theta & \widehat{\partial}_\beta \widehat{U}_\phi \\ \partial_\theta \widehat{U}_r - \widehat{U}_\theta & \partial_\theta \widehat{U}_\theta + \widehat{U}_r & \partial_\theta \widehat{U}_\phi \\ -\widehat{U}_\phi & -\widehat{U}_\phi \cot\theta & \widehat{U}_\theta \cot\theta + \widehat{U}_r \end{pmatrix}, \\
\widehat{\Delta}_{\text{sph}} \widehat{U} &:= \cot^2\beta \cos\beta \left(\cot\theta \partial_\theta \widehat{U} + \frac{1}{4}(2\sin 4\beta \partial_\beta \widehat{U} + \sin^2 2\beta(\partial_{\beta\beta}\widehat{U} - 3\widehat{U})) + \partial_{\theta\theta}\widehat{U} \right) \\
&\quad + \cot^2\beta \cos\beta \left(-2\widehat{U}_r - 2(\cot\theta \widehat{U}_\theta + \partial_\theta \widehat{U}_\theta), 2\partial_\theta \widehat{U}_r - \frac{\widehat{U}_\theta}{\sin^2\theta}, -\frac{\widehat{U}_\phi}{\sin^2\theta} \right), \\
\widehat{\nabla}_{\text{sph}} \widehat{P} &:= \frac{\cos^2\beta}{\sin\beta}(\widehat{\partial}_\beta \widehat{P}, \partial_\theta \widehat{P}, 0), \\
\widehat{\text{div}}_{\text{sph}} \widehat{U} &:= \frac{\cos^2\beta}{\sin\beta} \left(\frac{1}{2}\sin 2\beta \partial_\beta \widehat{U}_r + \frac{1}{2}(3 + \cos 2\beta)\widehat{U}_r + \frac{1}{\sin\theta}\partial_\theta(\widehat{U}_\theta \sin\theta) \right).
\end{aligned}$$

E Eigenfunction in the Ball

In this section, we aim to prove Lemma 4 and Lemma 5.

Proof [Proof of Lemma 4]

Step 1: Variational formulation. The problem (6.2) can be equivalently written as

$$\lambda_n^s = \sup_{\dim(V_n)=n-1} \inf_{\|u\|_\Omega^2=1, u\in V, u\perp V_n} \|\nabla u\|_\Omega^2.$$

We apply a variational approach to reformulate it as an eigenvalue problem. Consider the Lagrangian functional with multiplier p and λ:

$$\mathfrak{L}(u,p,\lambda) = \frac{1}{2}\|\nabla u\|_\Omega^2 - \frac{\lambda}{2}(\|u\|_\Omega^2 - 1) - \langle p, \operatorname{div} u\rangle_\Omega.$$

Taking variations gives

$$\delta\mathfrak{L} = \langle \nabla u, \nabla \delta u\rangle_\Omega - \lambda\langle u, \delta u\rangle_\Omega - \langle p, \operatorname{div}\delta u\rangle_\Omega = \langle -\Delta u + \nabla p - \lambda u, \delta u\rangle_\Omega + \langle \partial_{\vec{n}} u^b - p^b\vec{n}, \delta u\rangle_{\partial\Omega},$$

where we integrate by parts in the second step. The corresponding eigenvalue problem reads:

$$-\Delta_{\mathrm{sph}} u^b + \nabla_{\mathrm{sph}} p^b = \lambda^b u^b, \quad \operatorname{div}_{\mathrm{sph}} u^b = 0, \tag{E.1}$$

subject to the homogeneous Neumann boundary condition on $\partial\Omega$ with the unit vector $\vec{n}$:

$$\partial_{\vec{n}} u^b - p^b\vec{n} = 0.$$

Here u is constrained to the divergence-free subspace of axisymmetric vector fields.

Step 2: Expansion in Spherical Harmonics. We expand u^b and p^b in the vector spherical harmonics as follows:

$$u^b = \sum_{l=0}^{+\infty} (u_l^Y(r)Y_l(\theta) + u_l^X(r)X_l(\theta) + u_l^Z(r)Z_l(\theta)), \quad p^b = \sum_{l=0}^{+\infty} p_l(r)S_l(\theta).$$

From (E.1), taking the divergence yields $\Delta_{\mathrm{sph}} p = 0$. Thanks to (5.12), we obtain for each l,

$$\Delta_r p_l(r) - \frac{\mu_l}{r^2} p_l(r) = 0.$$

The regular solution is $p_l(r) = C_l r^l$, while the singular branch r^{-l-1} is discarded. Substituting into (5.11)(5.14), the eigenvalue problem becomes

$$\begin{aligned} &-\Delta_r u_l^Y - \frac{1}{r^2}(2\mu_l u_l^X - (\mu_l+2)u_l^Y) + lC_l r^{l-1} = \lambda u_l^Y, \\ &-\Delta_r u_l^X - \frac{1}{r^2}(2u_l^Y - \mu_l u_l^X) + C_l r^{l-1} = \lambda u_l^X, \quad -\Delta_r u_l^Z + \frac{\mu_l}{r^2} u_l^Z = \lambda u_l^Z. \end{aligned} \tag{E.2}$$

Using (5.13), the divergence-free condition reduces to

$$\frac{\mathrm{d}}{\mathrm{d}r} u_l^Y + \frac{2}{r} u_l^Y - \frac{\mu_l}{r} u_l^X = 0. \tag{E.3}$$

And the boundary condition is

$$\frac{\mathrm{d}}{\mathrm{d}r} u_l^X(1) = \frac{\mathrm{d}}{\mathrm{d}r} u_l^Y(1) - p_l(1) = \frac{\mathrm{d}}{\mathrm{d}r} u_l^Z(1) = 0.$$

Hence the system decouples into an eigenvalue problem for u_l^Z and an eigenvalue system for u_l^Y and u_l^X.

Step 3: Solve u_l^Y and u_l^X. We first solve for u_l^Y and u_l^X. When $l = 0$, the divergence-free condition (E.3) forces $u_l^Y = 0$. Thus, we only consider $l \geqslant 1$. Plugging (E.3) into (E.2), we obtain:

$$-\frac{\mathrm{d}^2}{\mathrm{d}r^2}u_l^Y - \frac{4}{r}\frac{\mathrm{d}}{\mathrm{d}r}u_l^Y + \frac{1}{r^2}(l(l+1)-2)u_l^Y + lC_l r^{l-1} = \lambda u_l^Y. \tag{E.4}$$

A particular solution for this equation is

$$u_l^Y = lA_l r^{l-1}, \quad C_l = \lambda A_l.$$

The homogeneous equation is related to the Bessel ODE. Its solution is:

$$u_l^Y = B_l \tilde{j}_l(kr), \quad \lambda = k^2, \quad \tilde{j}_l(r) := \frac{J_{l+\frac{1}{2}}(r)}{r^{\frac{3}{2}}},$$

where $J_{l+\frac{1}{2}}$ is the first kind of Bessel function. Hence the general solution reads

$$u_l^Y = B_l \tilde{j}_l(kr) + lA_l r^{l-1}.$$

It follows that

$$u_l^X = \frac{B_l}{\mu_l}\left(r\frac{\mathrm{d}}{\mathrm{d}r} + 2\right)\tilde{j}_l(kr) + A_l r^{l-1} = \frac{B_l}{\mu_l}(rk\tilde{j}_l'(kr) + 2\tilde{j}_l(kr)) + A_l r^{l-1}.$$

It is not hard to check that the pair indeed solves (E.2).

Finally, we use the boundary condition to decide k. The boundary condition for u_l^Y is:

$$\frac{\mathrm{d}}{\mathrm{d}r}u_l^Y(1) - p_l(1) = B_l k\tilde{j}_l'(k) - (k^2 - l(l-1))A_l = 0. \tag{E.5}$$

For u_l^X, we simplify the condition $\frac{\mathrm{d}}{\mathrm{d}r}u_l^X(1) = 0$ into

$$\begin{aligned}\frac{\mathrm{d}}{\mathrm{d}r}u_l^X(1) &= \frac{B_l}{\mu_l}\left(r\frac{\mathrm{d}^2}{\mathrm{d}r^2} + 3\frac{\mathrm{d}}{\mathrm{d}r}\right)\tilde{j}_l(kr)|_{r=1} + (l-1)A_l \\ &= -\frac{B_l}{\mu_l}((k^2 - (l-1)(l+2))\tilde{j}_l(k) + k\tilde{j}_l'(k)) + (l-1)A_l,\end{aligned}$$

where we use that $\tilde{j}_l(kr)$ is a homogeneous solution to (E.4). By (E.5), this becomes

$$-B_l(k^2 - (l-1)(l+2))\tilde{j}_l(k) - (k^2 - l(l-1)(l+2))A_l = 0.$$

To ensure nontrivial solutions with A_l and B_l, we require that (6.4) holds:

$$(k^2 - l(l-1)(l+2))k\tilde{j}_l'(k) + (k^2 - l(l-1))(k^2 - (l-1)(l+2))\tilde{j}_l(k) = 0. \tag{E.6}$$

This condition determines all eigenvalues $\lambda = k^2$ and the corresponding coefficients A_l and B_l are uniquely determined up to normalization, when $k > 0$:

$$A_l = -(k^2 - (l-1)(l+2))\tilde{j}_l(k), \quad B_l = k^2 - l(l-1)(l+2).$$

Step 4: $k = 0$ case. When $k = 0$ and $l > 1$, we have $A_l = 0$. In this case, both u_l^X and u_l^Y vanish, since

$$u_l^X = \frac{B_l}{\mu_l}\left(r\frac{\mathrm{d}}{\mathrm{d}r} + 2\right)\tilde{j}_l(kr), \quad u_l^Y = B_l\tilde{j}_l(kr).$$

When $k = 0$ and $l = 1$, u_l^X and u_l^Y reduce to the constant functions:

$$u_l^X = u_l^Y = 1.$$

Since these solutions are nontrivial, we conclude that $\lambda_0^s = 0$ is also an eigenvalue with the corresponding eigenvector:

$$\psi_0^s = (\cos\theta, -\sin\theta, 0).$$

Step 5: Solve u_l^Z. We now turn to the component u_l^Z. The corresponding eigenpairs are given explicitly by

$$u_l^Z = \frac{J_{l+\frac{1}{2}}(kr)}{\sqrt{r}}, \quad \lambda = k^2.$$

The boundary condition yields

$$\frac{\mathrm{d}}{\mathrm{d}r} u_l^Z(1) = kJ'_{l+\frac{1}{2}}(k) - \frac{1}{2}J_{l+\frac{1}{2}}(k) = 0, \tag{E.7}$$

which characterizes all admissible values of k, and therefore determines the corresponding eigenvalues $\lambda = k^2$. In particular, $k = 0$ is excluded since u_l^Z vanishes, so $\lambda = 0$ is not an eigenvalue in this case.

Summary In summary, let α_{ml}^Y be the m-th nonzero root of equation (6.4) and α_{ml}^Z be the m-th root of equation (6.3). Then the eigenpairs are:

$$\lambda_{ml}^Y = (\alpha_{ml}^Y)^2, \quad A_{ml} = -((\alpha_{ml}^Y)^2 - (l-1)(l+2))J_{l+\frac{1}{2}}(\alpha_{ml}^Y), \quad B_{ml} = (\alpha_{ml}^Y)^2 - l(l-1)(l+2),$$

$$\psi_{ml} = (B_{ml}\tilde{j}_l(\alpha_{ml}^Y r) + lA_{ml}r^{l-1})Y_l(\theta) + \left(\frac{B_l}{\mu_l}(r\alpha_{ml}^Y \tilde{j}'_l(\alpha_{ml}^Y r) + 2\tilde{j}_l(\alpha_{ml}^Y r)) + A_l r^{l-1}\right) X_l(\theta),$$

and

$$\lambda_{ml}^Z = (\alpha_{ml}^Z)^2, \quad \psi_{ml}^Z = \frac{J_{l+\frac{1}{2}}(\alpha_{ml}^Z r)}{\sqrt{r}} Z_l(\theta).$$

Plus a zero eigenmode $(\lambda_0, \psi_0) = (0, (\cos\theta, -\sin\theta, 0))$. □

Remark 11 In practice, it is often inconvenient to evaluate the derivative $J'_{l+\frac{1}{2}}(r)$ directly. Instead, we make use of the recurrence identity

$$J'_{l+\frac{1}{2}}(r) = J_{l-\frac{1}{2}}(r) - \frac{l+\frac{1}{2}}{r} J_{l+\frac{1}{2}}(r).$$

Substituting this relation, equation (6.4) can be rewritten as:

$$k(k^2 - l(l-1)(l+2))J_{l-\frac{1}{2}}(k) + (k^4 - l(2l+1)k^2 + l(l-1)(l+2)(2l+1))J_{l+\frac{1}{2}}(k) = 0,$$

while equation (6.3) becomes:

$$kJ_{l-\frac{1}{2}}(k) - (l+1)J_{l+\frac{1}{2}}(k) = 0.$$

Similarly, the expression for u_l^X takes the form:

$$u_l^X = \frac{B_l}{\mu_l\sqrt{r}} \left(\alpha_l^Y J_{l-\frac{1}{2}}(kr) - \frac{lJ_{l+\frac{1}{2}}(kr)}{r}\right) + A_l r^{l-1}.$$

Proof [Proof of Lemma 5] First we consider the equation (6.4). Since $J_{l+\frac{1}{2}}(\gamma) \neq 0$ for $l \geqslant 2$, it can be written in the form:

$$\frac{kJ'_{l+\frac{1}{2}}(k)}{J_{l+\frac{1}{2}}(k)} - \frac{3}{2} + \frac{(k^2 - l(l-1))(k^2 - (l-1)(l+2))}{(k^2 - l(l-1)(l+2))} = 0.$$

If $l = 1$, the equation becomes:

$$\frac{kJ'_{l+\frac{1}{2}}(k)}{J_{l+\frac{1}{2}}(k)} - \frac{3}{2} + k^2 = 0.$$

Define:

$$R_l(k) = \frac{kJ'_{l+\frac{1}{2}}(k)}{J_{l+\frac{1}{2}}(k)}, \quad T_l(k) = \frac{(k^2 - l(l-1))(k^2 - (l-1)(l+2))}{(k^2 - l(l-1)(l+2))}, \quad F_l(k) = R_l(k) - \frac{3}{2} + T_l(k).$$

We observe that $F_l(k)$ is continuous except at $\tilde{\beta}_{l,j}$ $(j \geqslant 1)$. If $\tilde{\beta}_{l,j}$ is a zero of $J_{l+\frac{1}{2}}(x)$, then

$$\lim_{x \to \tilde{\beta}_{l,j}+} R_l(x) = +\infty, \quad \lim_{x \to \tilde{\beta}_{l,j}-} R_l(x) = -\infty,$$

and $T_l(\tilde{\beta}_{l,j})$ is finite. If $\tilde{\beta}_{l,j}$ is γ, we have

$$\lim_{x \to \tilde{\beta}_{l,j}+} T_l(x) = +\infty, \quad \lim_{x \to \tilde{\beta}_{l,j}-} T_l(x) = -\infty,$$

and $R_l(\tilde{\beta}_{l,j})$ is finite. Therefore, for every $\tilde{\beta}_{l,j}$, in both cases we obtain

$$\lim_{x \to \tilde{\beta}_{l,j}+} F_l(x) = +\infty, \quad \lim_{x \to \tilde{\beta}_{l,j}-} F_l(x) = -\infty.$$

At $\tilde{\beta}_{l,0} = 0$, the power series expansion

$$J_{l+\frac{1}{2}}(x) = \frac{(x/2)^{l+\frac{1}{2}}}{\Gamma(l+\frac{3}{2})}(1 - \frac{x^2}{4(l+\frac{3}{2})} + O(x^4))$$

shows that

$$F_l(k) = \frac{3(1+l)^2}{l(2+l)(3+2l)}k^2 + o(k^2).$$

Therefore, we obtain $F_l(k) > 0$ for sufficiently small k. We conclude that $F_l(k)$ has at least one root on every interval $(\tilde{\beta}_{l,j}, \tilde{\beta}_{l,j+1})$ with $j \geqslant 0$. The case $l = 1$ follows by a similar argument.

Next we derive a lower bound for the first root, and prove that assuming two zeros in the same interval leads to a contradiction. Since $F_l(\tilde{\beta}_{l,j}+) = \infty$ and $F_l(\tilde{\beta}_{l+1,j}-) = -\infty$, we denote $k_2 > k_1$ as the first two roots in $(\tilde{\beta}_{l,j}, \tilde{\beta}_{l,j+1})$, which implies that $F'_l(k_1) \leqslant 0$.

Straightforward calculation shows that

$$R'_l(k) = -\frac{R_l(k)^2 + k^2 - \left(l+\frac{1}{2}\right)^2}{k}, \quad T'_l(k) = 2k\left(1 - \frac{l(l-1)^3(l+1)(l+2)}{(k^2 - l(l-1)(l+2))^2}\right).$$

When $F_l(k) = 0$, we have $R_l(k) = \frac{3}{2} - T_l(k)$. Thus F'_l simplifies into:

$$F'_l(k) = -\frac{\left(\frac{3}{2} - T_l(k)\right)^2 + k^2 - \left(l+\frac{1}{2}\right)^2}{k} + T'_l(k) = -\frac{kQ_l(k^2)}{(k^2 - l(l-1)(l+2))^2},$$

where

$$Q_l(s) = s^3 - 4l^2s^2 + l(l-1)(6l^2 + 11l + 7)s - 3l(l-1)^2(l+1)^2(l+2).$$

It is easy to verify that for $l \geqslant 2$, we have by quadratic equations that

$$Q'_l(s) = 3s^2 - 8l^2s + l(l-1)(3l+7)(2l+1) > 0.$$

Therefore, $Q_l(s)$ has a unique root $s_l > 0$ such that $Q_l(s) < 0$ for $s < s_l$, and $Q_l(s)$ is positive and strictly increasing for $s > s_l$.

For $l = 1$, we have $Q_1(s) = s^3 - 4s^2$, which satisfies the same property.

Since $F'_l(k_1) \leqslant 0$, it follows that

$$k_1 \geqslant \sqrt{s_l},$$

and that $0 \leqslant Q_l(k_1^2) < Q_l(k_2^2)$. Hence, we obtain $F_l'(k_2) < 0$. Thus F_l cannot cross the axis at k_1, and it has to hold that $F_l(k_1) = F_l'(k_1) = 0$. We verify that $F_l(\sqrt{s_l}) \neq 0$. Hence, we reach a contradiction and conclude the proof of the lemma.

By a similar but simpler argument, the equation (6.3) has exactly one root in every interval $(\beta_{l,j}, \beta_{l,j+1})$ for all $l \geqslant 1, j \geqslant 0$. Moreover the first root satisfies the lower bound

$$\beta_{l,1} \geqslant \sqrt{l(l+1)},$$

provided that $\sqrt{l(l+1)}$ is not a root. □

F Proof of Propositions 3 and 4

Proof [Proof of Proposition 3] Recall that we will use induction to prove $U_{\text{near}} \in H^\infty$. As in the proof sketch, we have the equation for U_{near}

$$-\tfrac{1}{2}U_{\text{near}} - \tfrac{1}{2}\,\xi \cdot \nabla U_{\text{near}} + \Pi(\widetilde{U} \cdot \nabla \widetilde{U}) - \Delta U_{\text{near}} = F, \quad \nabla \cdot U_{\text{near}} = 0, \tag{F.1}$$

with the right-hand side

$$F := \tfrac{1}{2}U_{\text{far}} + \tfrac{1}{2}\,\xi \cdot \nabla U_{\text{far}} + \Delta U_{\text{far}}, \quad \nabla^k F(\xi) = O(|\xi|^{-3-k}) \ \ (k \geqslant 0). \tag{F.2}$$

Fix a standard mollifier ρ_ϵ with $\epsilon \in (0,1)$ and denote

$$u^\epsilon = \rho_\epsilon * U_{\text{near}}, \quad F^\epsilon = \rho_\epsilon * F. \tag{F.3}$$

We know that $u^\epsilon \in H^\infty$ is divergence-free, and satisfies the pointwise equation

$$-\frac{1}{2}u^\epsilon - \frac{1}{2}\xi \cdot \nabla u^\epsilon - \frac{1}{2}[\rho_\epsilon *, \xi \cdot \nabla] U_{\text{near}} + \rho_\epsilon * \Pi(\widetilde{U} \cdot \nabla \widetilde{U}) - \Delta u^\epsilon = F^\epsilon, \tag{F.4}$$

where the commutator is computed as

$$[\rho_\epsilon *, \xi \cdot \nabla] U_{\text{near}} = \rho_\epsilon * (\xi \cdot \nabla U_{\text{near}}) - \xi \cdot \nabla(\rho_\epsilon * U_{\text{near}}) = -\int \rho_\epsilon(y) y \cdot \nabla U_{\text{near}}(\xi - y) dy.$$

The commutator vanishes as $\epsilon \to 0$. More precisely, we have the estimate of its H^{k-1}-seminorm by Young's inequality as

$$\|\nabla^{k-1}[\rho_\epsilon *, \xi \cdot \nabla] U_{\text{near}}\|_{L^2} \leqslant \|\rho_\epsilon(y) y\|_{L^1} \|\nabla^k U_{\text{near}}\|_{L^2} \lesssim \epsilon \|U_{\text{near}}\|_{H^k} < \|U_{\text{near}}\|_{H^k}, \quad \forall k > 0. \tag{F.5}$$

We recall two basic facts that will be used repeatedly: the boundedness of the Leray projection in L^2, and that mollification is bounded in H^k via Young's inequality: for any integer $k \geqslant 0$,

$$\|\nabla^k u^\epsilon\|_{L^2} = \|\rho_\epsilon * \nabla^k U_{\text{near}}\|_{L^2} \leqslant \|\rho_\epsilon\|_{L^1} \|\nabla^k U_{\text{near}}\|_{L^2} = \|\nabla^k U_{\text{near}}\|_{L^2}. \tag{F.6}$$

Next, we will obtain an estimate of the H^{k-1}-seminorm of the nonlinear term. Recall $U_{\text{far}} \in W^{\infty,\infty}$ and $\nabla U_{\text{far}} \in H^\infty$. A canonical term in the expansion of $\nabla^{k-1}(\rho_\epsilon * \Pi(\widetilde{U} \cdot \nabla \widetilde{U}))$ has the form $\rho_\epsilon * \Pi(\nabla^i U_{\text{s}} \otimes \nabla^{k-i} U_{\text{t}})$, where $\text{s}, \text{t} \in \{\text{far}, \text{near}\}$, $0 \leqslant i < k$. By Young's inequality, all of the terms where at least one of s, t is far have L^2-norm bounded by $1 + \|U_{\text{near}}\|_{H^k}$. When $\text{s}, \text{t} = \text{near}$ and $i > 0$, we have by Young's inequality, Holder's inequality, and the Sobolev embedding that

$$\|\rho_\epsilon * \Pi(\nabla^i U_{\text{s}} \otimes \nabla^{k-i} U_{\text{t}})\|_{L^2} \leqslant \|\nabla^i U_{\text{near}}\|_{L^4} \|\nabla^{k-i} U_{\text{near}}\|_{L^4} \lesssim \|U_{\text{near}}\|_{H^k}^2. \tag{F.7}$$

Finally, when $\text{s}, \text{t} = \text{near}$ and $i = 0$, we have, via a commutator representation, that

$$\|\rho_\epsilon * \Pi(\nabla^i U_{\text{s}} \otimes \nabla^{k-i} U_{\text{t}})\|_{L^2} = \|\Pi(u^\epsilon \nabla^k u^\epsilon + \int \rho_\epsilon(y)(U_{\text{near}}(x-y) - u^\epsilon(x)) \nabla^k U_{\text{near}}(x-y) dy)\|_{L^2}$$

$$\leqslant \|u^\epsilon\|_{L^\infty} \|U_{\text{near}}\|_{H^k} + (\iint \rho_\epsilon(y)(U_{\text{near}}(x-y) - u^\epsilon(x))^2 dy dx)^{1/2} (\iint \rho_\epsilon(y)(\nabla^k U_{\text{near}}(x-y))^2 dy dx)^{1/2}$$

$$= \|u^\epsilon\|_{L^\infty} \|U_{\text{near}}\|_{H^k} + (\frac{1}{2}\iiint \rho_\epsilon(y)\rho_\epsilon(z)(U_{\text{near}}(x-y) - U_{\text{near}}(x-z))^2 dy dz dx)^{1/2} \|U_{\text{near}}\|_{H^k}$$

$$\leqslant (\|u^\epsilon\|_{L^\infty} + (\frac{1}{2}\iint \rho_\epsilon(y)\rho_\epsilon(z)(y-z)^2 dy dz)^{1/2} \|\nabla U_{\text{near}}\|_{L^2}) \|U_{\text{near}}\|_{H^k} \lesssim \|u^\epsilon\|_{L^\infty} \|U_{\text{near}}\|_{H^k} + \|U_{\text{near}}\|_{H^k}^2,$$

where we use the Cauchy-Schwarz inquality and (F.6) in the first inequality, the variance identity $E_y(y-E_y)^2 = 1/2E_{y,z}(y-z)^2$ in the second equality, and the difference-quotient bound $\|u(\cdot + h) - u(\cdot)\| \leqslant |h|\|\nabla u\|$ (via the Lebiniz's rule and Jensen's inequality) in the second inequality.

Combined with (F.7), we already collect a good nonlinear estimate for $k > 1$ by the Sobolev embedding and Young's inequality:

$$\|\nabla^{k-1}\rho_\epsilon * \Pi(\widetilde{U}\cdot\nabla\widetilde{U})\|_{L^2} \lesssim 1 + \|U_{\text{near}}\|_{H^k}^2. \tag{F.8}$$

When $k = 1$, we need to treat the term $\|u^\epsilon\|_{L^\infty}$ with special care using the Sobolev embedding as

$$\|u^\epsilon\|_{L^\infty} \lesssim \|u^\epsilon\|_{H^{7/4}} \lesssim \|u^\epsilon\|_{H^2}^{3/4}\|u^\epsilon\|_{H^1}^{1/4} \lesssim \|u^\epsilon\|_{H^2}^{3/4}\|U_{\text{near}}\|_{H^1}^{1/4},$$

where we use the interpolation inequality and (F.6) again. Hence, we conclude

$$\|\nabla^{k-1}\rho_\epsilon * \Pi(\widetilde{U}\cdot\nabla\widetilde{U})\|_{L^2} \lesssim 1 + \|U_{\text{near}}\|_{H^k}^2 + \|\nabla^{k+1}u^\epsilon\|_{L^2}^{3/4}\|U_{\text{near}}\|_{H^k}^{5/4}, \quad k = 1. \tag{F.9}$$

We are now ready to perform an induction on k to show that $U_{\text{near}} \in H^k$. It holds for $k = 0, 1$, and suppose it holds for any index no greater than k, at level $k > 0$ we take derivatives of (F.4):

$$-\frac{1+k}{2}\nabla^k u^\epsilon - \frac{1}{2}(\xi\cdot\nabla)\nabla^k u^\epsilon - \frac{1}{2}\nabla^k([\rho_\epsilon *, \xi\cdot\nabla]U_{\text{near}}) + \nabla^k(\rho_\epsilon * \Pi(\widetilde{U}\cdot\nabla\widetilde{U})) - \Delta\nabla^k u^\epsilon = \nabla^k F^\epsilon. \tag{F.10}$$

Take inner products with a smooth function $\chi_R\nabla^k u^\epsilon$, where χ_R is a standard cutoff function with radius R, for example $1 - \widetilde{\chi}(\xi/R)$, we get the following estimate as we take $R \to \infty$.

The drift term has the estimate via an integration by parts as

$$\langle(\xi\cdot\nabla)\nabla^k u^\epsilon, \chi_R\nabla^k u^\epsilon\rangle = -\frac{1}{2}\langle\nabla\cdot(\chi_R\xi)\nabla^k u^\epsilon, \nabla^k u^\epsilon\rangle = -\frac{3}{2}\langle\chi_R\nabla^k u^\epsilon, \nabla^k u^\epsilon\rangle + O(\int_{R<|\xi|<2R}|\nabla^k u^\epsilon|^2),$$

where we use the fact that $|\nabla\chi_R| \lesssim 1/R$. The diffusion term similarly yields

$$\langle-\Delta\nabla^k u^\epsilon, \chi_R\nabla^k u^\epsilon\rangle = \langle\nabla^{k+1}u^\epsilon, \chi_R\nabla^{k+1}u^\epsilon\rangle + \langle\nabla^{k+1}u^\epsilon, \nabla\chi_R\nabla^k u^\epsilon\rangle = \langle\nabla^{k+1}u^\epsilon, \chi_R\nabla^{k+1}u^\epsilon\rangle + O(\frac{1}{R}).$$

In the same fashion, the commutator term enjoys the estimate by (F.5)

$$|\langle\nabla^k([\rho_\epsilon *, \xi\cdot\nabla]U_{\text{near}}), \chi_R\nabla^k u^\epsilon\rangle| = |\langle\nabla^{k-1}([\rho_\epsilon *, \xi\cdot\nabla]U_{\text{near}}), \chi_R\nabla^{k+1}u^\epsilon\rangle| + O(\frac{1}{R}) \lesssim \|\nabla^{k+1}u^\epsilon\|_{L^2} + O(\frac{1}{R}),$$

and the nonlinear term enjoys a similar estimate by (F.8) and (F.9)

$$|\langle\nabla^k(\rho_\epsilon * \Pi(\widetilde{U}\cdot\nabla\widetilde{U})), \chi_R\nabla^k u^\epsilon\rangle \leqslant \|\nabla^{k+1}u^\epsilon\|_{L^2}(1 + \|\nabla^{k+1}u^\epsilon\|_{L^2}^{3/4}) + O(\frac{1}{R}).$$

Again, by Young's inequality, the right hand side of (F.10) has the trivial estimate

$$\langle\nabla^k F^\epsilon, \chi_R\nabla^k u^\epsilon\rangle \leqslant \|\nabla^k F^\epsilon\|_{L^2}\|\nabla^k u^\epsilon\|_{L^2} \leqslant \|F^\epsilon\|_{L^2}\|\nabla^k U_{\text{near}}\|_{L^2} \lesssim 1.$$

We can take the limit $R \to \infty$ and collect the estimates, treating $\|U_{\text{near}}\|_{H^k}$ as a known constant:

$$\|\nabla^{k+1}u^\epsilon\|_{L^2}^2 \lesssim 1 + \|\nabla^{k+1}u^\epsilon\|_{L^2}^{7/4},$$

and we conclude a uniform bound on $\|u^\epsilon\|_{H^{k+1}}$ independent of ϵ. Thus, we conclude that $U_{\text{near}} \in H^{k+1}$ by the theory of mollifiers. We can take a weakly convergent subsequence of u^ϵ in H^{k+1}. Since they converge to U_{near} in distributions, we know the limits are identical and conclude $U_{\text{near}} \in H^{k+1}$.

We conclude by induction that $U_{\text{near}} \in H^\infty$. □

Proof [Proof of Proposition 4] As in the proof sketch, we only need to elaborate on the procedure to show that $|\xi|U_{\text{near}}, |\xi|\nabla U_{\text{near}}, |\xi|^2\nabla^2 U_{\text{near}} \in L^2$.

Step 1: L^2-level estimate, that $|\xi|U_{\text{near}}, |\xi|\nabla U_{\text{near}} \in L^2$. Recall that U_{near} is smooth, and (F.1) holds in a strong sense with $F \in H^\infty$, with decay at the infinity $\nabla^k F = O(|\xi|^{-3-k})$. We rewrite (F.1) in the velocity-pressure formation

$$-\frac{1}{2}U_{\text{near}} - \frac{1}{2}\xi \cdot \nabla U_{\text{near}} + \widetilde{U} \cdot \nabla \widetilde{U} + \nabla P - \Delta U_{\text{near}} = F, \tag{F.11}$$

where we can represent the pressure term by taking divergence and using Riesz transform R_i as

$$\Delta P = -\operatorname{tr}((\nabla \widetilde{U})^2), \quad P = \sum_{i,j} R_i R_j (\widetilde{U}_i \widetilde{U}_j). \tag{F.12}$$

We introduce the following cutoff version of the radial weight $|\xi|^2$ as ϕ_L:

$$\phi_L = |\xi|^2 \chi_L + (2L)^2(1 - \chi_L).$$

It holds that $\phi_L = |\xi|^2$ if $|\xi| < L$, $\phi_L = |2L|^2$ if $|\xi| > 2L$, ϕ_L is radially increasing since χ_L is radially decreasing, and that $|\Delta \phi_L| \lesssim 1$ is uniformly bounded in L due to the estimates on derivatives of χ_L. Now we take inner products of (F.11) with $\chi_R \phi_L U_{\text{near}}$, where the cutoff radius R is much larger than L, and we get the following estimates as we take $R \to \infty$.

The drift term has the estimate via an integration by parts as

$$\begin{aligned}
&\langle -\frac{1}{2}\xi \cdot \nabla U_{\text{near}}, \chi_R \phi_L U_{\text{near}} \rangle = \frac{3}{4}\langle U_{\text{near}}, \chi_R \phi_L U_{\text{near}} \rangle + \frac{1}{4}\langle U_{\text{near}}, \xi \cdot \nabla(\chi_R \phi_L) U_{\text{near}} \rangle \\
\geqslant &\frac{3}{4}\langle U_{\text{near}}, \chi_R \phi_L U_{\text{near}} \rangle + \frac{L^2}{4} O\Big(\int_{R<|\xi|<2R} |U_{\text{near}}|^2\Big),
\end{aligned}$$

where we use again the fact that $|\nabla \chi_R| \lesssim 1/R$, and the radial increasing property of ϕ_L. To see this, since $\phi_L = \phi_L(|\xi|)$ is radially increasing, we have $\xi \cdot \nabla \phi_L = |\xi|\, \phi_L'(|\xi|) \geqslant 0$, hence

$$\xi \cdot \nabla(\chi_R \phi_L) = \phi_L\, \xi \cdot \nabla \chi_R + \chi_R\, \xi \cdot \nabla \phi_L \geqslant \phi_L\, \xi \cdot \nabla \chi_R.$$

Therefore, for a lower bound, we may discard the nonnegative contribution $\chi_R\, \xi \cdot \nabla \phi_L$ and bound the remaining term on $\operatorname{supp} \nabla \chi_R = \{R < |\xi| < 2R\}$ using $\phi_L = (2L)^2$ and $|\xi \cdot \nabla \chi_R| \lesssim 1$.

The diffusion term has a similar estimate via an integration by parts twice as

$$\begin{aligned}
&\langle -\Delta U_{\text{near}}, \chi_R \phi_L U_{\text{near}} \rangle = \langle \nabla U_{\text{near}}, \chi_R \phi_L \nabla U_{\text{near}} \rangle - \frac{1}{2}\langle U_{\text{near}}, \Delta(\chi_R \phi_L) U_{\text{near}} \rangle \\
\geqslant &\langle \nabla U_{\text{near}}, \chi_R \phi_L \nabla U_{\text{near}} \rangle + O\Big(\frac{L^2}{R^2} + \frac{L}{R}\Big) + O(\langle U_{\text{near}}, U_{\text{near}} \rangle),
\end{aligned}$$

where we use the uniform bound on the Laplacian of ϕ_L. The nonlinear term splits into

$$\begin{aligned}
&|\langle \widetilde{U} \cdot \nabla \widetilde{U}, \chi_R \phi_L U_{\text{near}} \rangle| = |\langle \widetilde{U} \cdot \nabla U_{\text{far}}, \chi_R \phi_L U_{\text{near}} \rangle - \frac{1}{2}\langle \widetilde{U} \cdot \nabla(\chi_R \phi_L), |U_{\text{near}}|^2 \rangle| \\
\lesssim &|\langle |\xi| \widetilde{U} \cdot \nabla U_{\text{far}}, \sqrt{\chi_R \phi_L} U_{\text{near}} \rangle| + \frac{L^2}{R} + \langle \sqrt{\chi_R \phi_L} U_{\text{near}}, U_{\text{near}} \rangle \lesssim \frac{L^2}{R} + \sqrt{\langle U_{\text{near}}, \chi_R \phi_L U_{\text{near}} \rangle},
\end{aligned}$$

where we use the divergence-free of $\widetilde{U}$ in the first equality, $\widetilde{U} \in L^\infty$ and the estimate $|\nabla \phi_L| \lesssim \sqrt{\phi_L}$ in the first inequality. For the second inequality, we use the fact by (2.5) and (2.6) that $|\xi| \nabla U_{\text{far}}, \widetilde{U} \in L^4 \cap L^\infty$, and then apply the Cauchy–Schwarz inequality.

The pressure term is controlled by (F.12) using Calderón–Zygmund theory $\|P\| \lesssim \|\widetilde{U}\|_{L^4}^2 \lesssim 1$:

$$|\langle \nabla P, \chi_R \phi_L U_{\text{near}} \rangle| = |-\langle P \nabla(\chi_R \phi_L), U_{\text{near}} \rangle| \lesssim \frac{L^2}{R} + \sqrt{\langle U_{\text{near}}, \chi_R \phi_L U_{\text{near}} \rangle}.$$

The forcing term has the trivial estimate by the Cauchy–Schwarz inequality

$$\langle F, \chi_R \phi_L U_{\text{near}} \rangle \lesssim \langle |\xi| F, \sqrt{\chi_R \phi_L} U_{\text{near}} \rangle \lesssim \sqrt{\langle U_{\text{near}}, \chi_R \phi_L U_{\text{near}} \rangle}.$$

We can take $R \to \infty$ and collect the estimates that

$$\frac{1}{4}\langle U_{\rm near}, \phi_L U_{\rm near}\rangle + \langle \nabla U_{\rm near}, \phi_L \nabla U_{\rm near}\rangle \lesssim 1 + \sqrt{\langle U_{\rm near}, \phi_L U_{\rm near}\rangle}.$$

As a consequence, $\langle U_{\rm near}, \phi_L U_{\rm near}\rangle + \langle \nabla U_{\rm near}, \phi_L \nabla U_{\rm near}\rangle$ has a uniform bound in L and we can take the limit $L \to \infty$ to conclude that

$$|\xi| U_{\rm near} \in L^2, \qquad |\xi| \nabla U_{\rm near} \in L^2. \tag{F.13}$$

Step 2: H^1-level estimate, that $|\xi|^2 \nabla U_{\rm near}, |\xi|^2 \nabla^2 U_{\rm near} \in L^2$. Take derivatives of (F.11) to get

$$-\nabla U_{\rm near} - \frac{1}{2}\xi \cdot \nabla^2 U_{\rm near} + (\nabla \widetilde{U})^2 + \widetilde{U} \cdot \nabla^2 \widetilde{U} + \nabla^2 P - \Delta \nabla U_{\rm near} = \nabla F. \tag{F.14}$$

Now we take inner products of (F.14) with $\chi_R \phi_L |\xi|^\alpha \nabla U_{\rm near}$, where the cutoff radius R is much larger than L, and we get the following estimates as we take $R \to \infty$. We will first take $\alpha = 0$ to derive an intermediate result $|\xi| \nabla^2 U_{\rm near} \in L^2$, and then take $\alpha = 2$ to conclude.

For $\alpha = 0, 2$, the drift term has a similar estimate as that in Step 1:

$$\begin{aligned}
&\langle -\frac{1}{2}\xi \cdot \nabla^2 U_{\rm near}, \chi_R \phi_L |\xi|^\alpha \nabla U_{\rm near}\rangle = \frac{\alpha+3}{4}\langle \nabla U_{\rm near}, \chi_R \phi_L |\xi|^\alpha \nabla U_{\rm near}\rangle + \frac{1}{4}\langle \nabla U_{\rm near}, |\xi|^\alpha \xi \cdot \nabla(\chi_R \phi_L) \nabla U_{\rm near}\rangle \\
&\geqslant \frac{\alpha+3}{4}\langle \nabla U_{\rm near}, \chi_R \phi_L |\xi|^\alpha \nabla U_{\rm near}\rangle + \frac{L^2}{4} O\Big(\int_{R<|\xi|<2R} |\xi|^\alpha |\nabla U_{\rm near}|^2\Big).
\end{aligned}$$

The diffusion term has a similar estimate

$$\begin{aligned}
&\langle -\Delta \nabla U_{\rm near}, \chi_R \phi_L |\xi|^\alpha \nabla U_{\rm near}\rangle = \langle \nabla^2 U_{\rm near}, \chi_R \phi_L |\xi|^\alpha \nabla^2 U_{\rm near}\rangle - \frac{1}{2}\langle \nabla U_{\rm near}, \Delta(\chi_R \phi_L |\xi|^\alpha) \nabla U_{\rm near}\rangle \\
\geqslant &\langle \nabla^2 U_{\rm near}, \chi_R \phi_L |\xi|^\alpha \nabla^2 U_{\rm near}\rangle + O\Big(\frac{L^2}{R^2} + \frac{L+L^2}{R}\Big) + O(\langle \nabla U_{\rm near}, |\xi|^\alpha \nabla U_{\rm near}\rangle),
\end{aligned}$$

where we use the bound $\Delta(\phi_L |\xi|^\alpha) \lesssim |\xi|^\alpha$ uniformly in L. The first nonlinear term has the estimate

$$|\langle (\nabla \widetilde{U})^2, \chi_R \phi_L |\xi|^\alpha \nabla U_{\rm near}\rangle| \lesssim \| |\xi|^{\frac{2+\alpha}{2}} (\nabla \widetilde{U})^2 \|_{L^2} \sqrt{\langle \nabla U_{\rm near}, \chi_R \phi_L |\xi|^\alpha \nabla U_{\rm near}\rangle}.$$

When $\alpha = 0$, we have the estimate via (F.13) and the decay of $U_{\rm far}$:

$$\| |\xi|^{\frac{2+\alpha}{2}} (\nabla \widetilde{U})^2 \|_{L^2} \lesssim \| |\xi|^{\frac{1}{2}} \nabla U_{\rm far} \|_{L^4}^2 + \| |\xi| \nabla U_{\rm near} \|_{L^2} \| \nabla U_{\rm near} \|_{L^\infty} \lesssim 1,$$

and when $\alpha = 2$, we have the estimate by the Gagliardo–Nirenberg inequality that

$$\| |\xi|^{\frac{2+\alpha}{2}} (\nabla \widetilde{U})^2 \|_{L^2} \lesssim \| |\xi| \nabla U_{\rm far} \|_{L^4}^2 + \| |\xi| \nabla U_{\rm near} \|_{L^2}^{1/2} \| \nabla(|\xi| \nabla U_{\rm near}) \|_{L^2}^{3/2} \lesssim 1 + \| |\xi| \nabla^2 U_{\rm near} \|_{L^2}^{3/2}.$$

We collect the useful estimate for the first nonlinear term as

$$\| |\xi|^{\frac{2+\alpha}{2}} (\nabla \widetilde{U})^2 \|_{L^2} \lesssim 1 + \| |\xi|^{\alpha/2} \nabla^2 U_{\rm near} \|_{L^2}^{3/2}. \tag{F.15}$$

The second nonlinear term splits, similarly as in step 1, into

$$\begin{aligned}
&|\langle \widetilde{U} \cdot \nabla^2 \widetilde{U}, \chi_R \phi_L |\xi|^\alpha \nabla U_{\rm near}\rangle| = |\langle \widetilde{U} \cdot \nabla^2 U_{\rm far}, \chi_R \phi_L |\xi|^\alpha \nabla U_{\rm near}\rangle - \frac{1}{2}\langle \widetilde{U} \cdot \nabla(\chi_R \phi_L |\xi|^\alpha), |\nabla U_{\rm near}|^2\rangle| \\
&\lesssim |\langle |\xi|^2 \widetilde{U} \cdot \nabla^2 U_{\rm far}, \sqrt{\chi_R \phi_L |\xi|^\alpha} \nabla U_{\rm near}\rangle| + \frac{L^2}{R} + \langle \sqrt{\chi_R \phi_L |\xi|^\alpha} \nabla U_{\rm near}, \sqrt{|\xi|^\alpha} \nabla U_{\rm near}\rangle \\
&\lesssim \frac{L^2}{R} + \sqrt{\langle \nabla U_{\rm near}, \chi_R \phi_L |\xi|^\alpha \nabla U_{\rm near}\rangle}.
\end{aligned}$$

The pressure term is controlled by (F.12) using the Calderón–Zygmund theory and the fact that $|\xi|^\alpha$ is an A_2-weight for $-3 < \alpha < 3$ (see Thm. 5.24 in [26]), so that for $\alpha = 0, 2$, we have by (F.15) that

$$\| \nabla P |\xi|^{\alpha/2} \|_{L^2} \lesssim \| \nabla(\widetilde{U} \otimes \widetilde{U}) |\xi|^{\alpha/2} \|_{L^2} \lesssim \sqrt{\| |\xi|^{\frac{2+\alpha}{2}} (\nabla \widetilde{U})^2 \|_{L^2} \| \widetilde{U}^2 \|_{L^2}} \lesssim 1 + \| |\xi|^{\alpha/2} \nabla^2 U_{\rm near} \|_{L^2}^{3/4},$$

As a consequence we have

$$\begin{aligned}&|\langle\nabla^2 P, \chi_R\phi_L|\xi|^\alpha\nabla U_{\text{near}}\rangle| = |-\langle\nabla P, \nabla U_{\text{near}}^T\nabla(\chi_R\phi_L|\xi|^\alpha)\rangle|\\ \lesssim&\frac{L^2}{R} + (1+\||\xi|^{\alpha/2}\nabla^2 U_{\text{near}}\|_{L^2}^{3/4})\sqrt{\langle\nabla U_{\text{near}}, \chi_R\phi_L|\xi|^\alpha\nabla U_{\text{near}}\rangle}.\end{aligned}$$

Finally the forcing term has the trivial estimate by the Cauchy-Schwarz inequality

$$\langle\nabla F, \chi_R\phi_L|\xi|^\alpha\nabla U_{\text{near}}\rangle \lesssim \langle|\xi|^2\nabla F, \sqrt{\chi_R\phi_L|\xi|^\alpha}\nabla U_{\text{near}}\rangle \lesssim \sqrt{\langle\nabla U_{\text{near}}, \chi_R\phi_L|\xi|^\alpha\nabla U_{\text{near}}\rangle}.$$

We first choose $\alpha = 0$ and take $R\to\infty$ to conclude a uniform bound on $\langle\nabla^2 U_{\text{near}}, \phi_L\nabla^2 U_{\text{near}}\rangle$. Taking the limit $L\to\infty$ yields $|\xi|\nabla^2 U_{\text{near}}\in L^2$. Now we choose $\alpha = 2$ and take $R\to\infty$ to get

$$\frac{1}{4}\langle\nabla U_{\text{near}}, \phi_L|\xi|^2\nabla U_{\text{near}}\rangle + \langle\nabla^2 U_{\text{near}}, \phi_L|\xi|^2\nabla^2 U_{\text{near}}\rangle \lesssim 1 + \sqrt{\langle\nabla U_{\text{near}}, \phi_L|\xi|^2\nabla U_{\text{near}}\rangle}.$$

As a consequence, $\langle\nabla U_{\text{near}}, \phi_L|\xi|^2\nabla U_{\text{near}}\rangle + \langle\nabla^2 U_{\text{near}}, \phi_L|\xi|^2\nabla^2 U_{\text{near}}\rangle$ has a uniform bound in L and we can take the limit $L\to\infty$ to conclude that

$$|\xi|^2\nabla U_{\text{near}}\in L^2, \qquad |\xi|^2\nabla^2 U_{\text{near}}\in L^2. \tag{F.16}$$

We have hence conclude the proof. We remark that by the same argument, we can moreover show that $|\xi|^l\nabla^k U_{\text{near}}$ for any $l\leqslant k+1$ so that we can extract a decay of $O(|\xi|^{-5/2-k})$ for $\nabla^k U_{\text{near}}$ using the dyadic argument. This is not necessary for our purpose. □

References

[1] D. Albritton, E. Brue, and M. Colombo. Non-uniqueness of Leray solutions of the forced Navier-Stokes equations. *Annals of Mathematics*, 196(1):415–455, 2022.

[2] D. Albritton, E. Brué, and M. Colombo. Gluing non-unique navier–stokes solutions. *Annals of PDE*, 9(2):17, 2023.

[3] D. Albritton, E. Brué, M. Colombo, C. De Lellis, V. Giri, M. Janisch, and H. Kwon. Instability and nonuniqueness for the 2*d* Euler equations in vorticity form, after M. Vishik. *arXiv preprint arXiv:2112.04943*, 2021.

[4] J. Barzilai and J. M. Borwein. Two-point step size gradient methods. *IMA journal of numerical analysis*, 8(1):141–148, 1988.

[5] A. Bressan and R. Murray. On self-similar solutions to the incompressible Euler equations. *Journal of Differential Equations*, 269(6):5142–5203, 2020.

[6] A. Bressan and W. Shen. A posteriori error estimates for self-similar solutions to the Euler equations. *Discrete & Continuous Dynamical Systems: Series A*, 41(1), 2021.

[7] T. Buckmaster, C. de Lellis, L. Székelyhidi, and V. Vicol. Onsager's Conjecture for Admissible Weak Solutions. *Communications on pure and applied mathematics*, 72(2), 2019.

[8] T. Buckmaster and V. Vicol. Nonuniqueness of weak solutions to the Navier-Stokes equation. *Annals of Mathematics*, 189(1):101–144, 2019.

[9] L. Caffarelli, R. Kohn, and L. Nirenberg. Partial regularity of suitable weak solutions of the Navier–Stokes equations. *CPAM*, 35(6):771–831, 1982.

[10] A. Castro, D. Córdoba, and J. Gómez-Serrano. *Global smooth solutions for the inviscid SQG equation*, volume 266. American Mathematical Society, 2020.

[11] J. Chen. Vorticity Blowup in Compressible Euler Equations in Rd, d$\geq$ 3. *Annals of PDE*, 11(2):1–71, 2025.

[12] J. Chen, G. Cialdea, S. Shkoller, and V. Vicol. Vorticity blowup in 2D compressible Euler equations. *arXiv preprint arXiv:2407.06455*, 2024.

[13] J. Chen and T. Y. Hou. Stable nearly self-similar blowup of the 2D Boussinesq and 3D Euler equations with smooth data I: Analysis. *arXiv preprint: arXiv:2210.07191v3 [math.AP]*, 2022.

[14] J. Chen and T. Y. Hou. Singularity Formation in 3D Euler Equations with Smooth Initial Data and Boundary. *PNAS*, 122(27):e2500940122, 2025.

[15] J. Chen and T. Y. Hou. Stable nearly self-similar blowup of the 2D Boussinesq and 3D Euler equations with smooth data II: Rigorous numerics. *MMS*, 23(1):25–130, 2025.

[16] J. Chen, T. Y. Hou, and D. Huang. On the Finite Time Blowup of the De Gregorio Model for the 3D Euler Equation. *CPAM, https://doi.org/10.1002/cpa.21991*, 2021.

[17] J. Chen, T. Y. Hou, and D. Huang. Asymptotically self-similar blowup of the Hou-Luo model for the 3D Euler equations. *Annals of PDE*, 8(2):24, 2022.

[18] J. Chen, T. Y. Hou, V. T. Nguyen, and Y. Wang. On the stability of blowup solutions to the complex Ginzburg-Landau equation in R^d. *arXiv preprint arXiv:2407.15812*, 2024.

[19] A. Cheskidov, M. Dai, and S. Palasek. Instantaneous type˜ i blow-up and non-uniqueness of smooth solutions of the navier–stokes equations. *arXiv preprint arXiv:2511.09556*, 2025.

[20] A. Cheskidov and X. Luo. Sharp nonuniqueness for the Navier–Stokes equations. *Inventiones mathematicae*, 229(3):987–1054, 2022.

[21] A. Cheskidov and X. Luo. L 2-Critical Nonuniqueness for the 2D Navier-Stokes Equations. *Annals of PDE*, 9(2):13, 2023.

[22] M. P. Coiculescu and S. Palasek. Non-Uniqueness of Smooth Solutions of the Navier-Stokes Equations from Critical Data. *arXiv preprint arXiv:2503.14699*, 2025.

[23] T. M. Elgindi and F. Pasqualotto. From Instability to Singularity Formation in Incompressible Fluids. *arXiv preprint arXiv:2310.19780*, 2023.

[24] K.-J. Engel and R. Nagel. *One-parameter semigroups for linear evolution equations*. Springer, 2000.

[25] L. Escauriaza, G. Seregin, and V. Sverak. $L_{3,\infty}$-solutions to the Navier–Stokes equations and backward uniqueness. *Russian Mathematical Surveys.*, 58(2):211–250, 2003.

[26] L. Grafakos. *Classical Fourier Analysis*, volume 249 of *Graduate Texts in Mathematics*. Springer, New York, 3rd edition, 2014.

[27] J. Guillod and V. Šverák. Numerical investigations of non-uniqueness for the Navier–Stokes initial value problem in borderline spaces. *Journal of Mathematical Fluid Mechanics*, 25(3):46, 2023.

[28] E. Hopf. Über die Anfangswertaufgabe für die hydrodynamischen Grundgleichungen. *Math. Nachr.*, 4:213–231, 1951.

[29] T. Y. Hou, V. T. Nguyen, and Y. Wang. L^2-based stability of blowup with log correction for semilinear heat equation. *arXiv preprint arXiv:2404.09410*, 2024.

[30] P. Isett. A proof of Onsager's conjecture. *Annals of Mathematics*, 188(3):871–963, 2018.

[31] H. Jia and V. Sverak. Local-in-space estimates near initial time for weak solutions of the Navier-Stokes equations and forward self-similar solutions. *Inventiones mathematicae*, 196:2334–265, 2014.

[32] H. Jia and V. Sverak. Are the incompressible 3D Navier–Stokes equations locally ill-posed in the natural energy space? *Journal of Functional Analysis*, 268(12):3734–3766, 2015.

[33] H. Koch and D. Tataru. Well-posedness for the Navier–Stokes equations. *Advances in Mathematics*, 157(1):22–35, 2001.

[34] O. Ladyzhenskaya. Example of nonuniqueness in the Hopf class of weak solutions for the Navier–Stokes equations. *Mathematics of the USSR-Izvestiya*, 3(1):229–236, 1969.

[35] J. Leray. Sur le mouvement d'un liquide visqueux emplissant l'espace. *Acta Math.*, 63(1):193–248, 1934.

[36] F. Lin. A new proof of the Caffarelli–Kohn–Nirenberg theorem. *CPAM*, 51(3):241–257, 1998.

[37] J. Liu, Y. Wang, and T. Zhou. Finite time blowup for Keller-Segel equation with logistic damping in three dimensions. *arXiv preprint arXiv:2504.12231*, 2025.

[38] X. Liu. A framework of verified eigenvalue bounds for self-adjoint differential operators. *Applied Mathematics and Computation*, 267:341–355, 2015.

[39] X. Liu, M. T. Nakao, and S. Oishi. Computer-assisted proof for the stationary solution existence of the Navier–Stokes equation over 3D domains. *Communications in Nonlinear Science and Numerical Simulation*, 108:106223, 2022.

[40] X. Liu and S. Oishi. Verified eigenvalue evaluation for the Laplacian over polygonal domains of arbitrary shape. *SIAM Journal on Numerical Analysis*, 51(3):1634–1654, 2013.

[41] G. Luo and T. Y. Hou. Potentially singular solutions of the 3D axisymmetric Euler equations. *Proceedings of the National Academy of Sciences*, 111(36):12968–12973, 2014.

[42] G. Luo and T. Y. Hou. Toward the finite-time blowup of the 3D axisymmetric Euler equations: a numerical investigation. *Multiscale Modeling & Simulation*, 12(4):1722–1776, 2014.

[43] S. Palasek. Non-uniqueness in the Leray-Hopf class for a dyadic Navier-Stokes model. *arXiv preprint arXiv:2407.06179*, 2024.

[44] G. Prodi. Un teorema di unicita per le equazioni di Navier-Stokes. *Annali di Matematica pura ed applicata*, 48(1):173–182, 1959.

[45] J. Serrin. The initial value problem for the Navier–Stokes equations. Nonlinear Problems (Proceedings on Symposium, Madison, WI, 1962) pp. 69–98, 1963.

[46] H. Sohr. *The Navier-Stokes equations: An elementary functional analytic approach*. Springer Science & Business Media, 2012.

[47] G. Talenti. Best constant in Sobolev inequality. *Annali di Matematica pura ed Applicata*, 110:353–372, 1976.

[48] M. Vishik. Instability and non-uniqueness in the Cauchy problem for the Euler equations of an ideal incompressible fluid. Part I. *arXiv preprint arXiv:1805.09426*, 2018.

[49] M. Vishik. Instability and non-uniqueness in the Cauchy problem for the Euler equations of an ideal incompressible fluid. Part II. *arXiv preprint arXiv:1805.09440*, 2018.

[50] Y. Wang, M. Bennani, J. Martens, S. Racanière, S. Blackwell, A. Matthews, S. Nikolov, G. Cao-Labora, D. S. Park, M. Arjovsky, et al. Discovery of Unstable Singularities. *arXiv preprint arXiv:2509.14185*, 2025.

[51] Y. Wang, C.-Y. Lai, J. Gómez-Serrano, and T. Buckmaster. Asymptotic self-similar blow-up profile for three-dimensional axisymmetric Euler equations using neural networks. *Physical Review Letters*, 130(24):244002, 2023.

[52] Y. Wang, Z. Liu, Z. Li, A. Anandkumar, and T. Y. Hou. High precision PINNs in unbounded domains: application to singularity formulation in PDEs. *arXiv preprint arXiv:2506.19243*, 2025.